Enhancing T cell immunotherapy through dosing of memory transcription factors

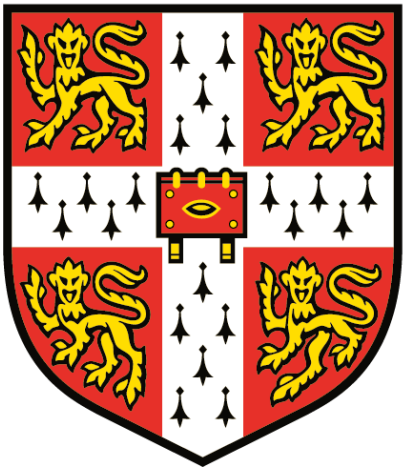

Alberto Gabriel Conti Negrin

Department of Pathology

University of Cambridge

This dissertation is submitted for the degree of *Doctor of Philosophy*

St Edmund's College

September 2025

Declaration

This thesis is the result of my own work and includes nothing which is the outcome of work done in collaboration except as declared in the preface and specified in the text. It is not substantially the same as any work that has already been submitted, or, is being concurrently submitted, for any degree, diploma or other qualification at the University of Cambridge or any other University or similar institution except as declared in the preface and specified in the text.

It does not exceed the prescribed word limit for the relevant Degree Committee.

Alberto Gabriel Conti Negrin

September 2025

Enhancing T cell immunotherapy through dosing of memory transcription factors

By Alberto Gabriel Conti Negrin

Summary

T cell therapies hold promise for treating solid tumours, but their efficacy is limited by poor persistence of transferred cells. Previous strategies to enhance persistence often relied on enforcing constitutively activated, and hence potentially toxic or oncogenic, T cell states. In contrast, physiological immune responses are sustained by quiescent, self-renewing progenitor T cells that depend on the memory transcription factor BACH2. These cells maintain stem-like potential while giving rise to short-lived effector cells. Here, I show that quantitative control of BACH2 dosage governs the physiological continuum of stem and effector $CD8^+$ T cell states, a principle that can be leveraged to engineer synthetic states with superior persistence and anti-tumour activity. Under physiological conditions, BACH2 is precisely regulated in $CD8^+$ T cells, with intermediate expression in memory and progenitor-exhausted subsets. Enforcing excessive levels of BACH2 locks cells in a quiescent state, disrupting the acquisition of effector functions necessary for tumour control. By contrast, low-dose BACH2 permits effector differentiation while preserving stem-like features, thereby enhancing persistence and therapeutic efficacy. Mechanistically, low-dose BACH2 partially restrains AP-1 occupancy at enhancers, attenuating highly AP-1–dependent genes without interfering with effector programmes. This dosage principle extends to other memory factors, as low-dose FOXO1 expression also augments T cell responses in an analogous manner. Thus, memory factor dosage emerges as a key regulator of T cell fate, suggesting that quantitative tuning of gene expression can drive qualitative improvements in cancer immunotherapy.

Acknowledgements

I remember vividly the day I first met Rahul. It was November 1st, 2019. That day should have been my father's birthday, but he was not here to celebrate it. He had passed away four years earlier due to the very same disease I would devote my career to: cancer. Witnessing this malady first-hand would prove key in my decision to forgo a medical degree in my home country of Spain and instead move my life to the United Kingdom to pursue a career in science and research.

After visiting Rahul's laboratory and walking with him through the Babraham Institute's campus, where he was based at the time, I thanked him for his time ready to make my way back home to York. Back then, I did not yet know whether I would secure a scholarship to carry out my PhD at the University of Cambridge, nor did he. But before I left, he said something that has stayed with me ever since: "*You know, I think you and I will achieve great things together*." After six years, several publications, grants and awards, three patents, one doctoral thesis and even one spin-out company, I guess it is fair to say he was onto something.

First and foremost, I would like to thank my supervisor and mentor, Rahul. Becoming a scientist happens only once in one's lifetime, and doing so under your supervision, mentorship and support has been a privilege. For the trust you have placed in me over the years, for reminding me what an honour it is to work in science, for fostering my scientific and creative freedom, for daring me to try, to think differently, and to take risks, for pushing me not to give up, and for placing my happiness and wellbeing above all else – for all of this, I am thankful.

Next, I would like to dispel a myth I have heard time and time again: that a PhD is a lonely endeavour, with little to no interaction with others, where one must face challenges, failures and obstacles alone. To anyone reading this, know this need not be the case. I would like to thank all the wonderful, talented and brilliant scientists I have had the privilege of working alongside. To Sarah: I still remember the day we went out for pizza a few weeks after I started – I was confused and overwhelmed, but you reassured me it would be okay, and over the following months you taught me the basics of flow cytometry and 'Rahul management', likely the two skills I have found most valuable throughout my time in Cambridge. To Charlotte: for teaching me how to process my very first spleen, for resolving an endless number of questions, doubts and fears, and for always being ready and happy to lend a helping hand. To Jie: for teaching me the ins and outs of animal research and for keeping me company on some of the longest days of my PhD. To Xan and Ardon: you guys are mad, and probably need some help,

but the lab would not be the same without you. To Teresa: for the unwavering support and for having my back during one of the most intense periods of my time in Cambridge. To Layla, Yumi, Jack, Aws, Randy and Lionel: for all the help with experiments and throughout the ups and downs of this journey.

But if there is anyone who deserves my deepest gratitude for their help and support at the bench, that is undoubtedly Alex. It is no exaggeration to say I have spent more time doing science with you than on my own – together we have accomplished more than I ever thought possible in a single PhD, and I have no doubt this is only the beginning. Power on.

Beyond the lab I have also had an unending stream of support and encouragement – during the toughest times of this degree, this has meant the world to me. Thank you to Marta: for the countless hours spent talking about our ups and downs, science and life. To Fabio: for being an unwavering pillar of support and kindness, and for being a friend unlike anyone I could have hoped to find in the UK. To Kai and Tanya: for having made Cambridge the vibrant and memorable experience it now occupies in my memories. To Adri, Carli, Bea, Becky, Laura and so many others who have been part of my life during these last few years: I am grateful to each and every one of you.

One person, however, has made Cambridge and my time here truly unforgettable. To Mariana, my partner in life and love. You have never failed to remind me of my worth, even when I doubted it most. Cambridge is where I met you, and even if I were to leave this place having failed every single experiment, having failed to make any contribution to science whatsoever, and having failed to defend this thesis and earn the title of ‘doctor’, meeting you alone would have made this journey worthwhile a million times over. Thank you.

Lastly, my most heartfelt thanks go to the most incredible people I have ever known: mum and dad. To mum: thank you for your unconditional love, for teaching me that one reaps what one sows, and for showing me that it is always the right time to learn, explore, and live fully. To dad: thank you for nurturing my love of science and discovery from an early age, and for instilling in me the values of resilience and hard work. Though you are not here to see this, I hope it would have made you proud. I can only imagine the sacrifices and effort it must have taken from both of you to give me a childhood so rich in stability, affection, and opportunity. Thank you for this life.

Acknowledgement of Assistance Received During Research

Training and Mentoring

Sarah Whiteside	Flow cytometry, *in vitro* assays, subcutaneous injections.
Charlotte Imianowski	Spleen/lymph node processing, *in vitro* assays.
Jie Yang	*In vivo* studies, tumour processing.
Katie Butcher	Intravenous injections.

Experimental Support

Alexander Evans	Tissue processing, *in vivo* experiments, *in vitro* assays, processing of bioinformatic data.
Teresa von Linde	Tissue processing, *in vivo* experiments, ATAC-seq assay.
Christian Deo T. Deguit	CUT&RUN assay.
Sarah Whiteside	Tissue processing.
Charlotte Imianowski	Tissue processing.
Alexander Wesolowski	Tissue processing.
Teresa von Linde	Tissue processing.
Yumi Yamashita-Kanemaru	Tissue processing.
Jack Chapman	Tissue processing.
Layla Dahmani	Tissue processing.
Jie Yang	Tissue processing.
Ardon M. Pillay	Tissue processing.
Randy Greaves	Tissue processing.
Aws Al-Deka	Tissue processing.

Technical Service Providers

Transnetyx	Genotyping of murine lines.
UBS Gurdon Facility	Housing and husbandry of mice.
Novogene	RNA and ATAC sequencing.
Peter MacCallum Cancer Centre Molecular Genomics Core	CUT&RUN sequencing.
Joana Cerveira, Mercedes Cabrera Jaran, Sameen Khan	Flow cytometry facility management, running cell sorters, and general flow cytometry support.
Department of Biochemistry	DNA sequencing.
VectorBuilder	Vector synthesis and assembly.

Abbreviations

ACT	Adoptive Cell Therapy
AGC	Automatic Gain Control
Akt	Protein Kinase B
AP-1	Activation Protein 1
APCs	Antigen-Presenting Cells
BACH2	Broad complex-tramtrack-bric a brac and Cap'n'collar homology 2
BATF	Basic Leucine Zipper ATF-like Transcription Factor
BCL-2	B cell lymphoma 2
BLIMP-1	B lymphocyte-induced maturation protein-1
BTB	Bric-a-brac–tramtrack–broad complex
CCR	C-C chemokine receptor
CD40L	CD40 ligand
CD	Cluster of differentiation
CDSs	Coding sequences
ChIP-seq	Chromatin immunoprecipitation sequencing
CTLA-4	Cytotoxic T-lymphocyte-associated protein 4
CTLs	Cytotoxic T lymphocytes
CUT&RUN	Cleavage under targets & release using nuclease
CXCR	C-X-C chemokine receptor
DAMPs	Damage-associated molecular patterns
DCs	Dendritic cells
DEGs	Differentially expressed genes
DIA	Data Independent Acquisition
FDA	Food and Drug Administration
FOXO1	Forkhead box protein O1
FOXO1^{AAA}	Constitutively active triple alanine FOXO1 mutein
ICTs	Immune checkpoint therapies
IDO	Indoleamine 2,3-dioxygenase
ID3	Inhibitor of DNA binding 3
IFN	Interferon
IL	Interleukin
IRF4	Interferon regulatory factor 4
ITAMs	Immunoreceptor tyrosine-based activation motifs
KO	Knock-out
LAG-3	Lymphocyte-activation gene 3

LCK	Lymphocyte-specific PTK
LNs	Lymph nodes
LTR	Long terminal repeat
MHC	Major histocompatibility complex
MSCV	Murine stem cell virus
MTD	Maximum tolerated dose
mTOR	Mechanistic target of rapamycin
NFAT	Nuclear factor of activated T-cells
NK	Natural killer
OE	Overexpression
PAMPs	Pathogen-associated molecular patterns
PD-1	Programmed death-1
PI3K	Phosphoinositide 3-kinase
pMHC	Peptide-MHC
PTKs	Protein tyrosine kinases
RFP	Red fluorescent protein
Slamf6	SLAM family member 6
STAT5	Signal transducer and activator of transcription 5
STAT5-CA	Constitutively active version of STAT5
STOP-TRM	STOP-translational readthrough motif
TAAs	Tumour-associated antigens
TCF1	T cell factor 1
TCR	T cell receptor
Tem	Effector memory
Teff	Short-lived effector T cells
Texh	Exhausted T cells
TFs	Transcription factors
Th	Helper T cells
TIL	Tumour infiltrating lymphocyte
TIM-3	T-cell immunoglobulin and mucin domain 3
Tint	Intermediate exhausted T cells
TLS	Tertiary lymphoid structures
TME	Tumour microenvironment
Tmp	Memory precursor T cells
TNF	Tumour necrosis factor
TOX	Thymocyte selection-associated high-mobility group box protein
Tpex	Exhausted progenitor T cells

Tregs	Regulatory T cells
TSAs	Tumour-specific antigens
Tscm	Stem cell memory
Ttex	Terminal exhausted T cells
UBS	University of Cambridge's Biomedical Services
WT	Wild-type

Contents

1. Introduction 1

1.1 A brief history of cancer immunotherapy 1

1.2 The cancer immunity cycle 2

1.2.1 Release and presentation of cancer cell antigens 2

1.2.2 T cell priming 2

1.2.3 Tumour trafficking and infiltration of T cells 3

1.2.4 Cancer cell recognition and killing by T cells 3

1.3 Priming and activation of T cells 5

1.3.1 Signal 1: recognition of tumour antigens 5

1.3.2 Signal 2: T cell co-stimulation 6

1.3.3 Signal 3: Cytokine signalling 7

1.4 $CD8^+$ T cells in the anti-tumour response 8

1.4.1 $CD8^+$ T cell-mediated killing 8

1.4.2 Differentiation states of $CD8^+$ T cells 9

1.4.3 $CD8^+$ T cell exhaustion 10

1.4.4 Transcriptional regulation during $CD8^+$ T cell exhaustion 13

1.5 Adoptive T cell therapy 14

1.5.1 TIL therapy 14

1.5.2 Genetically engineered antigen receptors 15

1.6 Improving T cell persistence in adoptive T cell therapy 19

1.6.1 Optimising T cell culture conditions 19

1.6.2 Controlling the level of T cell stimulation 19

1.6.3 Transcriptional regulators as targets for extending T cell persistence 20

1.6.4 Leveraging memory transcription factors for preventing terminal differentiation 22

1.7 BACH2 22

1.7.1 The basic leucine zipper TF family 23

1.7.2 The BACH subfamily 23

1.7.3 BACH2 in T cell biology 24

1.8 Leveraging BACH2 for improving T cell therapy in solid tumours 27

2. Material and methods 28

2.1 Mice 28

2.1.1 Experimental mice 28

2.1.2 Mice genotyping 28

2.2 Cell lines and cell culture reagents 28

2.2.1 Adherent cell lines 28
2.2.2 Primary cells 29
2.3 Tissue processing 29
2.3.1 Spleens and lymph nodes 29
2.3.2 Tumours 29
2.4 Retroviral T cell transduction 30
2.4.1 Construction of retroviral vector plasmids 30
2.4.2 Production of retroviral particles 30
2.4.3 Murine T cell transduction 31
2.5 Flow cytometry and cell sorting 31
2.6 Adoptive T cell transfers 32
2.7 Assessment of endogenous *Bach2* expression 32
2.8 *In vitro* chronic stimulation assay 33
2.8.1 Anti-CD3 plate coating 33
2.8.2 In vitro stimulation 33
2.9 Proteomics analysis 33
2.9.1 Proteomics sample preparation 33
2.9.2 Mass spectrometry 34
2.9.3 Proteomics data analysis 34
2.10 RNA sequencing and analysis 34
2.10.1 RNA sequencing 34
2.10.2 Processing and analysis of RNA sequencing data 35
2.11 ATAC-seq sequencing and analysis 35
2.11.1 ATAC sequencing 35
2.11.2 Processing and analysis of ATAC-seq data 36
2.12 CUT&RUN sequencing and analysis 36
2.12.1 CUT&RUN sequencing 36
2.12.2 Processing and analysis of CUT&RUN data 37
2.13 Human single-cell RNA sequencing analysis 37
3. Chapter 1: BACH2 overexpression in tumour-specific CD8$^+$ T cells ...39
3.1 Background 39
3.2 Results 39
3.2.1 Set-up of an in vivo solid tumour ACT model 39
3.2.2 BACH2 overexpression enhances stemness and prevents Ttex differentiation in tumour-specific T cells 46
3.2.3 BACH2 overexpression compromises the acquisition of effector functions and impairs ACT anti-tumour responses 48

3.3 Discussion 51
4. Chapter 2: Quantitative control of BACH2 in CD8$^+$ T cells 55
4.1 Background 55
4.2 Results 55
4.2.1 Intratumoral CD8$^+$ T cells display gradated expression of BACH2 mRNA 55
4.2.2 Low-dose expression of BACH2 preserves a stem-like phenotype without compromising effector functions in vitro 59
4.2.3 Dosed expression of BACH2 protects CD8$^+$ T cells from terminal differentiation without compromising their effector functions in vitro 68
4.2.4 Dosed expression of BACH2 imposes a unique transcriptional state featuring both Tpex and effector characteristics in vitro 70
4.2.5 Partial attenuation of AP-1 binding enables BACH2$_{DE}$ to selectively regulate genes with high levels of AP-1-dependency 77
4.3 Discussion 78
5. Chapter 3: BACH2 and FOXO1 dosing enhance anti-tumour responses *in vivo* 83
5.1 Background 83
5.2 Results 83
5.2.1 Low-dose expression of BACH2 enhances anti-tumour CD8$^+$ T cell therapy responses in vivo 83
5.2.2 Low-dose expression of BACH2 results in higher number of intratumoral T cells but does not affect the proportion of Tpex and Ttex 84
5.2.3 BACH2 dosing induces transcriptional changes in a subset-specific manner 90
5.2.4 BACH2 dosing preserves Slamf6$^+$ transcriptional features upon Slamf6$^-$ differentiation 91
5.2.5 Low-dose expression of FOXO1^{AAA} enhances anti-tumour CD8$^+$ T cell therapy responses in vivo 94
5.3 Discussion 98
6. Thesis Discussion 103
6.1 Summary of key findings 103
6.2 Limitations and future perspectives 105
6.3 Proposed conceptual model 109
7. Conclusion 112
8. References 113

1. Introduction

1.1 A brief history of cancer immunotherapy

Over the past decade, the advent of immunotherapies has transformed the treatment of cancer, marking a paradigm shift in the field of oncology. Yet, the concept of leveraging the immune system to combat cancer is far from new. Scientific observations hinting at the immune system's protective role against cancer, and its therapeutic potential, trace back to the late 19th century and even predate radiotherapy and chemotherapy[1,2]. In 1891, American surgeon and physician William B. Coley gathered several reports of tumour shrinkage following viral or bacterial infections and speculated that the immune reactions following those infections played a pivotal role in the observed regressions. This led him to develop a vaccine composed of heat-killed bacteria, now known as Coley's toxins, with which he treated his own patients – sometimes with remarkable success by the standards of the time [3-5]. Nonetheless, the unpredictable outcomes of the treatment, combined with a limited understanding of the immune system and the emergence of alternative approaches such as radiotherapy and chemotherapy in the early 20th century, led to a decline in interest in cancer immunology and immunotherapy within the scientific community[1,2].

The field would have to wait several decades until experiencing renewed scientific interest. This came during the 1960s and 1970s, an era that marked a turning point in our understanding of the interplay between the immune system and cancer. Pivotal work carried out during this time showed that mice lacking a functioning immune system develop cancer more readily[6-8]. In addition, it was during this same period that several key immune cell types were first described, such as T cells[9-11], dendritic cells (DCs)[12] and natural killer (NK) cells[13,14]. Subsequent research throughout the late 20th century continued to highlight the importance of immunity in cancer and deepened our knowledge of the molecular mechanisms through which these cell subsets contribute to cancer suppression and killing[15-19].

It was not until the beginning of the 21st century when the discoveries underpinning our understanding of cancer immunity were finally translated into commercially available therapies. In the 1990s, for instance, Tasuku Honjo and James P. Allison described programmed death-1 (PD-1)[20] and cytotoxic T-lymphocyte-associated protein 4 (CTLA-4)[21], respectively, as key checkpoint receptors exploited by cancer to suppress immune responses. Their work laid the foundation for the development of immune checkpoint inhibitors targeting these pathways, which gained approval in the 2010s and have since become the standard of care for

several types of cancer. Furthermore, the advent of adoptive cell therapy (ACT), which uses immune cells as living drugs, represents another significant milestone in cancer treatment and have positively impacted the lives of tens of thousands of patients.

1.2 The cancer immunity cycle

Despite the early observations from Coley and other pioneers, the idea that the immune system plays a significant role in the emergence and persistence of cancer was met with scepticism for much of the 20th century. Nonetheless, it is now understood that several cell types within the innate and adaptive immune compartments are actively involved in detecting and targeting malignant cells, in a process referred to as the cancer immunity cycle (**Fig. I-1**)[22,23].

1.2.1 Release and presentation of cancer cell antigens

Oncogenesis begins with the accumulation of genetic (e.g. somatic mutations) and epigenetic (e.g. aberrant gene expression or silencing) alterations within healthy cells. These alterations are critical for the start of the cancer immunity cycle as they can be recognised by the immune system and are broadly referred to as cancer or tumour antigens. Upon death of malignant cells, tumour antigens are released and captured by antigen-presenting cells (APCs), primarily DCs, for processing and presentation in the form of peptide fragments through major histocompatibility complex (MHC) surface molecules. Other soluble immunogenic factors are also released in the process, which activate APCs and induce the upregulation of co-stimulatory receptors necessary for mounting an adaptive immune response[24].

1.2.2 T cell priming

Once APCs have captured and processed cancer neoantigens, they migrate to secondary lymphoid organs such as lymph nodes (LNs) where they present them to naïve T cells. When a T cell receptor (TCR) on a naïve T cell successfully recognises and binds to a complementary antigen displayed in the context of an MHC molecule by an APC, and sufficient co-stimulatory signals are present, the T cell becomes activated – this is known as T cell priming (discussed later).

Upon priming, cluster of differentiation 4 $(CD4)^+$ T cells can differentiate into various subsets, including helper T cells (Th)1, Th2, Th17, or regulatory T cells (Tregs), depending on the affinity and context of the interaction. Each of these subsets possesses specialised functions that contribute to the anti-tumour immune response in distinct ways[25]. Conversely, activated

$CD8^+$ T cells (also known as cytotoxic T lymphocytes, CTLs) play a major role in direct targeting and killing of cancer cells.

While the role of LNs in T cell priming during anti-tumour responses has been studied extensively over the past two decades[26,27], an increasing volume of evidence has emerged in recent years highlighting the existence and importance of LN-like cell aggregates within solid tumours, termed tertiary lymphoid structures (TLS). The presence of TLS in tumours has been correlated with improved anti-tumour responses and is thought to enable *in situ* priming and expansion of T cells[28,29].

1.2.3 Tumour trafficking and infiltration of T cells

In the context of secondary lymphoid organ priming, the recognition of an APC presenting a tumour antigen is followed by T cell migration to the tumour. This process starts by downregulating receptors such as CD62L and C-C chemokine receptor (CCR) type 7 (CCR7), which are required for accessing and remaining in secondary lymphoid organs. At the same time, activated T cells upregulate the expression of receptors necessary for mediating migration and infiltration towards altered tissues. These include chemokine receptors such as C-X-C chemokine receptor (CXCR) type 3 (CXCR3) and CXCR6, which respond to various chemokine ligands produced in affected tissues and induce T cell trafficking to those sites. Upon ligand binding, these receptors induce upregulation and activation of other receptors such as lymphocyte function-associated antigen 1 and very late antigen 4, which mediate tissue adhesion and infiltration into the tumour site[30,31].

1.2.4 Cancer cell recognition and killing by T cells

Upon tumour infiltration, T cells initiate the process of identifying and eliminating malignant cells. $CD4^+$ T cells act primarily through the release of effector molecules within the tumour microenvironment (TME) in response to tumour antigens presented by APCs. These molecules include cytokines such as interferon gamma (IFN-γ), tumour necrosis factor (TNF) and interleukin (IL)-2, which support the activation and maintenance of several immune subsets and can also cause indirect tumour death[25,32]. In certain contexts, $CD4^+$ T cells have also been observed to directly engage and target tumour cells[33]. In contrast, $CD8^+$ T cells specialise in direct recognition and targeting of cancer cells[34] (discussed later). The death of tumour cells releases additional tumour antigens, effectively restarting the cycle and promoting the anti-tumour immune response[22].

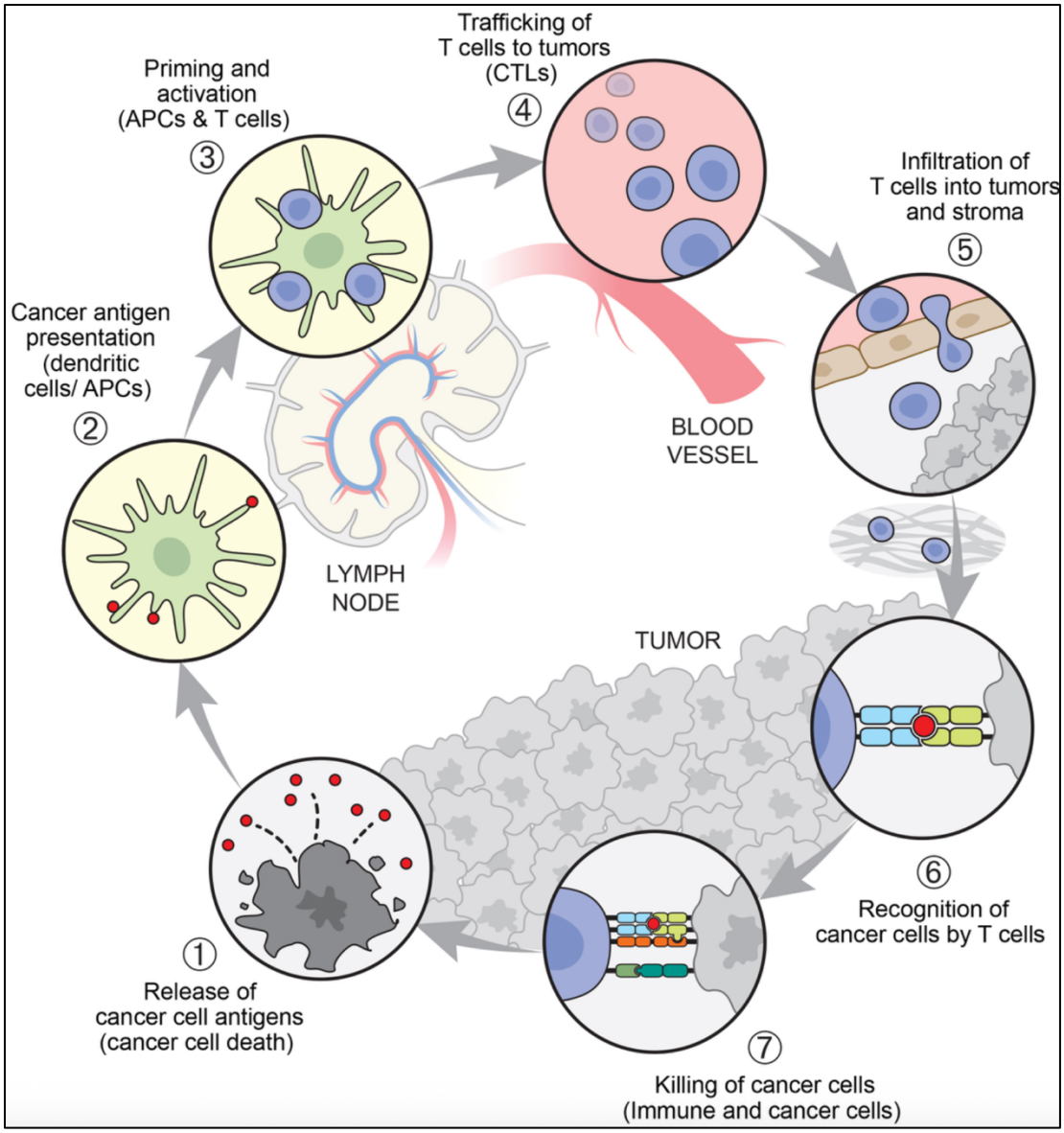

Figure I-1. The cancer immunity cycle. Visual representation of the different steps in the cancer immunity cycle, first conceived by Daniel S. Chen and Ira Mellman. Figure adapted from Chen, D. S. and Mellman I., *Immunity*, 2023.

1.3 Priming and activation of T cells

The diverse roles played by distinct immune subsets within the TME have been, and still are, an active area of investigation. Among these, T cells are critical mediators of cancer immunity, contributing to the recognition and elimination of transformed cells through a variety of mechanisms. The process through which T cells become activated and acquire effector functions is central to cancer immunity. Unsurprisingly, it is also tightly regulated and requires coordinated signals from multiple cell types.

1.3.1 Signal 1: recognition of tumour antigens

The recognition of a tumour antigen presented by an APC is the first step in the activation and expansion in a naïve $CD8^+$ T cell and is often referred to as 'Signal 1' during the process of T cell priming. This begins with APCs capturing tumour proteins, processing them into peptide fragments, and forming peptide-MHC (pMHC) complexes. These complexes are then displayed on the surface of APCs, where they interact with TCRs expressed by T cells.

Two main classes of MHC molecules exist: class I (MHC I) and class II (MHC II). Typically, MHC I molecules are expressed on all nucleated cells and display peptides derived from the cell's internal proteome. This provides the immune system with a mechanism to 'monitor' for the expression of viral or cancer-associated proteins across tissues. Conversely, MHC II molecules are expressed primarily on APCs and present peptides derived from captured extracellular proteins, such as those originating in pathogens or cancer cells. Notably, APCs can also present exogenous proteins through MHC I molecules via a process known as cross-presentation. This is important because, since CD4+ T cells recognise peptides presented exclusively in the context of MHC II molecules, and $CD8^+$ T cells interact only with MHC I molecules, cross-presentation enables APCs to prime $CD8^+$ T cells against virus- or cancer-derived antigens.

Importantly, the type of tumour antigen presented by APCs will also shape the nature of the anti-tumour response. Tumour antigens are broadly categorised into two groups: tumour-associated antigens (TAAs) and tumour-specific antigens (TSAs)[35]. TAAs derive from proteins present in both healthy and cancerous cells but are either aberrantly overexpressed or inappropriately expressed (e.g. re-expression of proteins unique to specific developmental stages) in cancer cells. In contrast, TSAs arise from aberrant protein alterations caused by mechanisms including somatic mutations, chromosomal rearrangements, or alternative

splicing. These alterations produce amino acid sequences unique to tumour cells, which is why TSAs are also referred to as neoantigens[35].

To elicit an anti-tumour response, the binding between a TCR and a pMHC complex must exhibit sufficiently high affinity. Since TAAs are derived from proteins present in healthy cells, there is a very limited repertoire of T cells capable of recognising them due to the elimination of self-reactive T cells during thymic maturation[36,37]. In contrast, the proportion of T cells expressing high affinity TCRs against neoantigens is much larger, making them highly immunogenic antigens and critical in the start of the cancer immunity cycle[35].

When an APC displaying a TSA interacts with a T cell bearing a TCR complementary for the displayed antigen, an immunological synapse is formed. This is a highly organised structure that facilitates the interaction of signalling molecules between the APC and T cell, initiating a complex signalling cascade that culminates in the activation and priming of the T cell. The cascade is initially triggered by the spatial clustering of receptors, such as the TCR, and co-receptors, such as CD4 or CD8. This clustering facilitates the recruitment of protein tyrosine kinases (PTKs), including lymphocyte-specific PTK (LCK), to the complex. LCK then phosphorylates immunoreceptor tyrosine-based activation motifs (ITAMs) located on the cytosolic tails of CD3 subunits within the TCR complex. This is followed by the recruitment of zeta-chain-associated protein kinase 70, which further activates other downstream adaptor proteins. The cascade ultimately culminates in the activation and translocation of transcription factors (TFs) that mediate T cell differentiation into effector subsets, including nuclear factor of activated T-cells (NFAT) and mechanistic target of rapamycin (mTOR), among others[38].

1.3.2 Signal 2: T cell co-stimulation

The formation of a strong TCR-pMHC interaction is an essential step for T cell priming, but it is not the only one. Additional layers of regulation are necessary to prevent inappropriate immune responses against self-antigens. Notably, approximately 4% of all mature T cells are estimated to express self-reactive TCRs at any given time[39]. To achieve effective T cell activation, a second essential requirement is the presence of co-stimulatory signals, often referred to as ‘Signal 2’.

APCs express molecules known as pattern recognition receptors, distributed both intracellularly and in the cell surface. These receptors recognise molecular structures characteristic of pathogens or apoptotic/damaged cells, generally referred to as pathogen-associated molecular patterns (PAMPs) or damage-associated molecular patterns (DAMPs)

respectively. Upon ligand binding, a cascade of intracellular signalling events is initiated that results in the upregulation of co-stimulatory receptors, including CD80 (also known as B7-1), CD86 (B7-2), on the surface of APCs[40].

During the formation of an immune synapse, CD80 and CD86 on APCs bind to the CD28 receptor on T cells. This interaction triggers the phosphorylation of CD28 by PTKs, which subsequently recruit phosphoinositide 3-kinase (PI3K). PI3K generates phosphatidylinositol (3,4,5)-trisphosphate at the plasma membrane, leading to the recruitment of downstream effectors such as protein kinase B (Akt). Ultimately, Akt leads to the amplification and stabilisation of the signals initiated by the TCR-pMHC interaction through the activation of key regulators, including NFAT and mTOR[38]. In addition to CD28, other co-stimulatory receptors have been identified including CD40 ligand (CD40L), OX40, 4-1BB and CD27.

In contrast to the function of co-stimulatory receptors, co-inhibitory receptors inhibit T cell activation and proliferation. A prime example is CTLA-4, which is expressed in T cells following activation, as well as in Tregs. CTLA-4 binds CD80/CD86 with higher affinity than CD28, preventing CD28-mediated co-stimulation while also inducing the expression of suppressive molecules such as indoleamine 2,3-dioxygenase (IDO). Other co-inhibitory molecules have also been identified, including PD-1, lymphocyte-activation gene 3 (LAG-3), T-cell immunoglobulin and mucin domain 3 (TIM-3), among others[41]. These receptors balance co-stimulatory signals and are implicated in the regulation of T cell priming and subsequent T cell activation and differentiation.

A strong TCR-pMHC interaction involving a naïve T cell, in the absence of sufficient co-stimulatory signalling, is characteristic of self-reactive T cells recognising self-antigens. Under such circumstances, T cells become tolerised and are unable to exert effector functions upon subsequent antigen encounter. This phenomenon, known as T cell anergy, is important to prevent unwanted activation from self-reactive T cells that have escaped thymic selection[42,43].

Co-stimulatory and co-inhibitory receptors in T cells have received considerable attention in the last decade, largely due to the clinical success of CTLA-4 and PD-1 antibody-based inhibitors and the incorporation of CD28 and 4-1BB intracellular domains in second- and third-generation CARs. Nonetheless, the precise molecular mechanisms underlying their signalling pathways in different contexts remain unknown or are still being elucidated[41].

1.3.3 Signal 3: Cytokine signalling

Along with a strong TCR-pMHC interaction and sufficient co-stimulation, a third stimulus is required for optimal T cell activation: cytokine signalling, sometimes referred to as 'Signal 3'. Without this third signal, T cells can fail to undergo effective activation and acquisition of effector functions[44,45]. The specific cytokine environment T cells are exposed to during priming, shaped in part by APCs, can dictate the type of T cell response or their differentiation trajectory. In the case of $CD4^+$ T cells, the different cytokine milieu will result in differentiation into different Th subsets. For instance, Th1 differentiation is promoted by IL-12, Th2 by IL-4, and Th17 by IL-6 and IL-23. For CD8+ T cells, IL-12 and IFN-α/β have been shown to be important to sustain a strong and long-lasting response[45,46]. The specific molecular bases for Signal 3 are still being elucidated, and the use of cytokines for supporting immunotherapies such as ACT is becoming an increasingly relevant therapeutic strategy[47,48].

1.4 $CD8^+$ T cells in the anti-tumour response

The role of $CD8^+$ T cells has long been recognised as pivotal for an effective anti-tumour immune response[34]. The existence of lymphocytes with cytotoxic properties was first observed in 1960 and shown to be CD8+ T cells during the 1970s[11,49-51]. Subsequent breakthroughs elucidated the specific mechanisms through which CD8+ T cells recognise foreign antigens, target malignant cells, and are regulated to prevent unwanted immune responses. These discoveries underpinned the translation of the first modern immunotherapies to the clinic, including immune checkpoint therapies (ICTs) and the use of systemic IL-2 administration for different cancer indications[52,53]. With the clinical traction gained by immunotherapies during the early 2000s, there has been heightened interest in understanding how $CD8^+$ T cells are impacted by these immunotherapies, how anti-tumour responses are sustained in the long-term, and why not all patients benefit from these therapies to the same extent.

1.4.1 $CD8^+$ T cell-mediated killing

Following effective priming by APCs, $CD8^+$ T cells acquire a wide range of effector functions. Unlike naïve $CD8^+$ T cells, a TCR-pMHC I interaction (Signal 1) with a target cell displaying a complementary antigen is sufficient to activate primed $CD8^+$ T cells and engage their cytotoxic functions. During an anti-tumour response, this signal tends to come from a malignant cell presenting a neoantigen.

A key mechanism of cytotoxicity is the release of cytotoxic granules. These consist of modified lysosomal vesicles containing effector proteins such as perforins and granzymes. In the absence of T cell activation, the conditions of these vesicles inhibit their activity, but upon antigen

recognition, the cytotoxic granules are delivered into the target cell. First, perforins create pores on the targeted cell, which cause direct damage while also acting as intercellular channels through which other cytotoxic molecules are delivered. Once in the target cells' cytosol, granzymes induce apoptosis by activating caspases (e.g. caspase 3 activation mediated by Granzyme B) or inducing mitochondrial damage (e.g. mitochondrial damage mediated by granzyme A and B). Notably, direct $CD8^+$ T cell cytotoxicity is specific towards the targeted cell and does not result in damage or death of bystander cells, nor of the T cell itself. Furthermore, engagement of the TCR induces synthesis of effector molecules, enabling $CD8^+$ T cells to replenish the supply of cytotoxic granules and to kill multiple target cells in succession (a property referred to as 'serial killing')[46,54].

Another method of contact-mediated cytotoxicity occurs through the membrane-bound Fas ligand, which can interact with Fas receptor in target cells and induce apoptosis. In addition to inducing cancer apoptosis in certain contexts, this mechanism is also relevant in modulating the magnitude of clonal expansion following T cell priming[55].

$CD8^+$ T cells also contribute to the anti-tumour response through the release of cytokines, including IFN-γ, IL-2 and TNF. IFN-γ is directly secreted to the extracellular medium and has pivotal roles in both anti-viral and anti-tumour responses, as it directly inhibits viral replication and induces upregulation of MHC I molecules for facilitating $CD8^+$ T cells recognition. IL-2 is also secreted by $CD8^+$ T cells and functions as a key stimulus for the proliferation and survival of both conventional $CD4^+$/$CD8^+$ T cells and Tregs. Instead, TNF exists both as soluble and membrane-bound forms and can trigger apoptosis directly by interacting with TNF receptors in target cells. In addition to their direct roles in cancer cells and T cells, these cytokines also interact with multiple other cell types and orchestrate various aspects of the TME[46].

1.4.2 Differentiation states of $CD8^+$ T cells

Our understanding of the differentiation trajectory and subtypes of $CD8^+$ T cells under different contexts has improved substantially over the past two decades, driven in part by the arrival of immunotherapies in the clinic. Nonetheless, it is worth noting that this remains a very active area of research, and that our appreciation of the specific subsets and mechanisms underlying their differentiation fates continues to evolve.

Upon activation, $CD8^+$ T cells differentiate into one of two major developmental branches[56,57]. The first one takes place in the context of acute viral infections or vaccinations where sufficient

stimulation and co-stimulation signals are available, where $CD8^+$ T cells differentiate into either short-lived effector T cells (Teff) or memory precursor T cells (Tmp)[58]. Teff exert high levels of cytotoxicity but have limited differentiation plasticity and are generally considered short-lived. In contrast, Tmp are long-lived and, upon antigen clearance, can give rise to multiple other memory subsets. These memory cells provide durable protective immunity through their ability to give rise to a new wave of Teff upon renewed antigen stimulation[59].

Depending on their function and tissue distribution, two distinct types of memory T cells exist: circulating and resident memory T cells. Among the circulating memory cells, several subsets with often distinct but overlapping functions have been described, including stem cell memory (Tscm), central memory (Tcm) and effector memory (Tem) T cells[58]. Alternatively, Tmp can also migrate to distinct tissues and generate resident memory T cells, which are thought to acquire functional characteristics associated with long-term tissue residence and immune surveillance[60].

A distinct developmental trajectory is adopted by $CD8^+$ T cells in the context of long-term TCR stimulation, such as chronic viral infections or tumours, referred to as T cell exhaustion. Exhausted T cells (Texh) are characterised by functional, phenotypic and epigenetic features distinct from those found in Teff or Tmp. First described in murine models of chronic infection[61,62], it is now evident that Texh are ubiquitously found in both cancer and chronic viral infection settings in both mouse and humans[63,64].

How and when $CD8^+$ T cells commit to the exhaustion differentiation pathway is not entirely understood. Nonetheless, recent findings suggest that key hallmarks of exhaustion during anti-tumour immune responses appear within just hours of antigen encounter[65]. Two core features of Texh are the expression of the TF thymocyte selection-associated high-mobility group box protein (TOX), which is key in the establishment of Texh subsets[66], and inhibitory receptors such as PD-1[67]. Initially, this led to the assumption that Texh were non-functional, but this view has since been updated. T cell exhaustion is likely to be an epigenetic and functional programme that enables T cells to withstand long periods of TCR stimulation while maintaining moderate functionality and avoiding excessive immunopathology[68,69]. This is supported by evidence showing that Texh are actively involved in sustaining immunity against chronic infections or cancer, and preventing the establishment of a T cell exhaustion programme has a negative impact on the outcome of anti-tumour immune responses[70].

1.4.3 $CD8^+$ T cell exhaustion

A key research focus over the past decade has been characterising the functional and phenotypic diversity found within the T cell exhaustion lineage. Initial observations highlighted that a Texh subset expressing T cell factor 1 (TCF1) was key for sustaining long-term anti-viral responses and constituted the primary responders to PD-1 blockade therapy[71], a finding that has since been recapitulated in both viral and cancer settings[72-77]. Despite the absence of a unified classification system, evidence from different groups converged to a model where Texh subtypes exist along a spectrum with varying states of differentiation. These have been grouped in three major subsets: exhausted progenitor T cells (Tpex), intermediate exhausted T cells (Tint) and terminal exhausted T cells (Ttex) (**Fig. I-2**)[56,57,78].

Tpex constitutes the least differentiated cell subtype among Texh. They are characterised by the expression of TCF1, as well as other markers such as SLAM family member 6 (Slamf6) or CXCR5, and absence of the inhibitory receptor TIM-3. Notably, Tpex have attracted substantial interest due to their role in sustaining long-term anti-tumour responses. Multiple studies, both in mouse and humans, have found strong correlations between the abundance of Tpex and positive therapeutic outcomes in the context of both ICT and ACT[75,76,79]. This is thought to be due to their ability to 'self-renew', which enables them to maintain a Tpex pool during chronic stimulation settings while simultaneously giving rise to more differentiated effector subsets. This is why Tpex are often also referred to as 'stem-like' T cells.

As their name suggests, Tint are considered to be an intermediate differentiation state between Tpex and Ttex. Unlike Tpex, they lack expression of TCF1, Slamf6 and CXCR5 and show intermediate levels of TIM-3. Tint also display expression of effector molecules such as IFN-γ and granzymes, which suggests they have an important role in direct targeting of malignant cells. Nonetheless, this subset displays considerable heterogeneity, and differences in the strategies for defining and identifying it have made comparisons among distinct studies difficult.

Lastly, Ttex are considered fully differentiated Texh subsets. As well as lacking TCF1, Slamf6 and CXCR5, they express high levels of TIM-3 and other inhibitory molecules, as well as CD39 and CD69. Ttex can also express some effector molecules such as granzymes, but to a much lower extent compared to Tint. Indeed, they may even contribute to immune suppression through the production of immunomodulators such as adenosine[80]. Conversely to Tpex, high abundance of Ttex is generally associated with poor anti-tumour responses and worse clinical

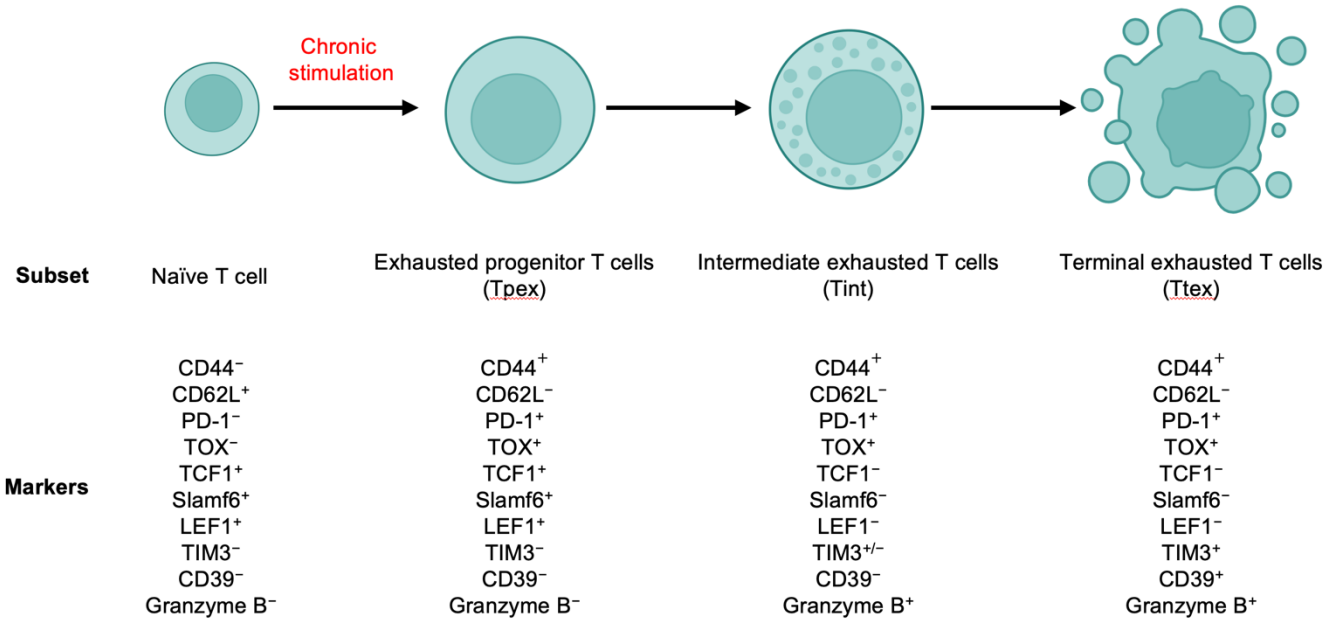

Figure I-2. Differentiation trajectory of exhausted CD8 T cells. Upon persistent stimulation (i.e. chronic viral infection or cancer), CD8 T cells enter an exhausted differentiation trajectory characterised by a spectrum of differentiation subsets. Commonly used markers for the identification of naïve and different CD8 exhausted T cell subsets in murine systems are shown.

outcomes. The Ttex differentiation state is considered short-lived, and the eventual fate of Ttex is likely to be deletion.

The precise lineage relationship between different Texh subsets is still under debate. Nonetheless, clonal lineage tracking data suggest that Tpex can give rise to both Tint and Ttex (referred to as branched differentiation model), and that Tint may also give rise to Ttex (linear differentiation model)[81,82]. It is likely that these two differentiation models co-exist, and specific immune milieu and level of antigen stimulation within the TME may determine which of the two is more prevalent in any given context. It is also important to emphasise that Texh exist in a continuum of differentiation states rather than as clearly defined subsets, which makes the categorisation of specific phenotypes into pre-defined states challenging.

The functional consequences of ICT in Texh has been an area of substantial debate. Early observations showing that PD-1 blockade reinvigorates Texh led to the hypothesis that this could be an effective strategy to reverse exhaustion. Nonetheless, it is now known this is not the case. T cell exhaustion is driven in part by chromatin and epigenetic changes that are not substantially altered upon PD-1 inhibition[83]. Rather, temporarily blocking PD-1 inhibitory signalling favours the differentiation of Tpex into Tint subsets with increased effector functions, leading to enhanced anti-tumour responses[75,76,84]. However, while reversible checkpoint inhibition has proven to be clinically transformative, long-term absence of these inhibitory signals can lead to a depletion of the Tpex pool and an increase in the proportion of Ttex. Indeed permanent knock-out (KO) of *Pdcd1* (which encodes PD-1) in T cell-based ACT does not lead to substantial improved responses and may compromise the persistence of tumour-targeting T cells[85,86].

1.4.4 Transcriptional regulation during CD8$^+$ T cell exhaustion

The mechanisms governing how different Texh subsets function during anti-tumour responses are controlled by several key transcriptional regulators. At its core lays the balance between two opposing epigenetic programmes: one relating to long-term maintenance, memory and stemness; and a second one involving T cell activation and the acquisition of effector functions[78,87].

Tpex are adapted to sustain prolonged periods of antigen stimulation and maintain a stable cell pool. They achieve this through TFs that modulate the activation of effector-associated gene networks and favour long-term maintenance. Initially, exhaustion starts with the induction of nuclear factor of activated T cells (NFAT) and NFAT2 instigated via TCR signalling. This leads

to the expression of PD-1 and other inhibitory receptors that modulate the level of stimulation and facilitate maintenance of the Tpex pool; as well as upregulation of TOX[66,67]. In turn, TOX shapes the exhaustion epigenetic landscape, stabilising the expression of PD-1 and committing T cells to the exhaustion lineage[88]. Another important factor is forkhead box protein O1 (FOXO1), a pioneer TF that directly regulates other key transcriptional Tpex regulators such as TCF1 and broad complex-tramtrack-bric a brac and Cap'n'collar homology 2 (BACH2)[89]. TCF1, a key marker of the Tpex subset, possess Tpex-stabilising properties through the induction of Eomesodermin and c-MYB, which silence the expression of genes involved with differentiation[90]. Similarly, BACH2 directly inhibits acquisition of Ttex features[91,92]. In addition, other factors that promote survival and maintenance, such as inhibitor of DNA binding 3 (ID3) and B cell lymphoma 2 (BCL-2), are also expressed in Tpex[78].

How the balance between Tpex and more differentiated Texh subsets is maintained during anti-tumour responses in not entirely understood. Nonetheless, it is now known that transition to an effector and eventually a terminally differentiated state involves silencing of the mechanisms preventing the expression of genes associated with these states. For instance, downregulation of TCF1 and BACH2 is a key feature of Tint and Ttex differentiation[90-92]. This releases the activity of factors including activation protein 1 (AP-1) family members such as c-Jun and JunD; as well as other key factors including interferon regulatory factor 4 (IRF4), basic leucine zipper transcription factor (BATF) and B lymphocyte-induced maturation protein-1 (BLIMP-1) [78]. The target genes from these TFs promote effector functions and terminal differentiation, driving the transition from Tpex to other subsets.

1.5 Adoptive T cell therapy

The discovery of the cytotoxic properties of $CD8^+$ T cells during the 1970s opened the doors to the possibility of leveraging their function therapeutically. At a similar time, IL-2 was identified as a key T cell growth factor playing an important role in promoting T cell survival and proliferation. This enabled the isolation, *in vitro* expansion and reinfusion of primary T cells for therapeutic purposes: an approach referred to as T cell-based ACT. For the first time, ACT allowed medicine to directly harness the cytotoxic properties of $CD8^+$ T cells and systematically direct it against cancer, adding a powerful new weapon to the arsenal of anti-cancer therapies. Broadly, there are two classes of T cell-based ACT: tumour infiltrating lymphocyte (TIL) therapy, and lymphocytes with genetically engineered antigen receptors.

1.5.1 TIL therapy

The general principle behind TIL therapy is that of using transplantable tumours as a source of tumour-specific lymphocytes[93]. This process starts with excision of the tumour mass and culture of the resulting fragments in high concentration of IL-2 for promoting T cell survival *ex vivo*. Subsequently, T cells undergo several rounds *in vitro* stimulation and expansion using IL-2, feeder cells, and activating antibodies that crosslink CD3 within the TCR complex. Finally, up to ~10^{11} expanded T cells can be obtained and reinfused into the patient, which can target both primary and metastatic tumour lesions.

By the late 1980s, the first demonstrations of the clinical potential of TIL therapy were observed in a trial using TILs and systemic IL-2 delivery on metastatic melanoma patients, with 60% of the cohort showing regressions[94]. Later trials also showed that the use of lymphodepleting chemotherapy prior to TIL therapy improved the engraftment, expansion and persistence of adoptive T cells[95]. This likely occurs through the clearance of the endogenous lymphocytes, which leads to an increase in the availability of T cell growth factors accessible to the adoptive T cells[96,97]. Nonetheless, despite several examples of powerful responses induced by TIL therapy, the complexity and cost of the process, and the variability in therapeutic outcomes, have made clinical translation difficult. Optimisations in the methods for isolation and expansion of TILs have been occurring ever since the first trials, and the Food and Drug Administration (FDA) approved a TIL therapy (lifileucel, sold under the brand name Amtagvi) for the first time in 2024 for the treatment of unresectable or metastatic melanoma[98].

1.5.2 Genetically engineered antigen receptors

Access to tumour-specific lymphocytes through cancer extirpation is a complex process and is limited only to resectable tumours. Nonetheless, peripheral T cells can be genetically engineered to express antigen receptors recognising tumour antigens of interest.

One approach consists of editing T cells to express a transgenic TCR. This type of therapy, called TCR T cell therapy, enables engineered T cells to target known cancer-associated peptides displayed through MHC I receptors. Historically, identifying suitable TCR sequences to be used therapeutically has been challenging due to the vast array of existing TCR clones and the lack of suitable technologies. Nonetheless, several common cancer-associated peptides had been identified by the early 2000s, and the first evidence of cancer regression in a clinical setting using TCR T cell therapy came in 2006[99].

TCR T cells can theoretically be used to target any intracellular protein through the MHC system. However, a major limitation of TCR T cell therapies is that TCR specificity is

determined not just by the sequence of the peptide presented via an MHC molecule, but also by the structure of the MHC molecule itself. In humans, MHCs are encoded by human leukocyte antigen (HLA) genes, which are among the most polymorphic genes in the genome. Consequently, a given TCR may recognise a peptide and form an immunological synapse when presented by the MHC of one individual, but not when presented from the MHC of a different individual. This phenomenon, known as HLA restriction, increases the diversity of peptides presented by a given population and maximises its likelihood of effectively responding to any potential pathogen, but also restricts the use of TCR T cell therapies to patients with a compatible HLA genotype[46,100]. Despite this challenge, work done over the past 20 years to identify TCRs specific to prevalent HLA alleles and to optimise the process of T cell editing and manufacturing have led to the first approval of a TCR T cell therapy (afamitresgene autoleucel) in 2024 for melanoma-associated antigen 4 (MAGE-A4)-positive advanced synovial sarcoma[101].

An alternative approach, pioneered in the 1980s, involves the use of chimeric antigen receptors (CARs). This type of receptors have an extracellular portion constructed by linking the light and heavy chains from the variable region of an antibody specific to an antigen of interest, referred to as single-chain variable fragment (scFv). The scFv is linked to intracellular domains derived from stimulatory or co-stimulatory signalling receptors through a transmembrane region. Once the scFv recognises an antigen on a target cell, clustering of CAR receptors occurs, emulating clustering of TCR receptors during the immune synapse and leading to downstream activation of stimulatory and co-stimulatory effector proteins[102]. CAR receptors can be designed to target any surface protein of interest regardless of a patient's HLA genotype, making them a more versatile approach than transgenic TCRs. Initial CAR designs ('first-generation' CARs) contained only a CD3ζ intracellular domain (part of the TCR complex). However, the addition of a second intracellular co-stimulatory domain from CD28 or 4-1BB ('second-generation' CARs) greatly improved their efficacy and propelled them into the clinic[102]. Since 2017, there have been several approvals by the regulatory agencies worldwide of CAR T cell therapies targeting either CD19 or B cell maturation antigen (BCMA) for various B cell malignancies, leading CAR T cell therapy to transform the treatment of haematological malignancies (**Fig. I-3** and **Table I-1**)[103,104].

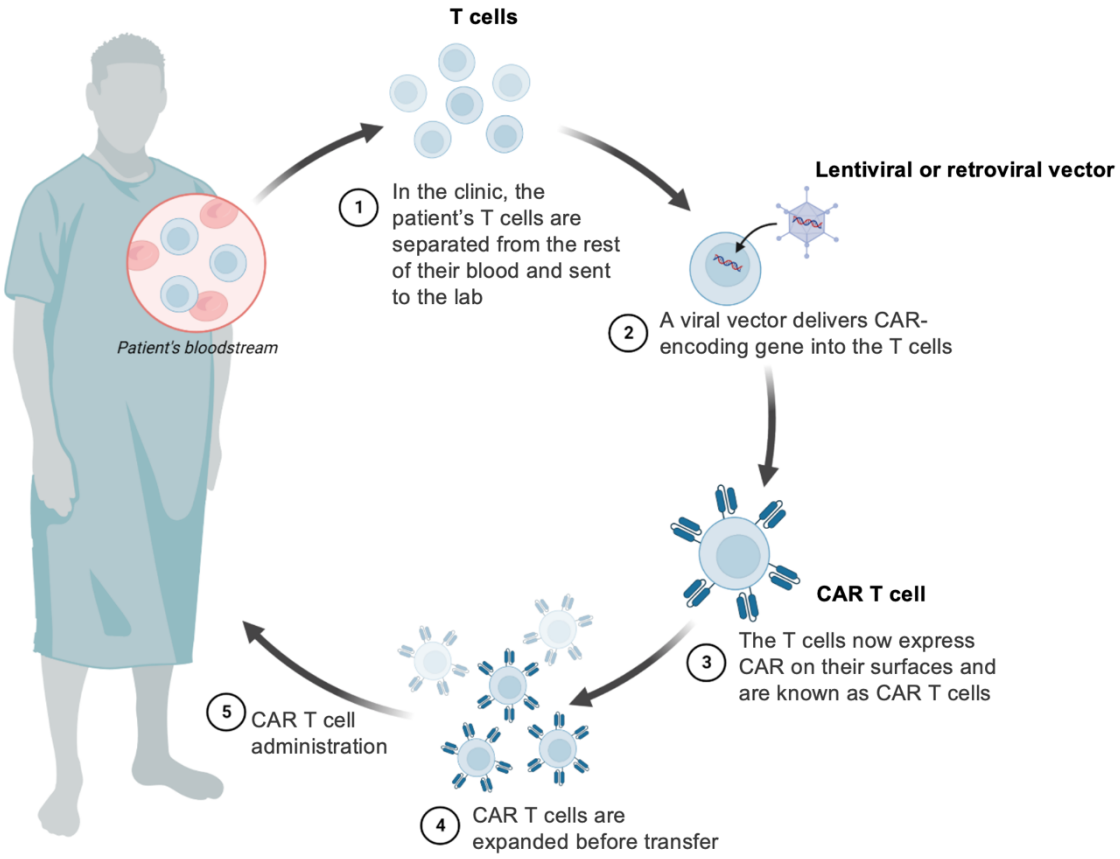

Figure I-3. The autologous CAR T cell therapy cycle. Diagram representing the autologous CAR T cell therapy cycle. First, patient blood gets obtained, from which T cells are isolated. Then, T cells are genetically engineered through the use of a viral vector encoding the CAR receptor to generate CAR T cells. CAR T cells are then expanded, characterised via flow cytometry and administered into the patient.

Table I-1. Summary of approved CAR T cells (US, UK and EU). Information regarding all approved CAR T products in the US, UK and EU territories. BMS, Bristol Myer Squid; J&J, Johnson & Johnson; ALL, acute lymphoblastic leukemia; R/R, refractory or relapsed; DLBCL, diffuse large B cell lymphoma; PMBCL, primary mediastinal B cell lymphoma; FL, follicular lymphoma; MCL, mantle cell lymphoma; MM, multiple myeloma; LV, lentivirus; GR, gamma-retrovirus.

Trade name	Generic Name	Developer	Target	Indication	Vector Type	Costimulatory Domain	Approval year (FDA)
Kymriah	Tisagenlecleucel	Novartis	CD19	ALL, R/R DLBCL	LV	4-1BB	2017
Yescarta	Axicabtagene ciloleucel	Kite (Gilead)	CD19	R/R DLBCL, PMBCL, FL	GR	CD28	2017
Tecartus	Brexucabtagene autoleucel	Kite (Gilead)	CD19	MCL, ALL	GR	CD28	2020
Breyanzi	Lisocabtagene maraleucel	BMS	CD19	R/R LBCL, FL, MCL	LV	4-1BB	2021
Abecma	Idecabtagene vicleucel	BMS / 2seventy bio	BCMA	R/R MM	LV	4-1BB	2021
Carvykti	Ciltacabtagene autoleucel	J&J / Legend Biotech	BCMA	R/R MM	LV	4-1BB	2022
Aucatzyl	Obecabtagene autoleucel	Autolus Therapeutics	CD19	ALL	LV	4-1BB	2024

1.6 Improving T cell persistence in adoptive T cell therapy

Both TIL and genetically engineered cell therapies have shown immense promise in the clinical setting. Nonetheless, limited T cell persistence following adoptive transfer has been a major challenge in both modalities. This is because T cells are exposed to long periods of antigen stimulation within the tumour, which promotes their differentiation into a Ttex state with limited effector functions and a short lifespan. Identifying strategies to extend the survival of adoptive T cells is hence of importance to the field[105].

1.6.1 Optimising T cell culture conditions

Consistent with the impairment of anti-tumour function driven by terminal differentiation, the presence of less differentiated T cell populations within the starting infusion product is correlated with improved expansion and persistence of adoptive cells in pre-clinical and clinical settings[75,79,106]. In light of this, several approaches have been employed to improve the starting phenotype of T cells prior to ACT.

One example is the use of biological or pharmacological interventions to 'uncouple' the *ex vivo* culture and expansion of lymphocytes (as part of the ACT treatment cycle) from effector and terminal differentiation. This can be particularly important in the context of TIL therapy, since the starting infusion material is derived from activated and antigen-experienced cells. For instance, using IL-7 and IL-15 during culture, as opposed to IL-2, results in T cells with a lower degree of differentiation[107]. Similarly, inhibitors of (AKT) and bromodomain inhibitors (disrupting the recognition of certain epigenetic marks by bromodomain-containing TFs) have been shown to restrain T cell differentiation without significantly compromising T cell expansion[108-110].

Another simple and cost-effective approach is that of reducing the expansion time of T cells prior to infusion. This may result in a lower number of lymphocytes in the infusion product, but the retention of a less differentiated phenotype results in an enhanced anti-tumour response[111,112]. Further, this can also reduce the treatment timelines for patients and, therefore, the cost of manufacturing. Nonetheless, despite the benefits and cost-effectiveness associated with optimising culture conditions, these approaches only yield transient improvements and do not address the acquisition of a Ttex state *in vivo*.

1.6.2 Controlling the level of T cell stimulation

A different strategy involves pharmacological interventions to modulate the level of T cell activation *after* the cells have been adoptively transferred. An example of one such approach is the use of a drug-regulatable CAR receptor, which can be stabilised (ON) or destabilised (OFF) *in vivo* via the administration of a drug. The use of an ON/OFF regimen was shown to improve the function of the CAR T cells by preventing prolonged, uninterrupted periods of stimulation and providing 'rest' intervals during the anti-tumour response[113]. The same group achieved similar results using an intermittent regimen of the kinase inhibitor dasatinib, known to disrupt T cell stimulation signalling.

As opposed to controlling the time of T cell stimulation, modulating the magnitude of the signal can also bear beneficial effects on the function of the T cells. For instance, multiple studies have shown that decreasing the affinity of the antigen receptor towards a specific antigen, or decreasing the number of ITAM motifs in the intracellular region of a CAR, can reduce the degree of terminal differentiation and have positive implications in the anti-tumour response[114-116].

Notably, while these approaches are promising, their clinical translation can be difficult. Strategies relying on the use of exogenous drugs for modulating T cell function face challenges including identifying the right regimen of drug administration, any potential side effects of the exogenous molecules, and intrinsic differences in T cell differentiation states among patients. On the other hand, designing antigen receptors with optimal affinity requires a preceding understanding of what constitutes 'optimal' in each context. Indeed, it is likely that this depends on multiple factors such as the level of antigen expression in target cells and the level of CAR expression in the T cells. For these reasons, finding the right antigen affinity of a transgenic receptor can be a time-consuming process, which would need to be repeated for each specific antigen.

1.6.3 Transcriptional regulators as targets for extending T cell persistence

As previously described, T cell differentiation states play an important role in dictating their ability to engage effector functions in scenarios of chronic stimulation. Leveraging the transcriptional regulators that control these states, either by disrupting or activating key adaptor proteins, could be an attractive strategy for improving the persistence and anti-tumour activity of T cells. Importantly, such approaches could be widely applied across different cell therapy modalities and cancer targets.

Critically, the suppression of effector functions associated with Ttex differentiation is a key mechanism of T cell deletion and therapeutic failure in ACT. To address this, a number of groups have attempted the overexpression (OE) of different TFs with the aim of restoring high levels of T cell function. These include factors belonging to the AP-1 family, which drive the expression of genes involved in T cell proliferation and cytokine production. For instance, OE of the AP-1 members c-Jun or basic leucine zipper ATF-like transcription factor (BATF) have independently been shown to enhance CAR T cell function in various pre-clinical tumour models[117,118].

Similarly, other attempts have involved the use of TFs involved in mediating T cell survival and proliferation. This was the case in a study that overexpressed a constitutively active version of signal transducer and activator of transcription 5 (STAT5-CA) – the principal mediator of transcriptional changes resulting from IL-2 signalling – which resulted in significant enhancement of the proliferative ability and engraftment of anti-tumour T cells by rewiring the terminal T cell differentiation state[119]. A related approach includes enforcing the expression of proteins bearing naturally occurring T cell-associated oncogenic mutations, such as the fusion of caspase recruitment domain-containing protein 11 and phosphoinositide-3-kinase regulatory subunit 3 (CARD11-PIK3R3), which resulted in improved persistence and increased AP-1 signalling[120].

Comparable results can also be obtained by disrupting the activity of negative regulators involved in antagonising stimulatory signals, which can favour the maintenance of T cell effector functions. For example, NR4A TFs have been shown to inhibit the function of AP-1 factors and promoting the expression of inhibitory receptors. Consequently, triple KO of three NR4A TFs can result in improved persistence and anti-tumour responses in pre-clinical models[121]. Similarly, disruption of negative regulators of T cell effector differentiation such as REGNASE-1 or suppressor of cytokine signalling 1 (SOCS1) can increase the number of T cells acquiring effector states and improve therapeutic outcomes in several pre-clinical ACT tumour models[122-124].

The generalisability of these approaches together with the positive data emerging from numerous pre-clinical studies has led to its widespread adoption among biotech companies developing the next generation of T cell therapies. Nonetheless, recently they have also raised concerns over their potential to exacerbate immune-based toxicities and even promote oncogenic T cell states among adoptive T cells. This has most notably been exemplified via a

warning issued by the FDA over potential cases of T cell-derived malignancies following ACT[125]. While the number of cases remains low, the clinical impact of strategies relying on actively driving T cell activation is still unclear. Indeed, the biological mechanisms exploited in some of the above-mentioned studies involve oncogenic-associated genetic edits. For instance, aberrant STAT5 activation, the CARD11-PIK3R3 fusion and disruption of SOCS1 have all been described in the context of cellular malignancy[120,126,127]. Therefore, the clinical risks and benefits of these approaches will need to be carefully evaluated in the coming years.

1.6.4 Leveraging memory transcription factors for preventing terminal differentiation

An alternative approach to actively promoting the acquisition of effector characteristics is instead that of delaying or preventing terminal differentiation. Memory factors are attractive candidates for this strategy, because they are associated with differentiation and maintenance of memory and Tpex states and are generally known to oppose T cell differentiation[56].

Recently, two groups independently showed that OE of the memory-associated TF FOXO1 limits the degree of terminal differentiation in a pre-clinical model of tumour-targeting CAR T cells, thereby enhancing their anti-tumour immunity[128,129]. This strategy is promising because memory factors likely carry a lower risk of causing T cell hyperactivation, resulting in a potentially safer alternative to other previously used TFs. Furthermore, it is likely widely applicable to different T cell therapy modalities, regardless of the specific CAR or TCR receptor used.

However, beyond FOXO1, efforts to harness memory factors remain limited. The FOXO1 studies from Weber's and Darcy's laboratories, published in 2024, were the first to demonstrate the effective use of memory factors in enhancing CAR T cell function. Some prior reports showed modest improvements using the Tpex-associated factor TCF1, but attempts at replicating these findings have yielded mixed results[128,130]. Nonetheless, given the growing body of evidence highlighting the importance of preventing Ttex differentiation among tumour-specific T cells, this is an area that warrants further investigation. In this context, BACH2 is a transcription factor of particular significance, since previous studies (including our own) have highlighted its role maintenance of both memory $CD8^+$ T cells and $CD8^+$ Tpex during acute and chronic viral infections, respectively[92,131].

1.7 BACH2

The dynamics of cell differentiation and the balance between different cellular subtypes is dictated by the function of transcriptional regulators, responsible for activating and suppressing different genetic programmes. Over the past decade, BACH2 has emerged as a key TF with important roles in different cell types, particularly those of the innate and lymphoid immune lineages.

1.7.1 The basic leucine zipper TF family

BACH2 is a 92 kDa transcriptional repressor that belongs to the basic leucine zipper (bZIP) family of TFs, a large evolutionarily conserved group of transcriptional regulators implicated in a wide range of biological processes. bZIP TFs are characterised by two functional domains: a conserved basic DNA-binding region, and a less conserved leucine zipper (ZIP) domain. The ZIP domain consists of a series of leucine residues forming an α-helical structure that allows bZIP proteins to dimerise (either as homodimers or heterodimers), which is essential for their function as transcription factors[132]. As dimers, bZIP TFs bind to DNA sequences containing one of two core palindromic motifs: 12-O-Tetradecanoylphorbol-13-acetate (TPA) response element (TRE, 5'-TGASTCA-3'), or cAMP response element (CRE, 5'- TGACGTCA-3')[132].

The dimeric nature of these factors contributes to their wide functional diversity. Different bZIP complexes with different DNA specificities can assemble based on the relative expression levels of individual members. This also enables individual non-functional monomers to form either activator or repressor complexes based on their specific partner. In humans, there are 53 bZIP members belonging to 21 distinct subfamilies, including the AP-1, the MAF and BACH TFs[132].

1.7.2 The BACH subfamily

BACH1 and BACH2 are the only two members of the BACH subfamily of TFs. Within immune subsets, BACH proteins display mutually exclusive patterns of expression: BACH1 is predominantly expressed in innate subsets, while BACH2 is primarily restricted to the lymphoid lineage[133]. BACH factors are the only known bZIP members containing bric-a-brac–tramtrack–broad complex (BTB) domains, which enables protein-protein interactions and is involved in the recruitment of transcriptional co-repressors. In addition, both BACH members possess cysteine-proline motifs (six in BACH1, five in BACH2). These regions enable binding to haem and enable the transcriptional activity of BACH proteins to be tightly regulated by haem levels[133].

The earliest known BACH-related gene ancestor is found in *Ciona intestinalis*, indicating its emergence predates the development of the adaptive immune system[134]. A second BACH-related gene developed in jawed vertebrates, likely as a result of gene duplication, coinciding with the appearance of adaptive immunity[135]. Notably, the evolutionary timeline of the BACH protein pair – spanning both before and after adaptive immunity's emergence – mimics the mutually exclusive expression of BACH1 and BACH2 in innate and lymphoid cells respectively[133].

Functionally, BACH1 and BACH2 are well-established transcriptional repressors. For instance, in murine macrophages, MAFK (bZIP factor belonging to the MAF subfamily) interacts with NRF2 to activate haem oxygenase 1 (HO1, encoded by *Hmox1*)[136]. Under high levels of haem, haem binding to BACH1 triggers its nuclear export and degradation. Conversely, at low haem concentrations, BACH1 binds MAFK and blocks NRF2-driven transcriptional activity by competing for the same genetic loci as NRF2-MAFK.

A similar mechanism has been described for BACH2 in lymphoid cells. By associating with AP-1 factors such as BATF, BACH2 can bind at the same loci as other AP-1 dimers and prevent their transcriptional activity (**Fig. I-4**)[131,137,138]. Like BACH1, the activity of BACH2 is also tightly regulated by its total availability. In T cells, BACH2 is differentially expressed among T cell subsets (see later), and phosphorylation at its S520 amino acid residue via TCR-mediated signalling leads to its nuclear export and degradation[131].

Beyond 'passive' inhibition of transcriptional activity through competition for target loci, the BTB domain characteristic of BACH members can also interact with co-repressors. This is exemplified by the ability of BACH2 to recruit histone deacetylase 3 (HDAC3), which in turn mediates epigenetic modifications resulting in transcriptional silencing of target genes[139].

1.7.3 BACH2 in T cell biology

BACH2 has been found to be expressed in a number of lymphocyte subsets, including B cells, T cells and NK cells[133]. Initial studies investigating the role of BACH2 in B cell class switching led to the development of a *Bach2*$^{-/-}$ mouse[140]. The resulting animals displayed a spontaneous inflammatory disorder that resulted in a median lifespan of 4.5-6 months and were characterised by immune infiltration of eosinophils, macrophages and conventional CD4^{+} T cells in lung and gastrointestinal tissues, as well as elevated levels of serum auto-antibodies[91]. To elucidate the underlying cause of this inflammatory phenotype, a series of elegant experiments were conducted using *Rag1*-deficient animals (lacking B and T cells) reconstituted

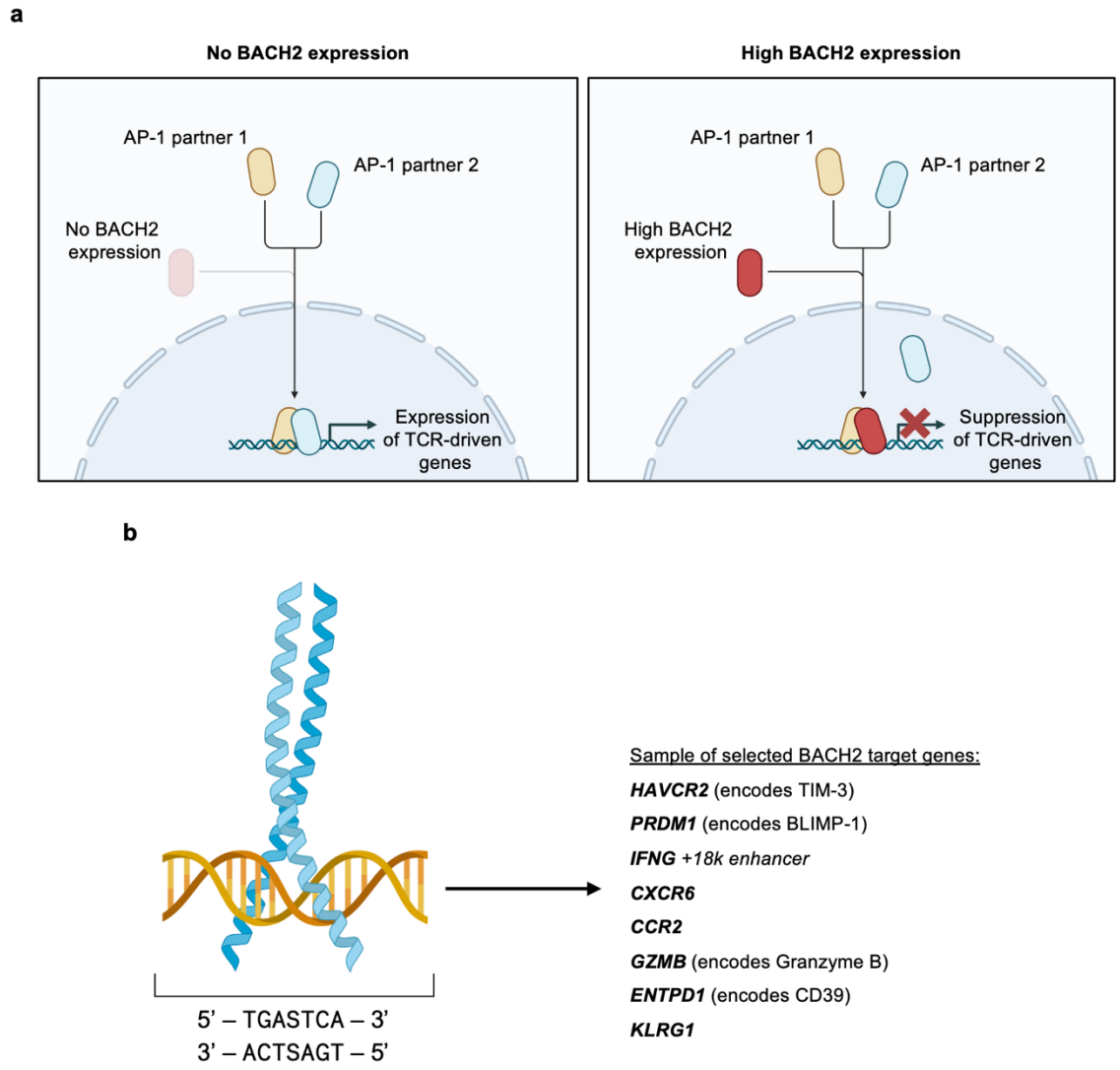

Figure I-4. Mechanism of action of BACH2. **a**, Diagram representing the mechanism of action of BACH2. In the absence of BACH2, AP-1 transcription factors are able to partner and activate the expression of genes associated with effector and terminal differentiation upon TCR stimulation (left). In contrast, when BACH2 is expressed at high levels, it disrupts AP-1-mediated gene expression by dimerising with other AP-1 factors and occupying AP-1 binding sites, therefore active as a passive repressor of expression (right). **b**, BACH2 and other AP-1 factors recognise the TRE DNA palindromic motif (5'-TGASTCA-3'). The basic region within the bZIP domain of each partner in a dimer bind a similar '5'-TGAS-3'' sequence.

with a mix of WT and *Bach2*$^{-/-}$ bone marrow-derived cells. A near-complete absence of thymic or splenic Tregs only in the *Bach2*$^{-/-}$ cell compartment was observed, suggesting an important cell-intrinsic role for BACH2 in both thymic and peripheral Treg development as the underlying cause of the observed inflammatory phenotype. This was further demonstrated through the recovery of a non-inflamed phenotype through the transfer of WT bone marrow cells containing CD4$^+$ Tregs[91].

Beyond Treg development, research performed over the past decade has shown that BACH2 also plays a crucial role in both CD4$^+$ and CD8$^+$ conventional T cell subsets. Functionally, through the inhibition of AP-1 signalling, BACH2 restrains activation of effector-associated genes.

In CD4$^+$ T cells, BACH2 regulates the expression of helper T cell cytokines such as IFN-γ, IL-5, IL-4, IL-13 or IL-17A. For instance, following *in vitro* stimulation under peripheral Treg-inducing conditions, naïve CD4$^+$ T cells lacking *Bach2* exhibit aberrant activation of gene expression programmes typically associated with helper T cell differentiation[91,141,142].

In CD8$^+$ T cells, restraint of TCR-driven effector programmes plays a crucial role in the formation of immunological memory. As previously discussed, the process of T cell differentiation from naïve to more effector subsets is tightly regulated and dependent on antigen stimulation. The progressive differentiation model proposes that, over time, maintained TCR signalling induces changes in the expression of genes that mediate the differentiation process and acquisition of effector functions, many of which are driven by AP-1 factors. BACH2 regulates this process by acting as a negative regulator of differentiation and TCR-driven signalling[92,131,141].

Mechanistically, *Bach2* mRNA levels are highest in naïve CD8$^+$ T cells, intermediate in memory subsets, and are nearly absent in fully differentiated effector cells. Through this graded expression pattern, BACH2 modulates TCR signalling across multiple T cell subsets differently, shaping the transcriptional response to antigen stimulation accordingly[131,133]. This regulatory mechanism helps preserve the lymphoid tissue homing and long-lived properties in the case of memory T cells, and the 'self-renewal' and functional properties in that of Tpex. Consequently, the lack of *Bach2* in T cells responding to viral and bacterial infections leads to compromised acquisition of a central memory phenotype and caused an elevated rate of apoptosis and terminal differentiation compared to WT T cells[131]. This is consistent with an observed downregulation of anti-apoptotic factors in cells lacking *Bach2*, including BCL-2,

BCL-X_L and myeloid cell leukaemia 1 (MCL1). As a result, *Bach2*$^{-/-}$ CD8$^+$ T cells displayed a diminished capacity for controlling bacterial titres using a model antigen-specific *in vivo* model of *L. monocytogenes* infection, and a decreased level of clonal expansion in viral infection models[131].

Conversely, overexpression of BACH2 has been shown to promote the formation of memory and Tpex CD8$^+$ T cells in various contexts, while abolishing Ttex differentiation[92,131]. This was evident from higher levels of expression of markers such as CD62L, in the case of acute infections, or TCF-1 and Slamf6, in the case of chronic stimulation models. Similarly, the levels of effector and Ttex markers, such as CD44, KLRG1 or TIM-3, were significantly downregulated in these same models, and lower levels of apoptosis were measured. BACH2-overexpressing CD8$^+$ T cells under chronic stimulation conditions also showed transcriptomic and epigenetic profiles resembling those observed in Tpex subsets.

1.8 Leveraging BACH2 for improving T cell therapy in solid tumours

The observations implicating BACH2 in the formation of Tpex and its role in preventing terminal differentiation - combined with growing appreciation over the past decade that poor T cell persistence and a tendency toward Ttex differentiation are major limitations in ACT - point to a compelling hypothesis: could BACH2 overexpression improve the persistence and functionality of tumour-specific CD8$^+$ T cells? By inhibiting terminal differentiation and maintaining the defining features of the Tpex subset, BACH2-mediated transcriptional programming may enhance therapeutic efficacy and counteract the detrimental effects associated with terminal differentiation. The present work focuses on examining the hypothesis that ectopic expression of BACH2 can be leveraged to improve the performance of T cells in the context of ACT.

2. Material and methods

2.1 Mice

2.1.1 Experimental mice

OT-I and *Ptprc*^{a} (CD45.1) congenic mice were sourced from the Jackson Laboratory. Tandem red fluorescent protein (RFP) *Bach2* (*Bach2*$^{tdRFP/+}$) reporter mice were generated as previously described and supplied by Tomohiro Kurosaki (Osaka University)[143]. 3xFLAG-tagged *Bach2* mice (BACH2^{FLAG} mice) were generated as previously described and supplied by Richard A. Flavell (Yale School of Medicine)[144]. Wild-type (WT) C57BL/6 mice were acquired from Charles River Laboratories (Wilmington, MA, USA) and acclimatised for one week prior to any experiment. All experiments utilised 8–12-week-old mice, matched within groups for age and sex. Animals were housed within the Gurdon Institute Facility at the University of Cambridge's Biomedical Services (UBS). All procedures adhered to UK Home Office regulations under the project license PP2448972 and received approval from the University of Cambridge Animal Welfare and Ethics Review Board.

2.1.2 Mice genotyping

Mice were genotyped using Transnetyx® Inc. (Memphis, TN, USA) by collecting ear biopsies from mice, placing them in 96-well plates and posting them. Genotype results were confirmed 72 hours following receipt of biopsies.

2.2 Cell lines and cell culture reagents

2.2.1 Adherent cell lines

The murine melanoma cell line B16-F10 was obtained from the American Type Culture Collection (ATCC). The murine melanoma cell line B78Ch-ovalbumin-mCherry (B16-OVA) was generously provided by Prof M. Krummel (University of California, San Francisco). The murine colorectal adenocarcinoma cell line MC38-ovalbumin (MC38-OVA) was purchased from Vitro Biotech. Platinum-E retroviral packaging cell line (Plat-E) was purchased (Cell Biolabs). All cell lines were maintained in Dulbecco's Modified Eagle Medium (DMEM, Gibco) supplemented with 10% heat-inactivated foetal bovine serum (FBS) (Sigma), 100 U/ml streptomycin and penicillin antibiotics (Gibco), 2 mM glutamine (Gibco), 0.1 mM non-essential amino acids (Gibco) and 1 mM sodium pyruvate (Gibco), termed DMEM complete medium (DCM). Cells were passaged by dissociating them using TrypLE dissociation reagent

(Gibco) following the manufacturer's instructions, reseeding them in tissue culture-treated T175 flasks at an appropriate dilution using DCM and cultured at 37 ºC, 5% CO_2.

2.2.2 Primary cells

Murine-derived primary splenocytes and T cells were cultured in Roswell Park Memorial Institute (RPMI) medium supplemented with 10% heat-inactivated FBS, 100 U/ml streptomycin and penicillin antibiotics (Gibco), 2 mM glutamine (Gibco), 0.1 mM non-essential amino acids (Gibco) and 1 mM sodium pyruvate (Gibco), termed RPMI complete medium (RCM). Murine-specific anti-CD3 (clone 145-2C11, BioLegend) and anti-CD28 (clone 37.51, BioLegend) were used for *in vitro* stimulation and co-stimulation of primary T cells. Human recombinant interleukin (IL)-2 (rhIL-2, PeproTech) was aliquoted and stored at –80 ºC prior to use. Cells were either used directly in experiments and analyses or cultured at 37 ºC, 5% CO_2.

2.3 Tissue processing

2.3.1 Spleens and lymph nodes

Following sacrifice of experimental mice, spleens and tumour-draining lymph nodes were carefully dissected and transported into the laboratory in ice-cold phosphate buffered saline (PBS). The tissues were placed in 40 µm cell strainers (Falcon), mechanically dissociated using sterile plastic 5 ml syringe plungers and washed with PBS. Erythrocytes were lysed using ACK Lysing Buffer (Gibco) at room temperature for 3 minutes (splenocytes only). Samples were filtered through a 40 µm cell strainer, washed twice in PBS and resuspended in RCM.

2.3.2 Tumours

Following sacrifice of experimental mice, tumours were carefully dissected and transported into the laboratory in ice-cold PBS. The tumours were weighed and placed in 7 ml Bijou containers (Thermo Scientific Sterilin) containing 2 ml DCM with 20 µg/ml DNase I (Roche) and 1 mg/ml collagenase (Sigma). Tumour samples were finely cut using scissors and incubated at 37 ºC for 30 minutes for digestion. Following digestion, tumour samples were mechanically dissociated using sterile plastic 5 ml syringe plungers and washed twice with PBS. TILs were enriched using Lympholite®-M solution (Cedarlane) following the manufacturer's instructions. Samples were washed twice in PBS and resuspended in RCM prior to analysis. For evaluating cytokine production, single-cell suspensions were resuspended in RCM containing either 20 ng/ml phorbol myristate acetate (PMA, Sigma) and 1 µg/ml

ionomycin (ION, Sigma), or 5 µg/ml anti-CD3; together with 5 µg/ml monensin (Sigma) and 5 µg/ml brefeldin A (Sigma).

2.4 Retroviral T cell transduction

2.4.1 Construction of retroviral vector plasmids

Murine stem cell virus (MSCV)-based backbone vectors, consisting of DNA plasmids containing a 5' long terminal repeat (LTR) sequence, an MSCV Ψ+ RNA packaging signal, a 3' LTR sequence, an origin of replication and an ampicillin-resistance cassette, were used for all retroviral transductions. Coding sequences (CDSs) encoding the transgenes of interest were introduced between the 5' and 3' LTR regions, either by Gibson assembly or by commissioning the synthesis to an external supplier (VectorBuilder).

Vectors used for the ectopic expression of BACH2 and of the constitutively active triple alanine FOXO1 mutein ($FOXO1^{AAA}$) contained a single open reading frame (ORF) with the CDS of the transduction reporter Thy1.1 followed by a self-cleavage T2A motif and the CDS of murine BACH2 (CCDS51135.1) or $FOXO1^{AAA}$, both tagged with a 3xFLAG tag at its corresponding N-termini. The three alanine mutations in $FOXO1^{AAA}$ correspond to T24A, S253A and S316A in the CDS of murine WT FOXO1 (CCDS17343.1)[145]. To achieve different doses of BACH2 and $FOXO1^{AAA}$, specific STOP-translational readthrough motifs (TRMs)[146] were placed between the Thy1.1 and T2A sequences. Vectors used as 'empty vector' (EV) control contains an internal ribosome entry site (IRES) sequence followed by an ORF encoding Thy1.1.

2.4.2 Production of retroviral particles

Plat-E cells were used to produce retroviral particles following the manufacturer's instructions from Mirus Bio. Briefly, ~1.1 x 10^7 Plat-E cells were seeded in DCM in a T175 flask (Thermo Fisher Scientific) ~24 hours prior to transfection to ensure a confluency of ~70% at the time of transfection. On the day of transfection, 6.3 µg pCL-ECO retroviral packaging plasmid (Addgene plasmid #12371) and 28.5 µg retroviral packaging plasmid of interest were mixed in 3.2 ml serum-free OptiMEM medium (Gibco) containing 95 µl TransIT-293 transfection reagent (Mirus Bio). The resulting solution was incubated for 30 minutes at room temperature and added dropwise into Plat-E cells. Transfected Plat-E cells were incubated at 37 ºC, 5% CO_2. The following day, Plat-E cell media was discarded, and 32 ml DCM were carefully added. 48 hours post-transfection, Plat-E cell supernatant containing retrovirus was harvested

and stored at –80. DCM was then replenished and newly harvested 72 hours post-transfection for storage at –80 ºC.

2.4.3 Murine T cell transduction

Murine splenocytes from OT-I mice were isolated as previously described and incubated in RCM supplemented with 100 U/ml rhIL-2, 10 µg/ml anti-CD3 and 10 µg/ml anti-CD28 for at 2 x 10^6 cells/ml, 37 ºC, 5% CO_2 during 24 hours for inducing T cell activation and expansion. The following day, virus-containing supernatant (produced as previously described) was thawed and supplemented with 100 U/ml rhIL-2 and 8 µg/ml polybrene (Merck) and used for resuspending activated T cells at 1 x 10^6 cells/ml. Cells were plated in non-tissue culture-treated plates, span down at 2,000 g, 32 ºC for 2 hours and incubated a further 4 hours at 37 ºC, 5% CO_2. Following incubation, cells were resuspended in RCM supplemented with 100 U/ml rhIL-2 at 1 x 10^6 cells/ml and incubated at 37 ºC, 5% CO_2 for at least 24 hours prior to any experiment or analysis to enable adequate levels of transgene expression.

2.5 Flow cytometry and cell sorting

Single-cell suspensions were washed twice in PBS and stained with Fixable Viability Dye eFluor 780 (Thermo Fisher Scientific) for 30 minutes protected from light at 4 ºC. Cells were washed twice in fluorescence-activated cell sorting (FACS) buffer (PBS, 0.5M ethylenediaminetetraacetic acid (EDTA), 2% FBS) and blocked with anti-mouse CD16/32 Fc block (BioXCell, clone 2.4G2) for 30 minutes protected from light at 4 ºC. For surface staining, a surface staining master mix containing all relevant antibodies at appropriate dilutions was prepared in FACS buffer with 10% Brilliant Stain Buffer Plus (BD Biosciences). Cells were washed twice in FACS buffer and incubated with the surface staining master mix for 30 minutes protected from light at 4 ºC. For intracellular staining, an intracellular staining master mix containing all relevant antibodies at appropriate dilutions was prepared in permeabilisation buffer with 10% Brilliant Stain Buffer Plus using either eBiosciences Foxp3/Transcription Factor Staining Buffer Kit (Invitrogen) for staining transcription factors, or BD Cytofix/Cytoperm Fixation/Permeabilisation Kit (BD Biosciences) for staining cytokines. Cells were washed twice in PBS and fixed using fixing solution from the corresponding kit for 20 minutes protected from light at room temperature. Cells were then washed twice in the corresponding permeabilisation buffer and incubated with the intracellular staining master mix overnight protected from light at 4 ºC. Following staining, cells were washed twice with FACS buffer and resuspended in FACS buffer with 123count eBeads (Invitrogen) for absolute cell

counting. Stained samples were analysed using a 5-laser Cytek Aurora cytometer and data analysed using FlowJo v10 (Tree Star Inc.). Uniform Manifold Approximation and Projection (UMAP) visualisations were performed using the CyTOF workflow with a cofactor of 150 and 0-to-1 scaling[147].

For cell sorting, cells were stained using surface staining as previously described. Cells were sorted into RCM supplemented with 50% FBS. Cell sorting was performed using MoFlo Astrios (Beckman Coulter) or BD Aria cell sorters.

2.6 Adoptive T cell transfers

B16-OVA or MC38-OVA cells passaged as previously described were harvested, counted and resuspended at a concentration of 1.25 x 10^6 cells/ml (B16-OVA) or 3 x 10^6 cells/ml (MC38-OVA) in DMEM. WT C57BL/6 mice were anaesthetised by inhalation of 2% isoflurane and subcutaneously injected with 100 µl of the cell line suspension (1.25 x 10^5 cells/animal for B16-OVA or 3 x 10^5 cells/animal for MC38-OVA) into the flank and monitored for tumour growth during 12-14 days prior to any additional experimental procedures. Tumour-bearing mice were pre-selected and randomised into experimental groups before receiving 2.5 Gy (MC38-OVA-bearing mice) or 3.5 Gy (B16-OVA-bearing mice) total body X-ray irradiation. Later the same day or the following day, T cells derived from an OT-I spleen (OT-I T cells) transduced as previously described and rested for 48h in RCM supplemented with 100 U/ml IL-2 were harvested, counted and resuspended at 5 x 10^6 cells/ml in Hanks' balanced salt solution (HBSS, Gibco), before being intravenously injected using 100 µl/animal. Following administration of transduced OT-I T cells, tumour growth was monitored every 3-4 days using electronic callipers (tumour area and volume were calculated as length x width and length x width^2, respectively). For analysis of tumour-infiltrating cells, tumours were dissected and processed 12-21 days after adoptive T cell transfer as previously described.

2.7 Assessment of endogenous *Bach2* expression

Bach2$^{tdRFP/+}$ reporter mice received subcutaneous injection of B16-F10 cells as previously described using B16-F10 cells (1.25 x 10^5 cells/animal). For analysis of lymphocytes in the spleen, lymph nodes, and tumour, tissues were dissected and processed 16 days after tumour inoculation as previously described. Staining and cell acquisition via flow cytometry was performed as previously described, avoiding fixatives or permeabilisation to retain intracellular RFP signal.

2.8 *In vitro* chronic stimulation assay

2.8.1 Anti-CD3 plate coating

To produce an anti-CD3-coated plate, murine-specific anti-CD3 (clone 145-2C11, BioLegend) was diluted at 1 μg/ml in PBS, and 100 μl/well of the suspension were transferred to a flat-bottom tissue culture-treated 96-well plate. The plate was incubated at 37 ºC for >1 hour. Immediately before seeding the cells, the anti-CD3 solution was removed from the plate, and wells were washed twice with PBS.

2.8.2 In vitro stimulation

Murine OT-I splenocytes were isolated and transduced as previously described. The day following transduction, cells were harvested and resuspended in RCM supplemented with 100 U/ml rhIL-2 at 1 x 10^6 cells/ml. The cells were then seeded into the anti-CD3-coated plate (chronic stimulation condition) or a non-coated plate (acute stimulation condition) at 200 μl/well and incubated at 37 ºC, 5% CO_2 for 48 hours. Following the 48-hour incubation, cells were harvested and resuspended again in rhIL-2-supplemented RCM and seeded in a new anti-CD3-coated plate (chronic stimulation condition) or a non-coated plate (acute stimulation condition) for an additional 48 hours. For analysis of cytokine polyfunctionality following chronic or acute stimulation, cells were harvested, resuspended in RCM supplemented with rhIL-2, 5 μg/ml brefeldin-A and 5 μg/ml monensin and seeded into an anti-CD3-coated plate for 4 hours. Cells were then transferred to a new plate and stained for flow cytometry analysis or cell sorting as previously described.

2.9 Proteomics analysis

2.9.1 Proteomics sample preparation

$CD8^+$ T cells were transduced and subjected to chronic stimulation as previously described. Sorted cells were lysed in 80 μL of buffer containing 5% SDS, 10 mM TCEP, and 50 mM TEAB, followed by heating at 100 °C for 5 minutes and sonication with a BioRuptor (15 cycles of 30 s on/30 s off). The lysates were then treated with benzonase for 15 minutes at 37 °C, and protein concentration was determined using the EZQ Protein Quantitation Kit (Thermo Fisher Scientific) according to the manufacturer's instructions. Proteins were alkylated by adding iodoacetamide to a final concentration of 20 mM and incubating for 1 hour at room temperature in the dark. Samples were then loaded onto S-Trap mini columns (ProtiFi) following the manufacturer's guidelines, and proteins were digested with trypsin at a 20:1 protein-to-enzyme

ratio. Digestion was carried out at 47 °C for 2 hours. Resulting peptides were eluted from the columns, dried, and resuspended in 1% formic acid.

2.9.2 Mass spectrometry

Peptide samples were analysed using single-shot Data Independent Acquisition (DIA). For each run, 200 ng of peptide material was injected onto a C18 reverse-phase chromatography system (Vanquish, Thermo Scientific) and ionised by electrospray into an Astral Orbitrap mass spectrometer (Thermo Fisher Scientific). Chromatographic separation was performed using buffer A (0.1% formic acid) and buffer B (80% acetonitrile, 0.1% formic acid) under a gradient optimised for 30 samples per day. Peptides were resolved on an Aurora Ultimate column (IonOpticks), and data were collected in DIA mode.

Each scan cycle included a full MS scan covering an m/z range of 380–980 with a resolution of 240,000, a custom automatic gain control (AGC) target of 500%, and a maximum injection time (IT) of 3 ms. This was followed by DIA MS/MS scans using isolation windows of 2 Th without overlap, spanning an m/z range of 150–2000. DIA spectra were acquired with an AGC target of 500% and a maximum IT of 3 ms, with normalised collision energy set to 25%. MS data were collected in profile mode, while DIA MS/MS events were recorded in centroid mode.

2.9.3 Proteomics data analysis

Raw mass spectrometry data were processed with Spectronaut (Biognosys, v19). Searches were performed against the mouse SwissProt/TrEMBL database (November 2023 release) using the directDIA workflow, with a 1% false discovery rate (FDR). Variable modifications included protein N-terminal acetylation and methionine oxidation, while carbamidomethylation of cysteine residues was specified as a fixed modification. Protein copy numbers were estimated using Perseus software following the approach described by Tyanova *et al*. and normalised to total protein mass per cell[148].

2.10 RNA sequencing and analysis

2.10.1 RNA sequencing

Intratumoral transduced OT-I T cells from Slamf6^{+} and Slamf6^{-} compartments of B16-OVA-bearing mice (CD45.1^{+} Thy1.1^{+} Slamf6$^{+/-}$) following an adoptive T cell transfer experiment, or chronically stimulated transduced OT-I T cells (CD45.1^{+} Thy1.1^{+}) following an *in vitro* chronic stimulation experiment, were sorted as previously described. All samples were

resuspended in 40 µl RNAlater Stabilization Solution (ThermoFisher), left at 4 ºC overnight and stored at -80 ºC until use. Total RNA was extracted using the RNeasy Plus Mini kit (QIAGEN) as per manufacturer's instructions, and further downstream processing was outsourced to an external service provider (Novogene). In brief, the extracted RNA was used for complementary DNA (cDNA) library preparation using the SMARTer Universal Low Input RNA Kit (Takara). The quality and concentration of the resulting libraries was assessed, and high-quality samples of sufficient concentration were selected and sequenced using an Illumina NovaSeq 6000 instrument.

2.10.2 Processing and analysis of RNA sequencing data

The quality of the FASTQ files resulting from the RNA-seq workflow were checked using FastQC, and the reads were aligned to the GRCm38 *Mus musculus* genome assembly using the Spliced Transcripts Alignment to a Reference (STAR) RNA-seq read mapper. Differential expression analysis was performed using DESeq2 (v1.42.0) in R (4.3.2)[149]. Principal component analysis (PCA) was performed using variance stabilising transformed counts generated via DESeq2. Heatmaps of gene expression data were generated using the R package pheatmap (v1.0.12). Gene set enrichment analysis (GSEA) was performed using the R package fgsea (v1.28.0), using 10,000 permutations for statistical analysis. Additional analyses and visualisations were performed in R.

2.11 ATAC-seq sequencing and analysis

2.11.1 ATAC sequencing

Genome-wide assay for transposase-accessible chromatin with sequencing (ATAC-seq) was performed on OT-I T cells transduced as previously described and subjected to chronic stimulation assays as previously described. Following the chronic stimulation assay, transduced cells (Thy1.1$^+$) were sorted using FACS as previously described and processed following the protocol from Grandi *et al*. with minor modifications. In brief, 5 x 10^4 sorted cells were washed twice in PBS, lysed using ATAC lysis buffer (0.01% digitonin, 0.1% Tween-20, 0.1% Igepal, 3mM $MgCl_2$, 10 mM NaCl, 10 mM Tris-HCl pH 7.5) for 5 min on ice, and nuclei were pelleted by centrifugation (500 xg, 10 min, 4 ºC). Nuclei were incubated in a 50 µL transposition mixture composed of 2× TD buffer and 2.5 µL TDE1 transposase (Illumina Tagment DNA Enzyme and Buffer), with the addition of 0.01% digitonin and 0.1% Tween-20. The reaction was carried out at 37 °C for 30 minutes under gentle mixing. DNA was then isolated using the MinElute PCR Purification Kit (Qiagen). To prepare ATAC-seq libraries, the DNA was

amplified via PCR with the NEBNext High-Fidelity 2× PCR Master Mix (New England Biolabs) and indexed using custom i5/i7 primers. The resulting products were cleaned up with the QIAquick PCR Purification Kit (Qiagen), quantified using the NEBNext Library Quant Kit by qPCR, and normalised to 10 nM for equimolar pooling. Sequencing was performed by Novogene on an Illumina NovaSeq X Plus platform, generating 150 bp paired-end reads.

2.11.2 Processing and analysis of ATAC-seq data

FASTQ files sequencing reads were aligned to the Mus musculus reference genome (GRCm38/mm10) using Bowtie2. Reads mapping to mitochondrial DNA, unpaired fragments, or unmapped sequences were filtered out with Samtools. PCR duplicates were removed with Picard, and regions listed in the ENCODE blacklist were excluded. Peak calling was carried out using MACS2 with an FDR threshold of $q < 0.01$ and a consensus peak set was obtained by merging peaks from all samples with bedtools merge and retaining only those present in more than one sample. Differentially accessible regions were defined with DiffBind ($q < 0.1$, log2 fold change > 1). Enrichment profiles surrounding BACH2 binding sites were generated with deepTools (v3.5.6).

2.12 CUT&RUN sequencing and analysis

2.12.1 CUT&RUN sequencing

OT-I T cells were isolated, transduced, and chronically stimulated as described previously. Transduced populations (Thy1.1$^+$) were sorted by FACS and processed for Cleavage Under Targets & Release Using Nuclease (CUT&RUN) using the CUTANA ChIC/CUT&RUN Kit (EpiCypher) with slight protocol adjustments. For each reaction, 5 x 10^5 cells were washed in buffer containing spermidine and protease inhibitors, then immobilised on pre-activated Concanavalin A (ConA) beads. Cells were permeabilised with 0.001% digitonin and incubated overnight at 4 °C with 1 µL Rabbit anti-JunB antibody (clone C37F9, Cell Signaling Technologies) in antibody buffer. The following day, pAG-MNase was added and incubated at room temperature for 10 minutes. Chromatin cleavage and release were initiated by $CaCl_2$ addition, followed by a 2-hour incubation at 4 °C. The reaction was stopped with buffer containing *E. coli* spike-in DNA. CUT&RUN DNA was purified using SPRIselect beads (Beckman Coulter) and quantified on a Qubit Fluorometer (Thermo Fisher Scientific).

Sequencing libraries were prepared using either the CUTANA CUT&RUN Library Prep Kit (EpiCypher) or the NEBNext Ultra II DNA Library Prep Kit for Illumina (New England Biolabs), following manufacturer protocols. Library quality was assessed with an Agilent TapeStation and D1000 ScreenTape (Agilent). Sequencing was performed on an Illumina NextSeq 2000 platform with 100 bp paired-end reads at the Peter MacCallum Cancer Centre Molecular Genomics Core.

2.12.2 Processing and analysis of CUT&RUN data

Raw CUT&RUN sequencing reads from mouse samples, which included *E. coli* K12-MG1655 spike-in DNA, were processed using custom bash pipelines. Adapter removal and quality trimming were performed with BBDuk (bbmap v35.19) (https://github.com/BioInfoTools/BBMap), and read quality was assessed before and after trimming with FastQC (v0.11.5). Potential contamination and alignment rates to the E. coli spike-in were evaluated using FastQ Screen (v0.15.3) (https://www.bioinformatics.babraham.ac.uk/projects/fastqc/). Reads were then mapped to the Mus musculus GRCm38 (mm10) reference genome with Bowtie2, and alignment files were processed using SAMtools (v1.9) and Sambamba (v0.6.7).

Normalization of BAM files was carried out using the CUT&RUN Greenlist approach. In this method, a curated set of high-confidence CUT&RUN regions ("greenlist") served as an internal reference to minimise technical variation across samples. For each sample i, the total read signal within greenlist regions (S_i) was calculated by summing per-base coverage across those intervals. A scaling factor was then derived as $scale_i = \bar{S} / S_i$, where $\bar{S}$ represents the average greenlist signal across all samples. Normalised coverage tracks were generated by multiplying per-base values by the appropriate $scale_i$. These adjusted tracks were output in both BigWig and bedGraph formats for downstream visualization and analyses. Signal enrichment around BACH2 binding sites was assessed using deepTools (v3.5.6).

2.13 Human single-cell RNA sequencing analysis

Published single-cell RNA sequencing (scRNA-seq) data from a human pan-cancer TIL dataset was obtained from a public repository[63]. Downstream analyses, including quality control, filtering, dimensionality reduction and clustering, were performed using Seurat (v5.1.0) in R (v4.3.2). Visualisations were performed using Scanpy (v1.9.1) in Python (v3.11.1). As per the author's recommendations, a number of genes were excluded ('blacklisted' genes, including ribosome-protein-coding genes, proliferation genes and immunoglobulin genes) prior to the

analysis. Raw counts were subsequently normalised, scaled and transformed using the SCTransform workflow with regression of mitochondrial and cell cycle-associated genes. To generate UMAP visualisations, the first 25 principal components were used. Cluster annotations were performed manually according to signature genes in each cluster.

3. Chapter 1: BACH2 overexpression in tumour-specific CD8$^+$ T cells

3.1 Background

Over the past decade, an expanding body of evidence has highlighted the pivotal role of CD8$^+$ T cell differentiation in shaping the efficacy of anti-tumour responses in ACT. Increased rates of differentiation towards a terminally exhausted state – characterised by diminished effector function and limited proliferative capacity – have been consistently associated with suboptimal therapeutic outcomes. In contrast, the presence of the less differentiated, Tpex subset is strongly correlated with improved persistence and enhanced anti-tumour activity.

BACH2 has been shown to play a key role in modulating the intensity of TCR-mediated signalling upon antigen stimulation, which in turn controls the rate of CD8$^+$ T cell differentiation. Consequently, T cells lacking BACH2 are short-lived and have a high propensity to become terminally differentiated[131]. On the other hand, overexpression of BACH2 prevents Ttex formation and favours the acquisition of a Tpex phenotype[92]. These observations raise the question of whether genetically editing T cells to enforce BACH2 expression could result in diminished Ttex differentiation, and consequently in improved anti-tumour responses, in the context of ACT.

3.2 Results

3.2.1 Set-up of an in vivo solid tumour ACT model

In order to test the hypothesis of whether overexpression of BACH2 can enhance the therapeutic outcome of tumour-specific CD8$^+$ T cells, I first needed to establish an appropriate ACT model. T cell differentiation dynamics in the context of chronic stimulation have been studied extensively using both *in vitro* and *in vivo* settings. Nonetheless, the complexity of the TME – including the complex milieu of different cell types, cytokines and suppressive factors – are challenging to recapitulate outside of a developing tumour. For this reason, establishing an *in vivo* model that could allow me to faithfully emulate these conditions became my initial priority.

An ideal model is one that establishes an optimal compromise between faithfully recapitulating the conditions found in the 'real world' (e.g. a patient's tumour) while at the same time enabling the execution and analysis of experiments with sufficient statistical power and within a reasonable timeframe (i.e. days or weeks, rather than months). This led me to the decision of using a syngeneic solid tumour mouse model. These models involve the use of a tumour-

derived murine cell line, which can be inoculated into mice through various routes (e.g. subcutaneous injection, intravenous injection, intraperitoneal injection, etc…). Upon inoculation, cells become established and grow relatively rapidly, resulting in established tumours within 2-3 weeks.

The B16-F10 tumour model is widely used within the field of cancer immunology[121,150-153]. Originally derived from a murine melanoma, this cell line can be inoculated subcutaneously into WT C57BL/6 mice, and the growth of the deriving tumours can be readily measured using callipers. To model an ACT setting, I used the B16-OVA cell line, a variant of B16-F10 that has been engineered to express the chicken-derived ovalbumin (OVA) protein. A fragment of this protein is processed and presented on the surface of tumour cells in the context of a pMHC complex, allowing recognition by T cells expressing the OT-I TCR (OT-I T cells). As a result, the adoptive transfer of OT-I T cells into B16-OVA-bearing mice serves as a preclinical model analogous to TIL or CAR T cell therapies used in cancer treatment.

One of the key advantages of using syngeneic models is that, unlike other in vivo systems, the recipient mice do not need to be immunocompromised, as the tumour cells are not spontaneously rejected. This preserves the full spectrum of the host's immune system, allowing for a more physiologically relevant assessment of tumour growth and anti-tumour immune responses. Crucial immunological features are retained, including the complex cytokine milieu produced by various immune cell types within the TME, the presence of immunosuppressive populations such as tumour-associated Tregs, and endogenous T cells reactive to neoantigens, among others.

Nonetheless, adoptive T cells generally engraft poorly in an immunocompetent host. This is because the available pool of cytokines and growth factors required for surviving and proliferating in the new host is limited due to competition with the endogenous immune system, and this is true both in murine models and in the clinical setting. This can be circumvented by transiently depleting the host’s immune system prior to undergoing ACT. In a clinical setting, patients undergo a cyclophosphamide and fludarabine chemotherapy regimen to achieve this. A similar result can be obtained in murine models employing whole-body sub-lethal irradiation prior to the adoptive transfer of tumour-specific T cells.

To set up the ACT model, I first needed to determine the ideal dose of irradiation to use in ACT experiments to achieve transient lymphodepletion while preserving the safety and wellbeing of the animals. The great majority of published murine ACT studies rely on gamma-source

irradiators to achieve lymphodepletion, but I only had an X-ray-source irradiator at my disposal. Since a given dose of gamma or X-ray irradiation affects animals differently[154], and since many published studies report only the dose – but not the source – of irradiation, I decided to experimentally determine the maximum tolerated dose (MTD) of irradiation for my own studies. I defined the MTD as the highest dose of irradiation that could be delivered to mice without any obvious impact in the health and wellbeing of the animals. Using this dose for ACT studies would maximise the likelihood of T cell engraftment and minimise the required number of adoptive T cells needed to observe a therapeutic response.

To do this, I divided a cohort of WT mice into experimental groups (7 mice per group), each exposed to a different dose of irradiation ranging from 0 Gy to 5 Gy. Health and vitality indicators – such as mobility, activity, and attentiveness – were monitored daily for up to five weeks, a time estimated to be longer than a typical ACT experiment (**Fig. 1-1a**). If any mouse in a group showed early signs of health deterioration, the entire group was euthanised to prevent further adverse effects, and the corresponding dose of irradiation was deemed to exceed the MTD.

Mice exposed to irradiation levels ranging from 2.5-3.5 Gy did not display any clinical symptoms for the duration of the study and showed comparable levels of vitality to mice that received no irradiation (0 Gy). Instead, mice exposed to 4 Gy, or 4.5 Gy, displayed piloerection, adopted a hunched position and showed reduced levels of mobility 14 days following irradiation, and a similar behaviour was observed in mice that received 5 Gy at day 7 post-irradiation (**Fig. 1-1b**). Therefore, I determined the MTD to be 3.5 Gy and established that as the dose to be used in subsequent ACT studies.

Next, I sought to confirm that a dose of 3.5 Gy was sufficient to enable visible therapeutic responses in an ACT model. WT mice received B16-OVA cells subcutaneously and were monitored every 2-3 days for tumour growth. Once established tumours had formed (tumour area of 20-25 mm^2), mice were either exposed to either 3.5 Gy or no irradiation, and either treated with 0.5 x 10^6 OT-I T cells transduced with an EV control, or untreated (vehicle) (**Fig. 1-2a**). In the absence of irradiation, administration of tumour-specific T cells to tumour-bearing mice had no effect on the tumour growth kinetics relative to the untreated group, indicating that the treatment was ineffective. Nonetheless, administering the same number of T cells to mice that had been exposed to a dose of 3.5 Gy a day prior led to a significant enhancement in tumour control (**Fig. 1-2b**). These data confirm that pre-conditioning with 3.5 Gy irradiation

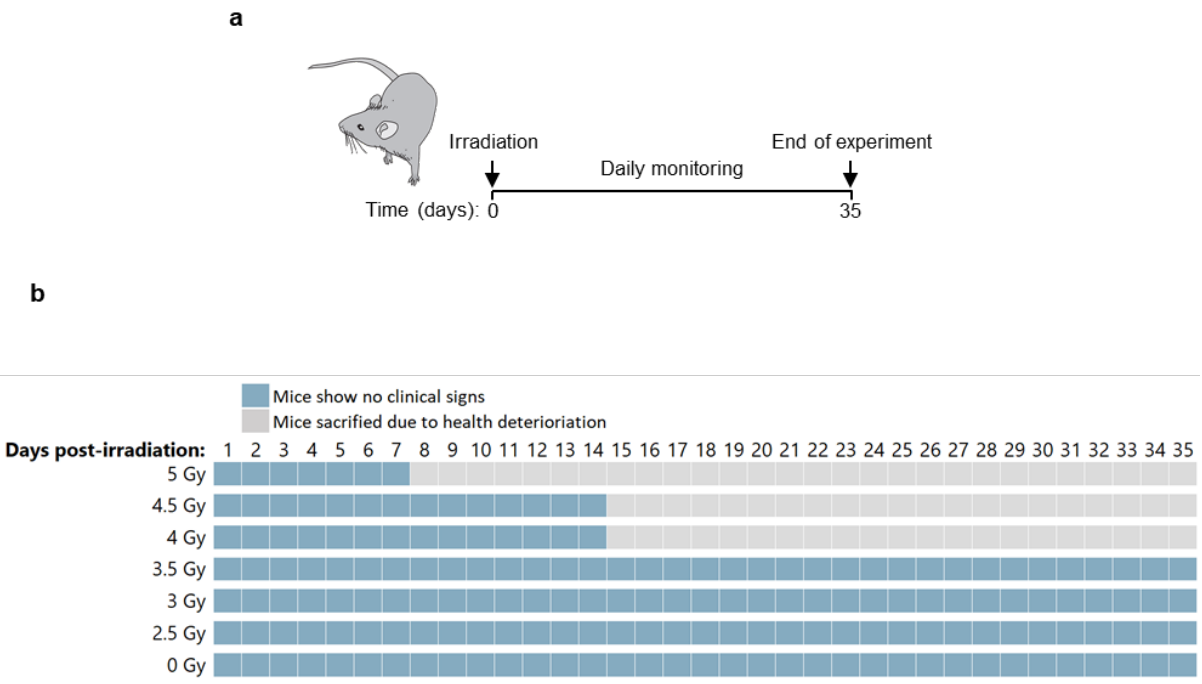

Figure 1-1. Irradiation pre-conditioning enhances the therapeutic response of tumour-specific T cells *in vivo*. a, Experimental schema. WT mice were exposed to different doses of irradiation ranging from 0 Gy (no irradiation) to 3.5 Gy and monitored daily. **b**, Tracking of animal clinical signs. Blue boxes indicate mice showed no adverse effects; grey boxes indicate at least one mouse in the group displayed adverse effects, leading to the removal of the group from the experiment.

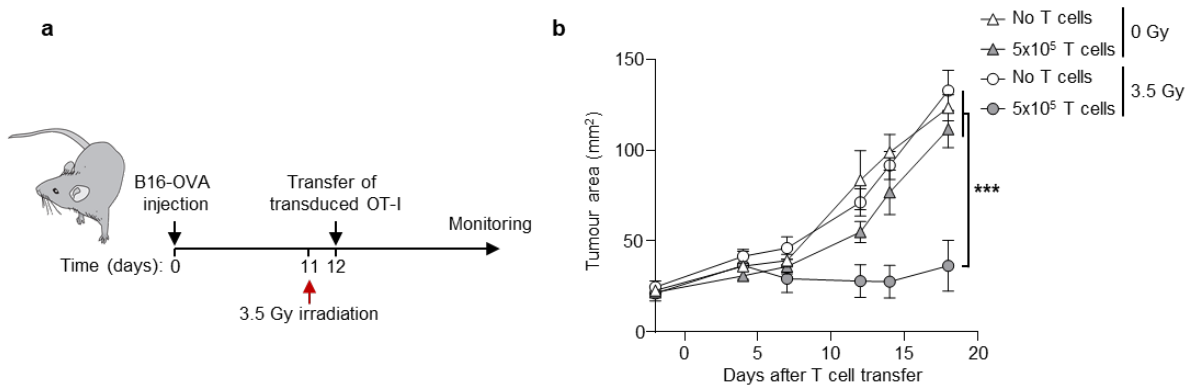

Figure 1-2. Irradiation pre-conditioning enhances the therapeutic response of tumour-specific T cells *in vivo*. a, Experimental schema. WT mice were subcutaneously injected with B16-OVA and tumour bearing-mice were exposed to either no irradiation (0 Gy) or 3.5 Gy irradiation a day prior to intravenous administration of OT-I T cells. **b**, Tumour measurements of B16-OVA-bearing mice exposed to either no irradiation (0 Gy) or 3.5 Gy and treated with either vehicle control (no T cells) or $5x10^5$ OT-I T cells. Statistical significance refers to differences in tumour area at the final day of the experiment. Data are representative of two independent experiments with five to eight mice per group. ns, non-significant ($P > 0.05$); *, $P < 0.05$; **, $P < 0.01$; ****, $P < 0.0001$. One-way ANOVA with Dunnett's multiple comparison correction (**b**).

enables a reliable therapeutic response following ACT. Moreover, they demonstrate that 3.5 Gy alone does not visibly affect tumour progression in this model.

With the ACT model established, I next wanted to assess how easily intratumoral adoptive T cells could be studied in this system. The intratumoral compartment of a tumour can be analysed using flow cytometry, which enables quantification of the expression of a panel of proteins of interest at single-cell resolution. Nonetheless, in order to reliably study the effects of BACH2 overexpression in the phenotype of transferred T cells in an ACT model, it is necessary to distinguish these cells from both transferred cells not bearing the construct of interest (i.e. untransduced OT-I T cells) and the endogenous T cells population. To distinguish transduced from untransduced OT-I T cells, the DNA payloads used to engineer T cells throughout my experiments included a truncated Thy1 reporter (also known as CD90). While this marker is ubiquitously expressed in all T cells, both the OT-I T cells and the recipient tumour-bearing WT mice expressed the Thy1.2 allelic variant, while the reporter used in my construct was the Thy1.1 variant. Similarly, two congenically distinct CD45 alleles were used to distinguish T cells from donor mice (i.e. OT-I T cells), which expressed CD45.1; from those in the recipient mice, expressing CD45.2.

To test this strategy, B16-OVA-bearing mice were irradiated with 3.5 Gy and treated with OT-I T cells transduced with an EV. 14 days following ACT treatment, mice were euthanised and the tumours were dissected and processed into single-cell suspensions prior to flow cytometry staining. To identify the T cell compartment, I used a standard gating strategy, whereby live cells, singlet events and lymphocytes were selected based on live/dead stain and forward/side scatter signal. The $CD8^+$ T cells could be reliably detected by selecting cells positive for both CD3 and CD8. As expected, $CD45.1^+$ cells (i.e. adoptive OT-I T cells) were exclusively found within the $CD8^+$ T cell compartment, and the transduction reporter Thy1.1 was expressed exclusively within $CD45.1^+$ cells (**Fig. 1-3**). Therefore, through this gating strategy, endogenous $CD8^+$ T cells ($CD3^+$ $CD8^+$ $CD45.1^-$), untransduced adoptive OT-I T cells ($CD3^+$ $CD8^+$ $CD45.1^+$ $Thy1.1^-$) and transduced adoptive OT-I T cells ($CD3^+$ $CD8^+$ $CD45.1^+$ $Thy1.1^+$) can be readily distinguished.

Together, these data confirm that the B16-OVA model, in combination with pre-conditioning irradiation, can be reliably used for evaluating the $CD8^+$ T cell-mediated tumour responses in the context of ACT. With this system in place, I was now positioned to assess how ectopic

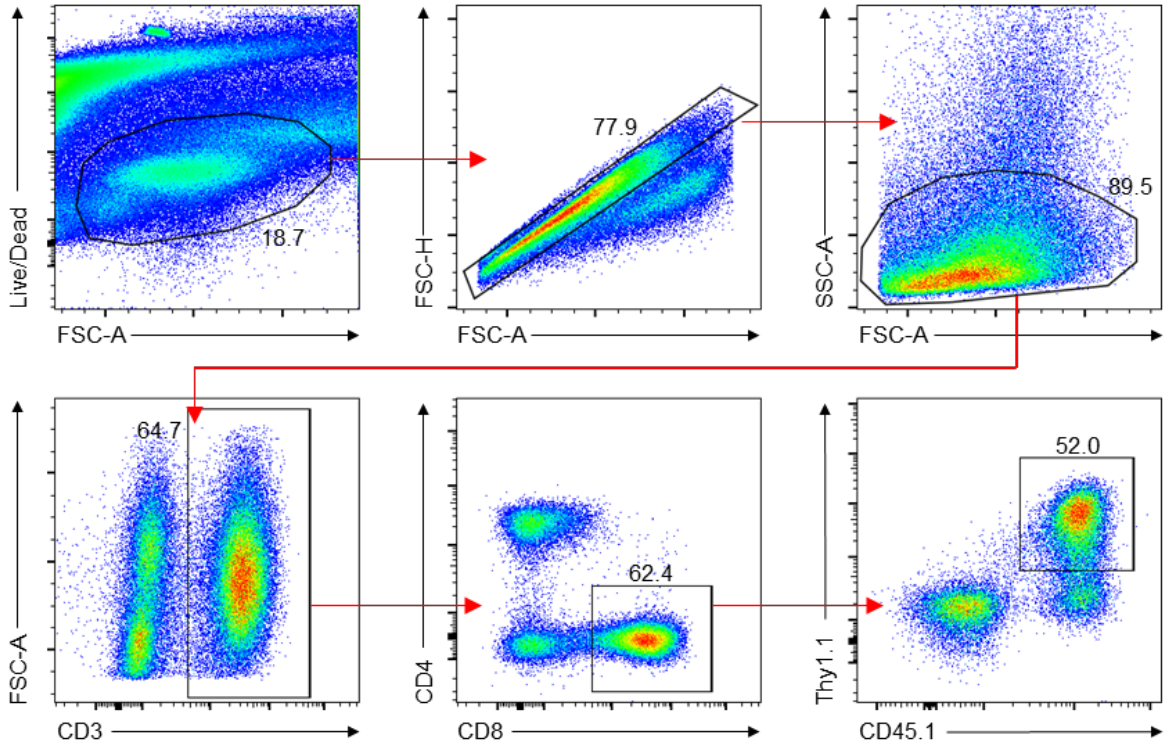

Figure 1-3. Transduced intratumoral adoptive T cells are readily detectable through flow cytometry. Representative gating strategy used for the identification of intratumoral T cells, including endogenous $CD8^+$ T cells, untransduced OT-I T cells and transduced OT-I T cells.

expression of BACH2 influences the differentiation, function, and therapeutic efficacy of tumour-specific $CD8^+$ T cells in a physiologically relevant context.

3.2.2 BACH2 overexpression enhances stemness and prevents Ttex differentiation in tumour-specific T cells

Having established a reliable *in vivo* solid tumour ACT model and confirmed the detectability of intratumoral T cells, I proceeded to analyse the impact of BACH2 overexpression in tumour-specific T cells. Previous work by my laboratory and others had already validated both the use of the selected CDS and the expected phenotype of T cells ectopically expressing BACH2 under conditions of chronic stimulation[92,131]. This groundwork allowed me to move to the *in vivo* setting from the outset.

BACH2 overexpression was achieved via retroviral transduction using an MSCV-based vector ($BACH2_{OE}$) encoding a single ORF comprising Thy1.1 and BACH2, separated by a self-cleaving T2A motif (**Fig. 1-4**). Given that the 5' LTR of MSCV vectors provides constitutive promoter activity, no additional promoter was included upstream of the Thy1.1-BACH2 cassette. As control, an EV construct containing Thy1.1 alone was used.

To test the impact of BACH2 overexpression in tumour-specific T cells, the previously established ACT model was employed. WT mice were subcutaneously injected with B16-OVA and tumour-bearing mice were irradiated (3.5 Gy) and administered with OT-I T cells transduced either with EV or $BACH2_{OE}$. 12 days after T cell administration, mice were euthanised and tumours were dissected and analysed via high-parameter flow cytometry (**Fig. 1-5a**). Initial analysis of intratumoral transduced OT-I T cells revealed substantial differences in the distribution of cells among T cell subsets. Unbiased analysis of the data via a clustering method distinguished both a stem-like cluster characterised by expression of TCF1 (Cluster 1) and two additional clusters lacking TCF1, likely representing more intermediate and terminally differentiated states (Cluster 2 and 3) (**Fig. 1-5b**). Cells transduced with EV displayed a broad range of phenotypes, with similar proportions between Cluster 1 and Clusters 2 and 3. In contrast, cells transduced with $BACH2_{OE}$ showed a significant bias towards Cluster 1, suggesting preferential retention of the Tpex phenotype under the conditions of chronic stimulation found intratumorally.

As previously discussed, there is no universally accepted unified nomenclature system for categorising distinct exhausted subsets. Nonetheless, the expression of TCF1, Slamf6, and TIM-3 on antigen-experienced PD-1^+ intratumoral T cells has been widely used to distinguish

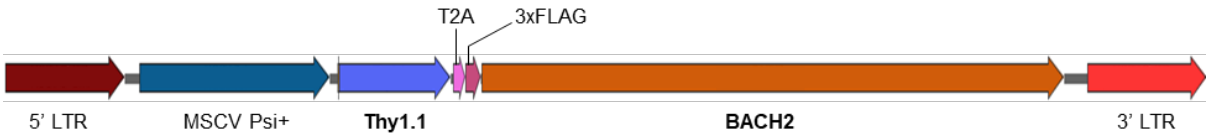

Figure 1-4. Construct for overexpression of BACH2. Diagram depicting the different cassettes featured in the BACH2 overexpression vector ($BACH2_{OE}$). LTR, long-terminal repeat; MSCV Psi+, Ψ RNA packaging signal.

between Tpex and Ttex populations. These markers were also used in my analyses to assess the presence of Tpex or Ttex subsets.

In the EV group, only about one-third of PD-1$^+$ OT-I T cells co-expressed the Tpex-associated markers TCF1 and Slamf6, while this was closer to 75% of PD-1$^+$ OT-I T cells in the BACH2$_{OE}$ group (**Fig. 1-5c**). Meanwhile, around one-third of PD-1$^+$ OT-I T cells in the EV group expressed the Ttex-associated marker TIM-3, whereas its expression was nearly absent in the BACH2$_{OE}$ group (**Fig. 1-5d**). This is consistent with the prior knowledge that overexpression of BACH2 enforces a Tpex phenotype, but this is the first time, to my knowledge, where this has been shown in intratumoral T cells.

Further to TCF1 and Slamf6, other markers have also been associated with a Tpex phenotype. Namely, markers associated with a memory state, such as CCR7 and CD62L, are among those that have been reported to be upregulated in this subset (even if not as noticeably as TCF1 and Slamf6). Indeed, both of these markers show significantly increased levels of expression in cells of the BACH2$_{OE}$ group compared to EV on a per-cell basis (**Fig. 1-5e**).

In all, these data confirm, that ectopic expression of BACH2 in tumour-specific T cells enforces a Tpex phenotype despite the high antigen density environment and prolonged stimulation period associated with the TME. These findings are in line with our prior knowledge regarding the function of BACH2 and its role in preserving stemness and memory in the context of chronic stimulation.

3.2.3 BACH2 overexpression compromises the acquisition of effector functions and impairs ACT anti-tumour responses

Next, I wanted to assess whether a reduction in terminal differentiation translates to a more favourable anti-tumour phenotype. To do this, I assessed effector and cytotoxic functions in tumour-specific T cells with and without BACH2 overexpression 12 days after OT-I T cell administration, focusing on markers such as CD44 and PD-1. I also assessed cytokine polyfunctionality by inducing pan-T cell stimulation following processing of tumour samples using PMA/ION in the presence of inhibitors of intracellular transport of the Golgi apparatus to prevent extracellular release of cytokines.

When comparing the median fluorescence intensity (MFI) of CD44 and PD-1 between EV- and BACH2$_{OE}$-transduced cells, I observed a significant decrease in the expression of both markers in the BACH2$_{OE}$ group relative to control (**Fig. 1-6a**). Furthermore, the expression of effector

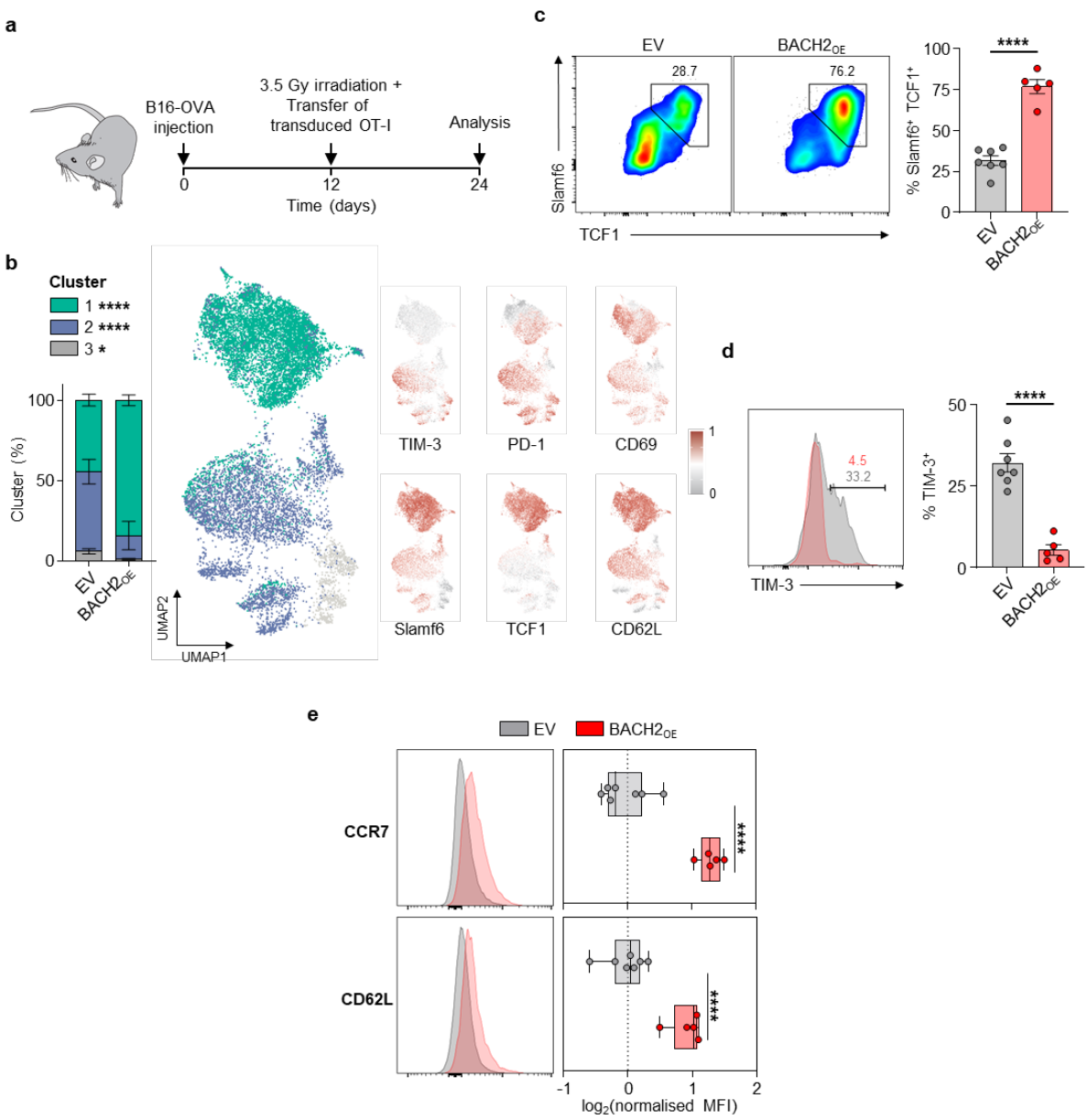
a
B16-OVA injection
3.5 Gy irradiation + Transfer of transduced OT-I
Analysis
0
12
24
Time (days)
b
Cluster
1 ****
2 ****
3 *
Cluster (%)
EV
BACH2OE
UMAP2
UMAP1
TIM-3
PD-1
CD69
Slamf6
TCF1
CD62L
c
EV
BACH2OE
28.7
76.2
Slamf6
TCF1
% Slamf6+ TCF1+
****
d
4.5
33.2
TIM-3
% TIM-3+
****
e
EV
BACH2OE
CCR7
CD62L
****
****
log2(normalised MFI)

Figure 1-5. BACH2 overexpression enforces a Tpex phenotype and prevents Ttex differentiation. a, Experimental schema. WT mice were subcutaneously injected with B16-OVA and tumour bearing-mice were irradiated and administered with EV- or $BACH2_{OE}$-transduced OT-I T cells. **b**, UMAP visualisation of high-parameter flow cytometry data from transduced intratumoral OT-I T cells, and relative expression of indicated markers across the UMAP. The proportion of EV and $BACH2_{OE}$ cells assigned to each cluster and significant differences in proportion between groups is shown. **c**, Proportion of $Slamf6^+$ $TCF1^+$ transduced intratumoral OT-I T cells and representative flow cytometry plots. **d**, Proportion of $TIM\text{-}3^+$ transduced intratumoral OT-I T cells and representative flow cytometry histogram plot. **e**, Normalised median fluorescence intensity (MFI) of CCR7 and CD62L in transduced intratumoral OT-I T cells and representative flow cytometry histogram plots. Data are representative of two independent experiments with five to eight mice per group. ns, non-significant ($P > 0.05$); *, $P < 0.05$; **, $P < 0.01$; ****, $P < 0.0001$. Unpaired two-tailed Student's *t* test (**c-e**). Bars and error indicate mean ± SEM (**b-d**). Box indicates interquartile range, vertical line indicates median, and error bars indicate range (**e**).

molecules such as IFN-γ and Granzyme B was significantly reduced upon BACH2 overexpression (**Fig. 1-6b-c**). This suggests that, despite the reduction in terminal differentiation and a strongly sustained Tpex phenotype, high levels of BACH2 resulted in reduced – not increased – effector functions.

I also decided to test how the $BACH2_{OE}$ phenotype impacted tumour control *in vivo*. For this, I used the same workflow as before; except this time tumour-bearing mice were not euthanised for analysis and were instead monitored every 2-3 days until a humane endpoint based on tumour size was met (this was considered to be an average length/width of 15 mm as per the project license under which the studies were performed). In addition, mice were randomised and grouped to ensure a similar average tumour size and tumour size distribution across experimental groups.

As previously observed, mice treated with OT-I T cells transduced with EV displayed higher tumour control than mice that received no T cells. Nonetheless, contrary to my initial hypothesis and in line with the observed reduction in effector functions, mice transduced with $BACH2_{OE}$ exhibited worse anti-tumour responses compared to the EV control (**Fig. 1-6d**). Concordantly, the latter group also showed a worsened survival throughout the experiment due to faster tumour outgrowth (**Fig. 1-6e**).

Collectively, these data show that BACH2 overexpression severely compromises the ability of $CD8^+$ T cells to exert the cytotoxic and effector functions necessary to mount an effective anti-tumour response. This is despite the fact that cells adopt a strong Tpex phenotype, which has traditionally been correlated with improved proliferative capacity and anti-tumour control.

3.3 Discussion

The data presented in this section address the initial hypothesis upon which my work is originally based: that ectopic expression of BACH2 improves the anti-tumour function of T cells in an ACT setting. The biological rationale underpinning this hypothesis assumed that, since terminal differentiation of T cells has been recognised to be a major reason for the short persistence (and in turn negative therapeutic outcomes) of T cell therapies, expression of a transcription factor known to prevent terminal differentiation would address this failure point and in turn lead to an improvement in ACT-mediated responses. Nonetheless, the results obtained here clearly and unequivocally indicate that this is not the case.

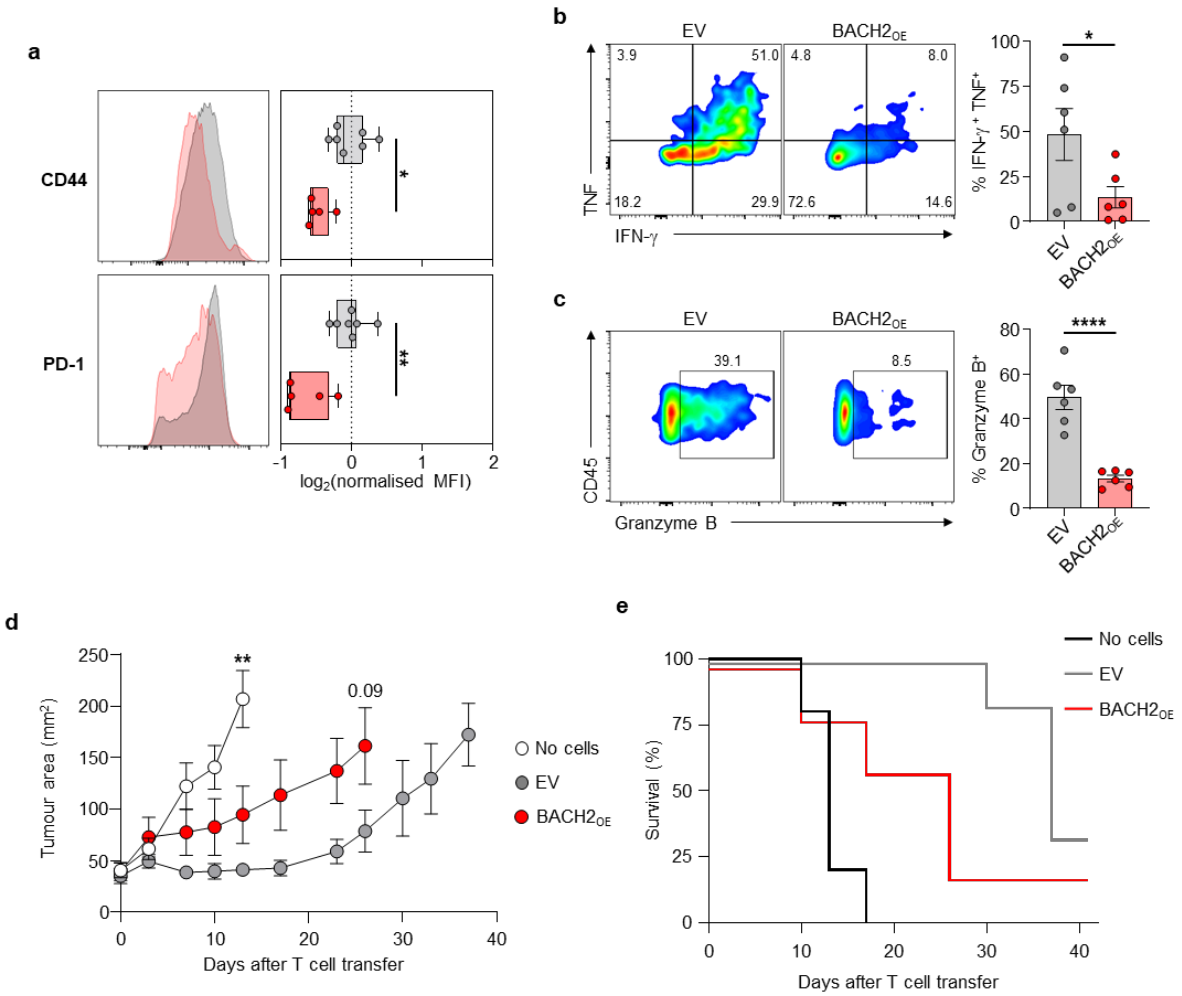

Figure 1-6. BACH2 overexpression compromises effector functions and impairs anti-tumour responses. a, Normalised MFI of CD44 and PD-1 in transduced intratumoral OT-I T cells and representative flow cytometry histogram plots. **b-c**, Percentage of IFN-γ^+ TNF$^+$ (**b**) and Granzyme B$^+$ (**c**) cells in transduced intratumoral OT-I T cells following *ex vivo* stimulation with PMA/ION and representative flow cytometry plots. **d-e**, Tumour measurements (**d**) and survival (**e**) of B16-OVA-bearing mice treated with either Hanks' balanced salt solution HBSS ('No cells') or OT-I T cells transduced with EV or BACH2$_{OE}$. Significant differences between EV and either 'No cells' or BACH2$_{OE}$ groups at the indicated day is shown (**d**). Data are representative of two independent experiments with five to eight mice per group. ns, non-significant ($P > 0.05$); *, $P < 0.05$; **, $P < 0.01$; ****, $P < 0.0001$. Unpaired two-tailed Student's *t* test (**c-e**). Bars and error indicate mean ± SEM.

It is worth noting, however, that the data are supportive of the notion that BACH2 prevents terminal differentiation in the context of tumour-mediated chronic stimulation. The markers used to make this assumption – including TCF1, Slamf6 and TIM-3 – have been used widely to define and characterise Tpex and Ttex populations. Furthermore, the observed phenotype is in line with that observed in previous studies characterising the role of BACH2 during chronic stimulation, which strongly suggests these cells constitute a *bona fide* Tpex population.

However, it is the second assumption in my initial hypothesis that may need to be revisited: that a reduction in Tpex differentiation would inexorably result in an improved anti-tumour response. As previously discussed, presence of Tpex and absence of Ttex in the tumour is correlated with improved anti-tumour responses, not just in the ACT setting but in other immunotherapy modalities as well[78,79]. Nonetheless, the relative proportion of subsets is only part of the whole picture. Tpex cells are characterised by their ability to generate more differentiated effector subsets with a higher degree of cytotoxic potential while maintaining a stable Tpex pool – a feature that has made this population also widely known in the field as 'stem-like' T cells (see 'Introduction'), and that is likely to be critical for the improved anti-tumour responses associated with this subset. My results, on the other hand, point to a severe decrease in the proportion of cells with effector functions despite an expanded Tpex population. Therefore, it is likely that the ability to generate more differentiated effector cells is being actively inhibited in $BACH2_{OE}$-transduced cells.

There are two major conclusions I can draw from these observations. The first one is that BACH2 overexpression promotes Tpex differentiation but inhibits progression to more differentiated subsets. While this results in a reduction of Ttex cells – as originally anticipated and as demonstrated by my results – this also causes a reduction in intermediate effector subsets, too. In other words, high levels of BACH2 'lock' T cells in a progenitor exhausted state, protecting them from terminal differentiation but simultaneously interrupting the acquisition of necessary functions to effectively fight tumours.

While discouraging, this first conclusion is not completely unexpected. BACH2, as previously mentioned, acts as an inhibitor of TCR-mediated signalling by competing with AP-1 factors, which are involved in driving both T cell activation and Ttex differentiation. Indeed, previous reports from my group already indicated a reduction in the expression of IFN-γ in BACH2 overexpressing cells under conditions of acute stimulation[131]. What I did not know, however, was whether the exposure to a high antigen density environment over a prolonged period of

time, together with a blockade of inhibitory mechanisms associated with the Ttex state, would overcome this reduction in activation and result in a net-positive anti-tumour phenotype. This is not the case.

The second conclusion is that, like in most of biology, T cell differentiation is a complex, highly regulated and dynamic process. Several reports have established a link between Tpex, the expression of BACH2 in the anti-tumour T cell compartment and positive therapeutic outcomes; and high levels of *BACH2* mRNA in tumour samples are associated with improved anti-tumour responses likely because of this reason[133,155]. Yet, as my results show, enforced expression of this TF in tumour-specific T cells compromises the therapeutic outcomes of ACT. This somewhat paradoxical finding hints at the fact that the regulation of BACH2 in $CD8^+$ T cells is dynamic in nature and may be important in maintaining the right balance of long-lived T cell survival and effector functions required for a durable anti-tumour response.

This line of thinking raised important biological questions that led to the next section of my work: how is BACH2 is regulated in $CD8^+$ T cells during physiological anti-tumour responses? And can a better understanding of the underlying expression dynamics of BACH2 during chronic stimulation provide insights into how to modify T cells for improved therapeutic outcomes in ACT? To my knowledge, these questions have never been addressed before, yet they may reveal, important insights into how to engineer T cells to achieve enhanced anti-tumour responses.

4. Chapter 2: Quantitative control of BACH2 in CD8$^+$ T cells

4.1 Background

The results obtained in the previous chapter strongly suggest that overexpression of BACH2 locks T cells in a Tpex state, unable to acquire effector functions which, in turn, display a limited ability to mount effective anti-tumour responses. Nonetheless, BACH2 is an important factor in mounting successful long-term anti-tumour responses, such as those observed in the context of tumours or chronic viral infections. This conundrum led me to hypothesise that the regulation of BACH2 in CD8$^+$ T cells is of crucial importance to ensure the right balance between long-term survival and anti-tumour cytotoxic activity.

However, to date, a detailed analysis of how BACH2 is regulated in tumour-specific T cells has not been performed. For instance, whether BACH2 expression in intratumoral CD8$^+$ T cells follows a binary distribution (i.e. either expressed or not expressed), or a more gradual expression pattern like in the case of naïve, memory and effector T cells in the context of acute stimulation, is not known. Similarly, whether different levels of expression of BACH2 are important in determining how T cells respond to given stimuli, such as TCR-driven stimulation, has never been studied in detail. Hence, I next decided to focus my efforts into elucidating how BACH2 activity is controlled in intratumoral T cells, with the conviction that a better understanding of its regulation dynamics may form the basis for a new strategy to enhance T cell persistence in the context of ACT.

4.2 Results

4.2.1 Intratumoral CD8$^+$ T cells display gradated expression of BACH2 mRNA

Previous reports already show that lack of BACH2 leads to unrestrained T cell differentiation. Similarly, cells in a terminally differentiated state express low levels of memory factors like BACH2[92,131]. Nonetheless, an unanswered question (and the one I first sought to answer in this chapter) is how exactly BACH2 is regulated throughout T cell differentiation in intratumoral responses. For instance, does BACH2 expression remain high until a specific differentiation state is reached before being rapidly downregulated (i.e. binary expression pattern)? Or is BACH2 expression extinguished in a more gradual manner as differentiation progresses, as it occurs in the context of acute T cell stimulation (i.e. gradual expression pattern)?

To start, I decided to leverage publicly available data from human TILs to study the expression of *BACH2* in different subsets. To this end, I relied on a recent study that assembled a pan-

cancer scRNA-seq atlas of $CD8^+$ T cells from a wide range of cancer types and over 300 donors, arguably constituting the most comprehensive study of its kind to date[63]. During the analysis, the data were processed in a manner consistent with the authors' guidelines to maximise consistency across studies and ensuring a high-quality output. In addition, labelling of different cell populations was performed using a similar criterion to that used in the original publication.

Following data processing, the scRNA-seq data of $CD8^+$ T cells were visualised through a UMAP plot with clusters labelled based on the transcriptomic profiles of the corresponding cells. Unsurprisingly, a wide span of phenotypes were observed, ranging from less differentiated $CD8^+$ T cell populations, such as those expressing transcripts associated with naïve-like (naïve-like cluster) and memory-like (*IL-7R* and *CCR7* clusters) T cells; to those displaying expression of transcripts linked with high differentiation states, such as terminally differentiated T cells (*ENTPD1*, which encodes for CD39) and T effector memory re-expressing CD45RA (TEMRA, a terminally differentiated subset of T cells that express CD45RA)[156,157] (**Fig. 2-1a**).

The classification of different subsets of T cells in subsets based on their differentiation state provided a useful starting point for evaluating subset-specific expression of different markers by looking at the average signal of different clusters. Some markers, such as *KLRG1* or *TOX*, displayed relatively sudden and rapid changes of expression across different clusters, while changes in the expression of markers like *PDCD1* (encoding PD-1) were gradual. Interestingly, *BACH2* mRNA expression corresponded to the latter category, following a gradual differentiation pattern (**Fig. 2-1b**). While its expression was highest in less differentiated subsets like naïve-like or memory-like clusters, it decreased gradually until reaching its minimum in TEMRA cells.

According to these data, while cells in the lowest differentiation states express the highest level of BACH2, those in intermediate state (which also correspond to those exerting the highest degree of effector functionality) express intermediate levels of BACH2. This suggests that, like in the context of acute stimulation, BACH2 expression is tightly controlled throughout the distinct differentiation states of Texh. However, the resolution of scRNA-seq data can be limited, which can be a problem especially for lowly-expressed genes such as those encoding TFs.To expand upon this initial finding, I decided to utilise a transgenic mouse model to track the expression of *Bach2* in different cell types: the *Bach2*$^{tdRFP/+}$ mouse strain. In this strain, one of

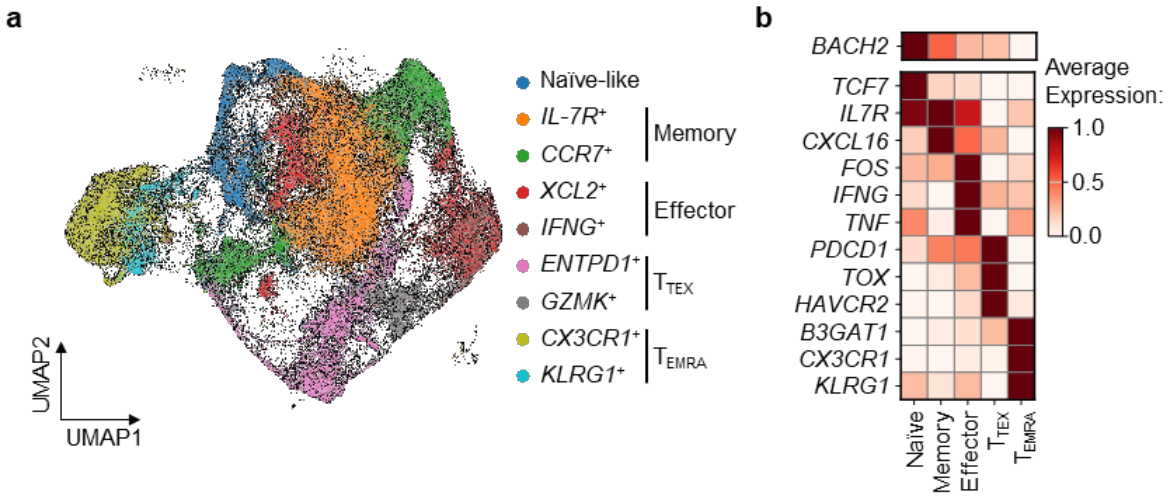

Figure 2-1. Intratumoral CD8$^+$ T cells across various human cancers display a gradual expression pattern of *BACH2* mRNA. a-b, UMAP plot visualization of CD8$^+$ TILs from various human cancers (**a**) and relative expression of the indicated markers across different CD8$^+$ T cell populations (**b**).

the two *Bach2* alleles has been replaced with a knock-in RFP gene, while the second *Bach2* allele remains intact (**Fig. 2-2a**)[143]. This is a particularly versatile model for the study of BACH2 expression for three different reasons. The first one is that *Bach2* is haplosufficient, meaning that a single copy of the gene produces enough protein to sustain its physiological functions[158]. This enables the use of this strain without confounding biases caused by the loss of one of the two alleles. Second, the detection of BACH2 in murine models is challenging even in naïve cells where BACH2 expression is the highest, because absolute protein levels are relatively low; and there is no commercially available anti-BACH2 antibody optimised for flow cytometry. And third, previous studies have confirmed that the expression of the RFP knock-in mimics reliably that of the endogenous *Bach2* mRNA because since all of the native cis-regulatory elements remain unaltered[143].

Bach2$^{tdRFP/+}$ mice were subcutaneously injected with B16-F10 tumour cells with the aim of investigating the dynamics of BACH2 expression in peripheral and intratumoral CD8$^+$ T cells. Tumour growth was monitored, and upon establishment of visible tumours, mice were euthanised and tumours, spleens, and draining LNs were harvested and processed for flow cytometric analysis.

Using a panel of various surface markers, I was able to study RFP expression in CD8$^+$ T cell subpopulations across different tissues. In the spleen and draining LNs, central memory (CD62L$^+$ CD44$^–$), effector memory (CD62L$^+$ CD44$^+$) and effector (CD62L$^–$ CD44$^+$) T cells showed a pattern of RFP expression similar to that described in previous studies, with less differentiated central cells showing the highest level of expression, and effector cells the lowest[131]. The pattern continues if I extend the analysis to PD-1$^+$ effector T cells, thought to be circulating cells that have experienced chronic antigen stimulation and therefore considered to be further in their differentiation trajectory[159] (**Fig. 2-2b-e**).

Notably, a similar pattern emerges when shifting to intratumoral CD8$^+$ T cells. Among these, non-exhausted PD-1$^–$ T cells – broadly considered to be bystander T cells not actively engaging the tumour – showed the highest level of RFP expression. When focusing on more differentiated T cells within the PD-1$^+$ TIM-3$^–$ compartment, a gradual decrease in the expression of RFP in different subpopulations defined by Slamf6 and CD69 becomes apparent, where Slamf6$^+$ CD69– showed the highest RFP expression, followed by Slamf6$^+$ CD69$^+$, Slamf6$^–$ CD69$^+$ and Slamf6$^–$ CD69– cells (**Fig. 2-2f-g**). Interestingly, this pattern resembles a proposed differentiation model by Beltra *et al.*, where a similar differentiation order (from less

to more differentiated) within Texh is proposed (Slamf6^{+} CD69^{-} > Slamf6^{+} CD69^{+} > Slamf6^{-} CD69 > Slamf6^{-} CD69^{-})[160]. Lastly, terminally differentiated cells (marked by activation and Ttex markers CD69 and TIM-3) showed the lowest level of RFP expression. Overall, these results are consistent with the notion that BACH2 expression is regulated in a gradual manner throughout the differentiation trajectory of intratumoral Texh, with an expression pattern that is inversely correlated with the cell's differentiation state.

Upon observing the differential expression of BACH2 across functionally distinct T cell subsets, both in peripheral and intratumoral settings, I made an important realisation. As I have previously discussed, BACH2 counteracts TCR-driven expression of different genetic programmes associated with T cell activation and differentiation. Importantly, however, the BACH2 expression levels change across different T cells subsets. This dynamic regulation of BACH2 likely serves to fine-tune the degree of stimulation each T cell subset receives, aligning with its specific functional requirements. Notably, when looking at its expression in intratumoral T cells, neither the cells with the highest BACH2 expression (e.g., the PD-1^{-} intratumoral population) nor those with the lowest levels (e.g., terminally differentiated TIM-3^{+} T cells) exhibit the greatest cytotoxic potential. Rather, the highest cytotoxic activity appears to reside within intermediate states: where BACH2 is expressed, but only at moderate levels.

This led me to propose the following hypothesis: could engineering CD8^{+} T cells to express *low but sustained* levels of BACH2 be a viable strategy to protect tumour-specific T cells from terminal differentiation without compromising the acquisition of effector functions? After all, the 'default' expression level achieved through standard retroviral constructs relying on the 5' LTR promoter (like in $BACH2_{OE}$) is likely supraphysiological compared to endogenous BACH2 levels. As a result, the balance between long-term immune cell persistence and the exertion of effector functions may become overly skewed toward the former during conventional BACH2 overexpression, and fine-tuning its expression may promote a more balanced state encompassing both persistence and cytotoxic functions.

4.2.2 Low-dose expression of BACH2 preserves a stem-like phenotype without compromising effector functions in vitro

The concept of modulating the level of expression of transgenes is hardly new in biotechnology. Applications for such technology vary widely, including controlling the delivery dose of biotherapeutics, optimizing molar ratios for improving the production of complex biologics

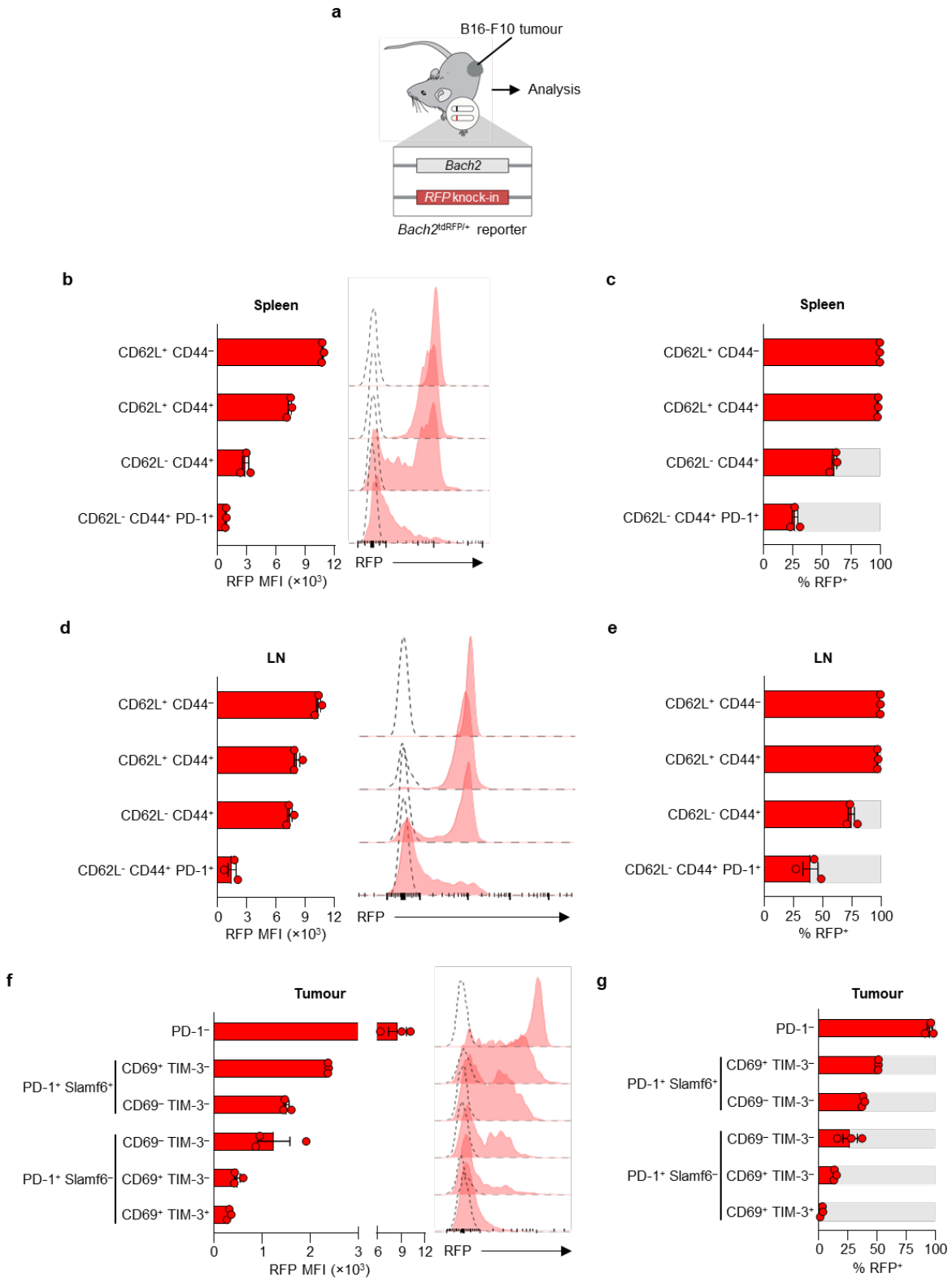
a
B16-F10 tumour
Analysis
Bach2
RFP knock-in
Bach2tdRFP/+ reporter
b
Spleen
CD62L+ CD44−
CD62L+ CD44+
CD62L− CD44+
CD62L− CD44+ PD-1+
0 3 6 9 12
RFP MFI (×10³)
RFP
c
Spleen
CD62L+ CD44−
CD62L+ CD44+
CD62L− CD44+
CD62L− CD44+ PD-1+
0 25 50 75 100
% RFP+
d
LN
CD62L+ CD44−
CD62L+ CD44+
CD62L− CD44+
CD62L− CD44+ PD-1+
0 3 6 9 12
RFP MFI (×10³)
RFP
e
LN
CD62L+ CD44−
CD62L+ CD44+
CD62L− CD44+
CD62L− CD44+ PD-1+
0 25 50 75 100
% RFP+
f
Tumour
PD-1−
PD-1+ Slamf6+
CD69+ TIM-3−
CD69− TIM-3−
PD-1+ Slamf6−
CD69− TIM-3−
CD69+ TIM-3−
CD69+ TIM-3+
0 1 2 3 6 9 12
RFP MFI (×10³)
RFP
g
Tumour
PD-1−
PD-1+ Slamf6+
CD69+ TIM-3−
CD69− TIM-3−
PD-1+ Slamf6−
CD69− TIM-3−
CD69+ TIM-3−
CD69+ TIM-3+
0 25 50 75 100
% RFP+

Figure 2-2. Peripheral and intratumoral CD8$^+$ T cell subsets display a gradual expression pattern of *Bach2*. a, Experimental schema. *Bach2*$^{tdRFP/+}$ were subcutaneously injected with B16-F10 tumour cells, and following tumour establishment, different tissues were harvested for flow cytometric analysis. **b-g**, MFI of RFP expression and representative histograms, or RFP$^+$ frequency, of the indicated CD8$^+$ T cell subpopulations in the spleen (**b-c**), draining LNs (**d-e**) or tumour (**f-g**).

like antibodies, and reducing unwanted metabolic byproducts in engineered microbes during biofuel or biopharmaceutical production[146,161,162]. As a result, a wide range of methods to modulate transgene expression have been developed.

With this in mind, I sought a strategy to fine-tune the expression of BACH2 that met three criteria. First, the approach needed to preserve the native structure of BACH2. Given that the function of BACH2 relies on complex interactions with other macromolecules (e.g. nuclear translocation, recognition and binding to target DNA sequences, interactions with protein partners such as co-repressors, etc…), adding exogenous domains could interfere with one or more of these processes, introducing confounding variables and potentially compromising its biological activity. Second, the selected method needed to allow modulation of BACH2 expression over a sufficiently broad range. Retroviral overexpression of a TF can lead to a level that are several-fold, or even orders of magnitude, higher than physiological amounts[163]. Therefore, in order to test my hypothesis, I decided to use an approach capable of reducing BACH2 expression by at least an order of magnitude relative to the 'default' 5'-LTR retroviral promoter. And third, I needed a method that was compact and simple to use. Large payload sizes can significantly impact retroviral titres and, in turn, the efficient of T cell transduction. Since the BACH2 CDS already spans over 2.5 kilobases (kbs), I avoided any method requiring the incorporation of large sequences (i.e. custom promoter sequences with additional synthetic TFs) in the retroviral vectors. Furthermore, approaches that depend on exogenous molecules to regulate transgene expression would be difficult to implement *in vivo*, where the pharmacokinetics properties of such molecules would complicate the control of transgene expression levels in adoptively transferred T cells.

After carefully considering various approaches, I decided to adopt an elegant method developed by Sillibourne *et al*., called the STOP-translational readthrough motif (STOP-TRM) system[146]. The STOP-TRM system exploits the natural phenomenon of translational readthrough to modulate downstream transgene expression. This mechanism is based on the principle that, under specific conditions, a ribosome may bypass the termination signal (STOP codon) and continue translation. This can happen, for example, when short cis-acting sequences (as short as 6 bp) flanking the termination signals lead to near-cognate transfer RNAs competing with the release factors necessary to interrupt the process of translation, resulting in the insertion of additional amino acids. Instances of translational readthrough have been described in different natural contexts, including in human transcripts (e.g. *LDHB* gene, which

encodes lactate dehydrogenase b in humans), and can result in the translation of protein variants with expanded amino acid sequences and altered functions[164].

Critically, the efficiency of translation downstream of a STOP-TRM sequence is substantially reduced, and this is the feature that Sillibourne *et al*. exploited to turn this natural regulatory mechanism into a tool for synthetically controlling the expression levels of specific transgenes (**Fig. 2-3**). By testing multiple combinations of canonical STOP codons and TRMs, the authors found that different sequences bypassed translation termination to different extents. In this way, they constructed a library of STOP-TRM sequences capable of inducing a decrease in downstream transgene expression ranging from ~6-fold to ~140-fold relative to uninterrupted rates of translation.

Sillibourne *et al*. implemented the STOP-TRM system to control the level of expression of transgenic IL-12 from CAR T cells. They did so by designing a retroviral vector containing a sequence for a CAR receptor, followed by a STOP-TRM, the self-cleavage peptide domain T2A, and IL-12. In this way, they produced CAR T cells expressing high levels of the CAR receptor (upstream of the STOP-TRM) but reduced levels of IL-12 (downstream of the STOP-TRM), enabling them to prevent the IL-12-induced toxicity observed after in the same murine ACT model. Evidently, this method is not restricted to cytokines and is easily generalisable to any transgene of interest, including TFs. Therefore, the STOP-TRM system provides an approach to modulate the expression of BACH2 in a way that (I) preserves its native structure, that (II) enables downregulation of over an order of magnitude relative to conventional overexpression, and that (III) is compact (the total size of the STOP-TRM is only 9 bp) and simple to implement (it can be easily incorporated into the standard retroviral vectors I have been using up to this point).

Therefore, I designed vectors for dosed expression of BACH2 ($BACH2_{DE}$) based on the same backbone and sequence disposition as in $BACH2_{OE}$ (**Fig. 1-4**), with the addition of a STOP-TRM sequence immediately upstream of the T2A self-cleavage motif. I decided to use two distinct STOP-TRMs which, based on Sillibourne *et al.* work, would result in a decrease in BACH2 expression of approximately 10- and 20-fold relative to the original dose – corresponding to expression levels of 10% and 5% of the original, respectively. I herein refer to these vectors as $BACH2_{DE\text{-}10\%}$ and $BACH2_{DE\text{-}5\%}$ (or $BACH2_{DE}$ collectively) (**Fig. 2-4a**).

To validate that the $BACH2_{DE}$ vectors led to the expected reduction in BACH2 expression, I transduced $CD8^+$ T cells with $BACH2_{OE}$ and $BACH2_{DE}$ vectors containing a 3xFLAG tag at

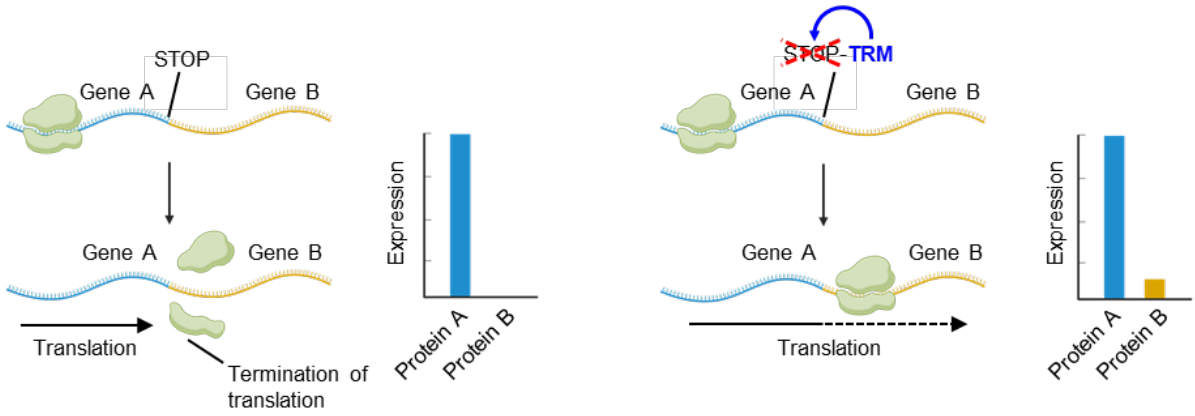

Figure 2-3. A STOP-translational readthrough motif (STOP-TRM) system can be used for controlling the expression of a transgene of interest. Generally, when a ribosome translates an mRNA, translation will be terminated upon reaching a STOP codon (left). However, if the STOP codon is followed by a TRM, translation is only partially suppressed, resulting in downstream translation occurring at lower levels of expression (right).

the N-terminus of BACH2. N-terminal tagging with 3xFLAG is unlikely to disrupt BACH2 function, as mice harbouring this identical modification exhibit no reported physiological abnormalities and the data generated previously using $BACH2_{OE}$ also contained a BACH2 tagged with an N-terminal 3xFLAG. Following transduction, cells were stained with a fluorochrome-conjugated anti-FLAG antibody to detect BACH2 expression via flow cytometry. I observed a clear signal corresponding with the anti-FLAG antibody only in cells transduced with $BACH2_{OE}$, but not in EV-transduced cells. As anticipated, the signal from cells transduced with $BACH2_{DE\text{-}10\%}$ and $BACH2_{DE\text{-}5\%}$ was approximately 10- and 20-fold lower than that of $BACH2_{OE}$, confirming the reliability of these vectors for subsequent experiments (**Fig. 2-4b**).

These data show that the STOP-TRM system enables dosing the expression of BACH2, but how these dosed levels compare to physiological levels of BACH2 remains an outstanding question. To answer this, I used $BACH2^{FLAG}$ mice, which carry a 3xFLAG tag at the N-terminus of the endogenous BACH2 gene (identical to the tag incorporated in our BACH2 expression constructs). This allowed a direct comparison of endogenous and vector-derived BACH2 by flow cytometry. $CD8^+$ T cells from both $BACH2^{FLAG}$ and WT mice were transduced with EV, $BACH2_{OE}$, or $BACH2_{DE}$ vectors and maintained under identical culture conditions (**Fig. 2-4c**). After 48 hours, all groups exhibited a central memory phenotype ($CD44^+$ $CD62L^+$), and any size differences were controlled by normalizing 3xFLAG fluorescence intensity to cell size (**Fig. 2-4d**). In $BACH2^{FLAG}$ mice, EV-transduced cells showed detectable 3xFLAG signal, reflecting endogenous BACH2 expression in central memory cells. Importantly, WT cells transduced with $BACH2_{DE\text{-}5\%}$ vectors expressed 3xFLAG at levels comparable to endogenous BACH2 in $BACH2^{FLAG}$ central memory T cells, while $BACH2_{DE\text{-}10\%}$ drove slightly higher expression and $BACH2_{OE}$ produced a much stronger signal (**Fig. 2-4e**). These results indicate that $BACH2_{DE}$ vectors achieve transgene expression close to physiological BACH2 levels in central memory T cells.

To validate these findings using an alternative method, I quantified BACH2 protein levels by mass spectrometry. This analysis revealed that $BACH2_{DE}$-transduced cells exhibited a total BACH2 copy number (endogenous + transgene) normalised to total protein that was similar to, or slightly higher than, that observed in central memory T cells (**Fig. 2-4f**). The modest differences between this measurement and our 3xFLAG flow cytometry results likely reflect that flow cytometry captured only transgene-derived BACH2, whereas mass spectrometry

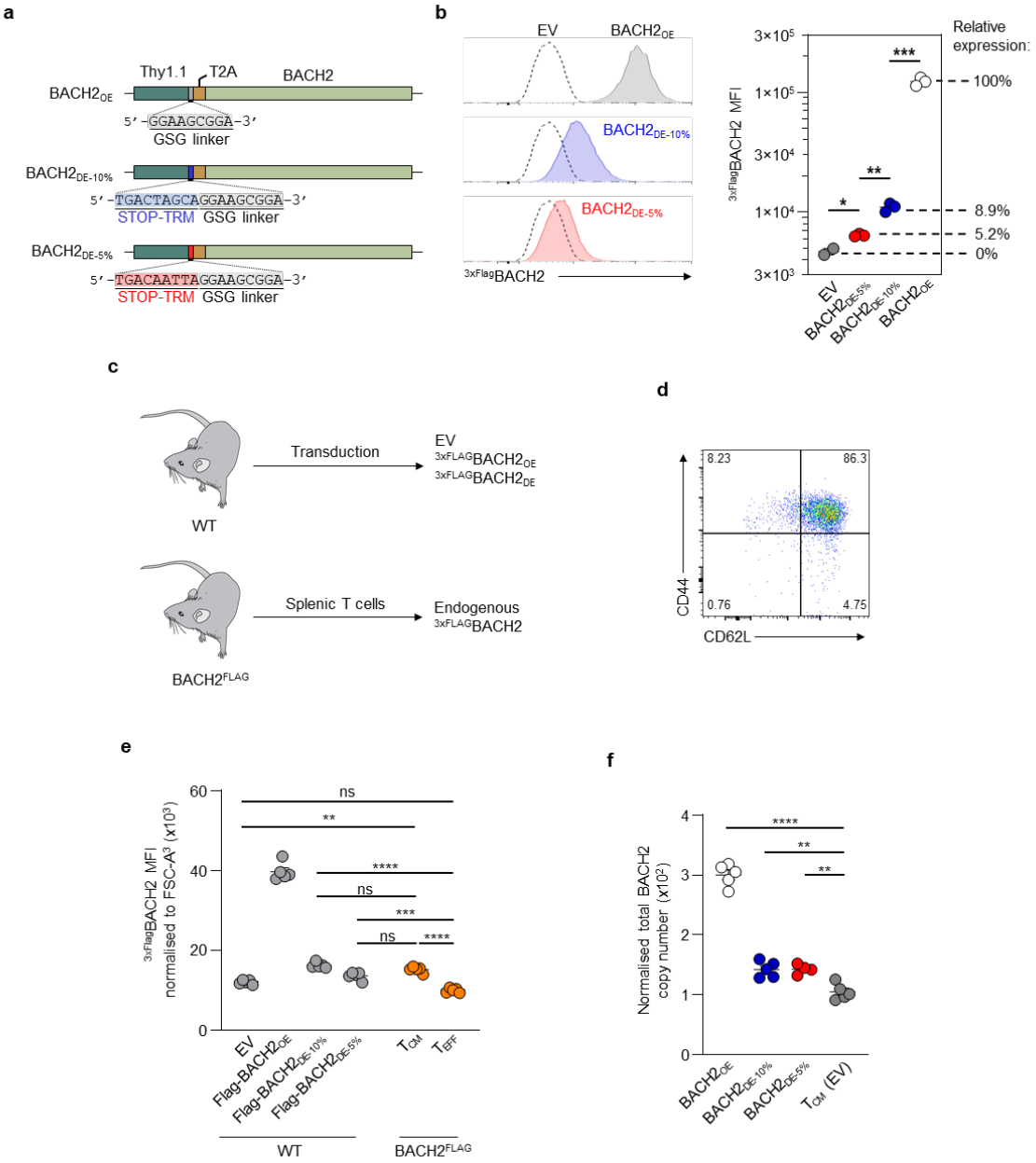
a
Thy1.1
T2A
BACH2
BACH2OE
5′-GGAAGCGGA-3′
GSG linker
BACH2DE-10%
5′-TGACTAGCAGGAAGCGGA-3′
STOP-TRM GSG linker
BACH2DE-5%
5′-TGACAATTAGGAAGCGGA-3′
STOP-TRM GSG linker
b
EV
BACH2OE
BACH2DE-10%
BACH2DE-5%
3xFlagBACH2
3xFlagBACH2 MFI
Relative expression:
100%
8.9%
5.2%
0%
EV
BACH2DE-5%
BACH2DE-10%
BACH2OE
c
Transduction
EV
3xFLAGBACH2OE
3xFLAGBACH2DE
WT
Splenic T cells
Endogenous
3xFLAGBACH2
BACH2FLAG
d
8.23
86.3
0.76
4.75
CD44
CD62L
e
3xFlagBACH2 MFI normalised to FSC-A3 (x10³)
ns
**
****
ns
***
ns
****
EV
Flag-BACH2OE
Flag-BACH2DE-10%
Flag-BACH2DE-5%
TCM
TEFF
WT
BACH2FLAG
f
Normalised total BACH2 copy number (x10²)
****
**
**
BACH2OE
BACH2DE-10%
BACH2DE-5%
TCM (EV)

Figure 2-4. Dosed expression of BACH2 can be achieved using a STOP-TRM system. **a**, Diagram depicting $BACH2_{OE}$ and BACH2 dosed expression ($BACH2_{DE}$) vector designs. All vectors were constructed using the Thy1.1 CDS (transduction reporter), followed by a glycine-serine-glycine (GSG) linker, a STOP-TRM sequence, a T2A self-cleavage motif, and the *Bach2* ORF (CCDS51135.1) tagged N terminally with a 3xFLAG (^{3xFLAG}BACH2). Two distinct STOP-TRM sequences were used: TGA-CTAGCA ($BACH2_{DE\text{-}10\%}$) and TGA-CAATTA ($BACH2_{DE\text{-}5\%}$). **b**, MFI of ^{3xFLAG}BACH2 expression on $CD8^+$ T cells transduced with $BACH2_{OE}$, $BACH2_{DE\text{-}10\%}$ and $BACH2_{DE\text{-}5\%}$. **c**, Diagram depicting experimental mice and vectors used. $BACH2^{FLAG}$-derived cells contain a 3xFLAG tag at the 5' terminus of endogenous *Bach2* loci identical to that present in the $BACH2_{OE}$ and $BACH2_{DE}$ vectors. **d**, Representative flow cytometry plot of CD44 and CD62L expression levels of cultured transduced $CD8^+$ T cells 48 hours post-transduction across all vectors. **e**, Normalised MFI of 3×FLAG–BACH2 in cells from either $BACH2^{FLAG}$ or WT mice transduced with the indicated vectors. 3×FLAG signal was adjusted to cell size to adjust for differences in cell size. The horizontal dotted line indicates the average normalised MFI of EV-transduced $BACH2^{FLAG}$ cells. **f**, Normalised BACH2 protein copy number in cells transduced with the indicated vectors, expressed relative to total cellular protein mass. Data are representative of two independent experiments. ns, non-significant ($P > 0.05$); *, $P < 0.05$; **, $P < 0.01$; ****, $P < 0.0001$. Multiple unpaired two-tailed Student's *t* test with Bonferroni correction (**b**). Horizontal line and error indicate mean ± SEM.

quantified both endogenous and transgenic protein, in addition to employing a different normalization approach.

Collectively, these data show that the STOP-TRM system can be reliably used to modulate the expression of BACH2 down to a range that is comparable to physiological T_{CM} levels, potentially avoiding the effects of supraphysiological expression while avoiding complete loss of expression during effector differentiation. This method can therefore be used to test my hypothesis of whether low but sustained expression of BACH2 leads to improvements in the function of $CD8^+$ T cells under conditions of chronic stimulation.

4.2.3 Dosed expression of BACH2 protects $CD8^+$ T cells from terminal differentiation without compromising their effector functions in vitro

Once I validated that $BACH2_{DE}$ vectors enabled dosed expression of BACH2, I sought to test their functional consequence on T cell differentiation and effector functions. To do that, first started with basic *in vitro* experiments involving multiple rounds of persistent stimulation of transduced T cells. These assays, generally referred to as chronic stimulation, T cell exhaustion or T cell dysfunction assays, have been used widely before to study the transcriptional, metabolic and epigenetic features in Texh[165,166].

For my experiments, I decided to implement a protocol relying on an initial round of stimulation (part of the standard retroviral T cell transduction protocol), followed by two additional rounds of 48-hour stimulations, induced by seeding transduced $CD8^+$ T cells in anti-CD3-coated plates. As a control, I also seeded transduced cells in a non-coated plate and cultured them in identical conditions as those undergoing stimulation. I refer to these experimental groups as 'acutely' and 'chronically stimulated, respectively (**Fig. 2-5a**). To confirm the effects of the chronic stimulation and evaluate the degree of T cell differentiation, I assessed the expression of PD-1 and TIM-3, both of which are known to be upregulated during prolonged periods of stimulation. A pilot test of the assay using EV-transduced $CD8^+$ T cells showed, as expected, that chronically stimulated cells exhibited robust expression of PD-1 and TIM-3, whereas their levels were markedly reduced in the acute stimulation group (**Fig. 2-5b**).

Next, I performed the experiment using OT-I T cells transduced with the EV, $BACH2_{OE}$, $BACH2_{DE\text{-}10\%}$, and $BACH2_{DE\text{-}5\%}$ constructs. Comparing the levels of $PD\text{-}1^+$ $TIM\text{-}3^+$ cells across groups revealed that, consistent with my previous *in vivo* observations, $BACH2_{OE}$ significantly restricted the acquisition of terminal differentiation features compared to EV. Notably, even though BACH2 expression in $BACH2_{DE}$ groups was 10- to 20-fold lower

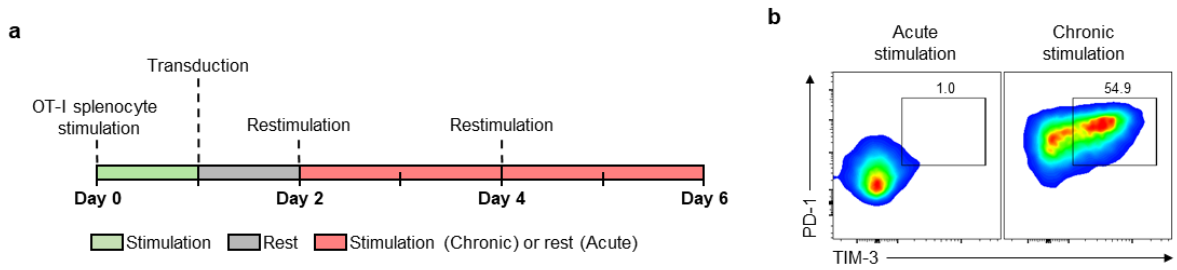

Figure 2-5. Chronic *in vitro* stimulation of CD8$^+$ T cells induces the expression of Texh markers PD-1 and TIM-3. a, Experimental schema. Splenocytes were isolated from OT-I mice, stimulated for 24 hours and rested for an additional 24 hours. Subsequently, cells were under subjected to two rounds of 48-hour stimulation (chronic stimulation) or rested in culture in the absence of stimulation (acute stimulation). **b**, Representative Representative flow cytometry plots showing the expression of PD-1 and TIM-3 in EV-transduced OT-I cells following acute or chronic stimulation.

compared to in $BACH2_{OE}$, cells transduced with $BACH2_{DE}$ vectors retained a phenotype comparable to $BACH2_{OE}$-transduced cells, with a PD-1^+ TIM-3^+ frequency significantly lower relative to EV and only slightly higher than in $BACH2_{OE}$ (**Fig. 2-6a**). An inverted pattern of expression was observed in the memory-associated marker CD62L, which was significantly increased in $BACH2_{OE}$ and, to a lower extent, in $BACH2_{DE}$ cells, relative to EV-transduced cells (**Fig. 2-6b**).

As part of the assay, I also evaluated features associated with acquisition of effector functions, such as cell size – correlated to forward scatter (FSC-A) – and secretion of effector cytokines following a 4-hour restimulation with anti-CD3. Interestingly, despite displaying reduced levels of terminal differentiation, acutely stimulated cells in $BACH2_{DE}$ groups displayed a comparable FSC-A relative to EV-transduced cells. This was not the case in $BACH2_{OE}$ cells, which displayed a lower FSC-A consistent with an impairment in activation-associated cell enlargement (**Fig. 2-6c**). In the same setting, $BACH2_{OE}$-transduced cells, but not $BACH2_{DE}$-transduced cells, displayed a significantly lower level of expression in IFN-γ and TNF relative to the EV group (**Fig. 2-6d**). When the same 4-hour restimulation was applied to chronically stimulated cells, all groups showed visibly decreased cytokine expression levels relative to acutely stimulated cells. In this context, EV and $BACH2_{OE}$ displayed a similar degree of cytokine expression. Nonetheless, cells in the $BACH2_{DE\text{-}10\%}$ group showed a moderately higher level of cytokine expression, while this was even higher in $BACH2_{DE\text{-}5\%}$ cells (**Fig. 2-6d**).

Collectively, these data hint at notable functional differences between $CD8^+$ T cells with high ($BACH2_{OE}$), low ($BACH2_{DE}$), and no (EV) ectopic BACH2 expression. While, like previously observed, $BACH2_{OE}$ protected transduced cells from terminal differentiation during chronic stimulation but at the expense of efficient acquisition of effector functions, cells in the $BACH2_{DE}$ displayed comparable levels of differentiation to the $BACH2_{OE}$ group while maintaining a similar degree of effector functions to the EV group. This data, therefore, suggest that fine-tuning the levels of expression of BACH2 could be an effective method to protect tumour-specific T cells from terminal differentiation without compromising effector functions.

4.2.4 Dosed expression of BACH2 imposes a unique transcriptional state featuring both Tpex and effector characteristics in vitro

To better understand how dosed expression of BACH2 affects $CD8^+$ T cells, I decided to evaluate their transcriptional profile. For achieving this, I employed the previously described chronic stimulation assay on $CD8^+$ T cells transduced with $BACH2_{OE}$, $BACH2_{DE\text{-}10\%}$,

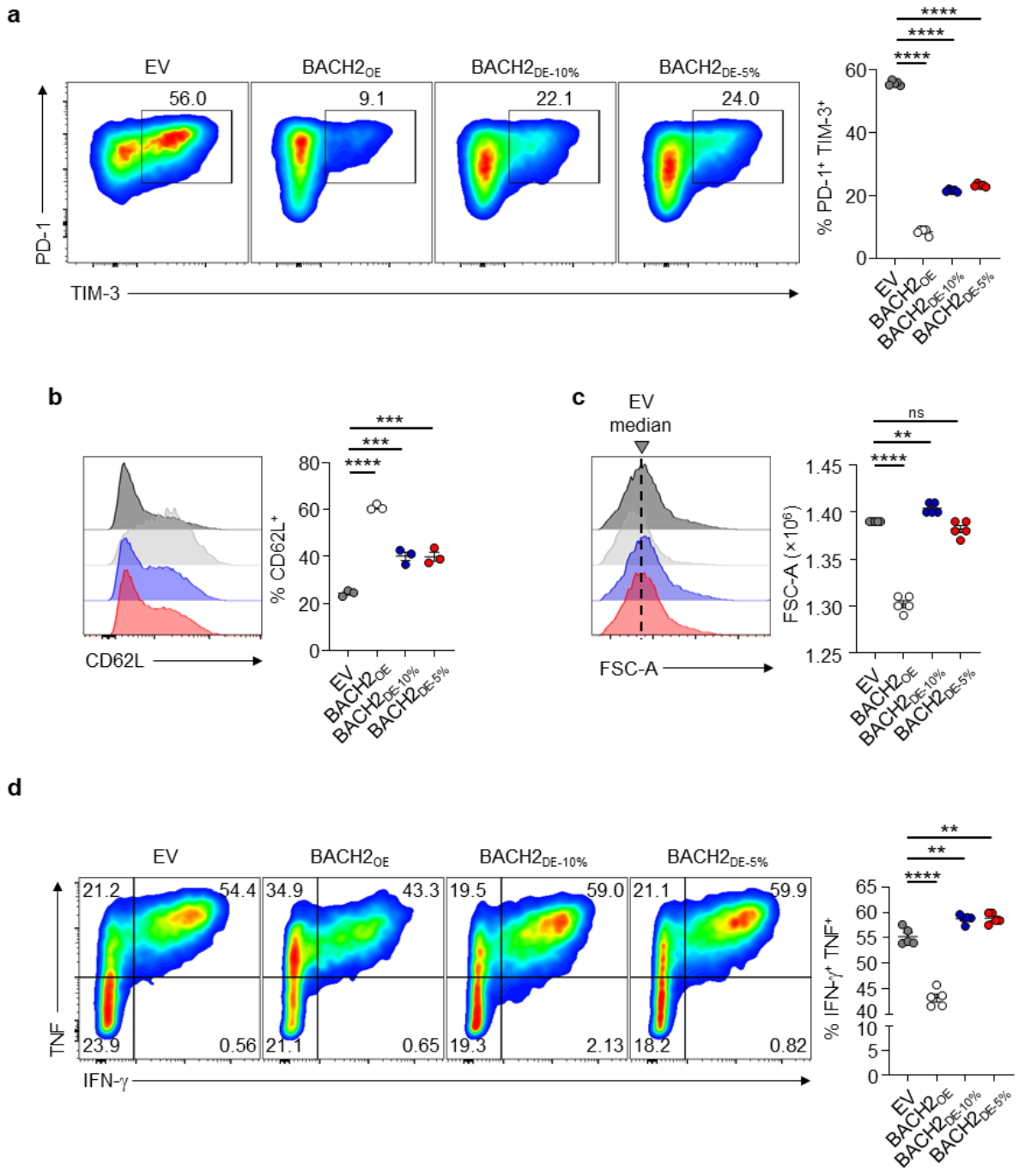
a
EV
BACH2OE
BACH2DE-10%
BACH2DE-5%
56.0
9.1
22.1
24.0
PD-1
TIM-3
% PD-1+ TIM-3+
b
CD62L
% CD62L+
c
EV
median
FSC-A
FSC-A (×10^6)
ns
d
21.2
54.4
23.9
0.56
34.9
43.3
21.1
0.65
19.5
59.0
19.3
2.13
21.1
59.9
18.2
0.82
TNF
IFN-γ
% IFN-γ+ TNF+

Figure 2-6. Dosed expression of BACH2 protects *in vitro* CD8$^+$ T cells from terminal differentiation without compromising their effector functions. a, Frequency of PD-1$^+$ TIM-3$^+$ OT-I T cells transduced with the indicated vectors following chronic stimulation and representative flow cytometry plots. **b**, Frequency of CD62L$^+$ OT-I T cells transduced with the indicated vectors following chronic stimulation and representative flow cytometry histograms. **c**, FSC-A of OT-I T cells transduced with the indicated vectors following acute stimulation and representative flow cytometry histograms. The median FSC-A for EV-transduced cells is indicated in the histogram for reference. **d**, Frequency of IFN-γ^+ TNF$^+$ OT-I T cells transduced with the indicated vectors following a 4-hour anti-CD3-mediated restimulation of acutely stimulated cells in the presence of monensin and brefeldin-A. Data are representative of three independent experiments. ns, non-significant ($P > 0.05$); *, $P < 0.05$; **, $P < 0.01$; ****, $P < 0.0001$. One-way ANOVA with Dunnett's multiple comparison correction (**a-e**). Horizontal lines and error indicate mean ± SEM.

$BACH2_{DE\text{-}5\%}$ and EV vectors, before sorting transduced cells ($Thy1.1^{+}$) via FACS and analysing the enriched populations for bulk RNA-seq.

Firstly, I employed a method of dimensionality reduction, called PCA, to visualise the overall differences in transcriptional profiles between groups. This method captures global variations in gene expression across samples and displays those differences through two unique dimensions (called principal components) that can be readily visualised. This revealed that $BACH2_{OE}$, $BACH2_{DE}$ and EV cells encompassed unique transcriptional profiles, shown through the clustering of the different samples in three distinct groups (**Fig. 2-7a**). The first principal component (PC1), which explained most of the transcriptional variation in the experiment, highlighted stark differences between $BACH2_{OE}$ and the rest of the groups, while PC2 hinted at distinctions between $BACH2_{DE}$ and EV. Notably, $BACH2_{DE\text{-}10\%}$ and $BACH2_{DE\text{-}5\%}$ clustered together in the PCA plot, indicating a high transcriptional similarity between these two groups.

I then proceeded to examine the differences in the expression of individual genes using a heatmap plot displaying all differentially expressed genes (DEGs, $q < 0.05$, $\log_2(FC) > 1$) across all conditions, sorted into clusters using an unbiased clustering algorithm. Interestingly, the gene expression profile of $BACH2_{DE}$ cells did not reflect an 'intermediate' state between the profiles of $BACH2_{OE}$ and EV groups, as it may have been initially assumed. Rather, $BACH2_{DE}$ cells displayed some transcriptional programmes with high similarity to those found in EV cells, while others resembled those in $BACH2_{OE}$ cells, and others still appeared to be completely unique (**Fig. 2-7b**).

In contrast with the EV group, $BACH2_{DE}$-transduced cells induced a set of transcriptional changes that resembled those in $BACH2_{OE}$ (Cluster A, D and F), as well as a set of unique transcriptional programmes (Cluster C). Genes upregulated by both $BACH2_{OE}$ and $BACH2_{DE}$ relative to EV include critical Tpex-associated transcripts, such as *Tcf7* (encoding TCF1), *Id3* (both in Cluster A) and *Slamf6* (Cluster D). Similarly, both groups also showed a notable decrease in the expression of known BACH2 targets associated with terminal differentiation relative to EV, such as *Prdm1* (encoding BLIMP-1), *Entpd1* (CD39) and *Havcr2* (TIM-3) (Cluster F). Among uniquely regulated profiles, $BACH2_{OE}$ (but not EV or $BACH2_{DE}$) shown downregulation of genes associated with effector functions, including *Ccr5*, *Gzma*, *Gzmc*, *Ccr2*, *Cxcr6* and *Id2* (Cluster E). Other genes were exclusively upregulated by $BACH2_{OE}$

condition, such as *Dnmt1*, *Ccl22*, *Kit* and *Socs3* (Cluster B), and a different set upregulated only in the $BACH2_{DE}$ condition, such as *Cd266*, *Il18* and *Ly6a* (Cluster C).

Notably, many of the genes displayed are known to have AP-1 binding motifs and have been previously shown to bind BACH2 directly through chromatin immunoprecipitation sequencing (ChIP-seq) analysis performed in activated $CD8^+$ T cells in a previous study (**Fig. 2-7b**). These include *Cxcr6* and *Ccr2*, both of which have been shown to be bound by BACH2 in their corresponding promoter regions under physiological conditions[131] (**Fig. 2-7c**). Interestingly, these represent two examples of effector-associated genes downregulated only in the context of high BACH2 expression ($BACH2_{OE}$), but not when BACH2 is dosed ($BACH2_{DE}$) as illustrated by the signal intensity of mRNA transcripts in each group. In the case of other genes, such as *Havcr2*, downregulation of mRNA expression happens instead at a similar rate in both $BACH2_{OE}$ and $BACH2_{DE}$.

Finally, I sought to compare how the overall transcriptomes in EV, $BACH2_{OE}$ and $BACH2_{DE}$ compared to reference Tpex and Ttex transcriptional signatures. To do this, I relied on GSEA – a method to estimate the degree of similarity between an RNA-seq dataset comparing two conditions and a pre-selected set of genes associated with a cellular state or phenotype of interest. Using DEGs identified in B16-OVA-derived OT-I Tpex in a different study as reference genes, the GSEA analysis showed that cells from $BACH2_{OE}$, $BACH2_{DE\text{-}10\%}$ and $BACH2_{DE\text{-}5\%}$ exhibited a transcriptional profile that is significantly more similar to that of the reference Tpex signatures compared to EV[75]. Instead, when using Ttex DEGs as reference genes, I observed the opposite: that EV showed, in all cases, a higher degree of similarity than the remaining conditions to a terminally differentiated state (**Fig. 2-7d**).

In summary, the transcriptional data observed here are consistent with the notion that dosed expression of BACH2 induces a unique transcriptional state consistent with a higher degree of retention of stemness-associated Tpex features following chronic stimulation, but without compromising the upregulation of effector-associated genes. Therefore, this suggests that a quantitative change in the expression of a transgene can lead to a qualitative functional difference, with implications for cell engineering strategies in therapeutic contexts such as ACT.

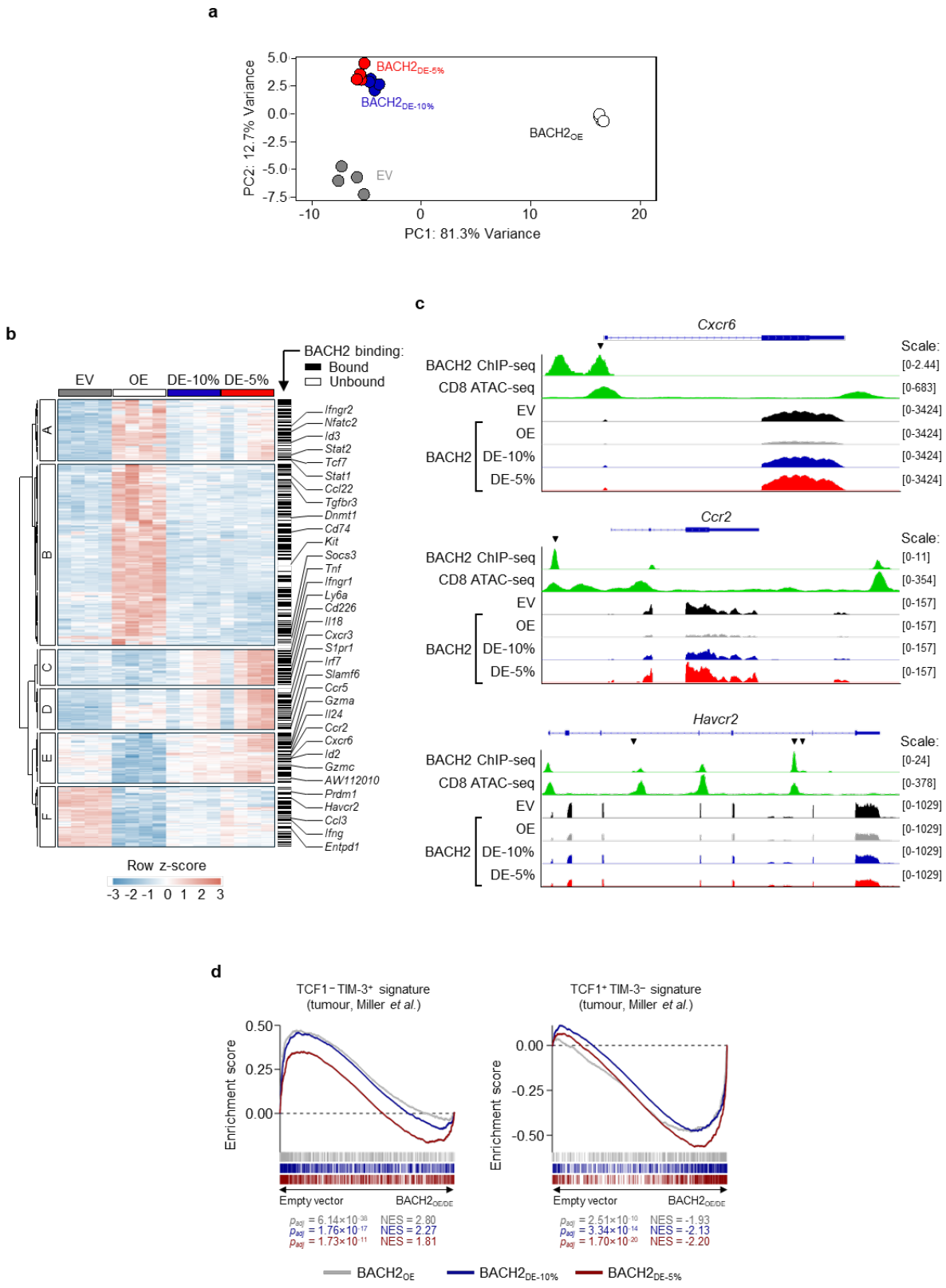
a
PC2: 12.7% Variance
PC1: 81.3% Variance
BACH2DE-5%
BACH2DE-10%
BACH2OE
EV
b
BACH2 binding:
Bound
Unbound
EV
OE
DE-10%
DE-5%
Ifngr2
Nfatc2
Id3
Stat2
Tcf7
Stat1
Ccl22
Tgfbr3
Dnmt1
Cd74
Kit
Socs3
Tnf
Ifngr1
Ly6a
Cd226
Il18
Cxcr3
S1pr1
Irf7
Slamf6
Ccr5
Gzma
Il24
Ccr2
Cxcr6
Id2
Gzmc
AW112010
Prdm1
Havcr2
Ccl3
Ifng
Entpd1
Row z-score
c
Cxcr6
Ccr2
Havcr2
Scale:
BACH2 ChIP-seq
CD8 ATAC-seq
BACH2
d
TCF1⁻TIM-3⁺ signature
(tumour, Miller et al.)
TCF1⁺TIM-3⁻ signature
(tumour, Miller et al.)
Enrichment score
Empty vector
BACH2OE/DE
padj = 6.14×10-36 NES = 2.80
padj = 1.76×10-17 NES = 2.27
padj = 1.73×10-11 NES = 1.81
padj = 2.51×10-10 NES = -1.93
padj = 3.34×10-14 NES = -2.13
padj = 1.70×10-20 NES = -2.20
BACH2OE
BACH2DE-10%
BACH2DE-5%

Figure 2-7. Dosed expression of BACH2 imposes a unique transcriptional state featuring both Tpex and effector characteristics *in vitro*. a, PCA plot displaying transcriptional differences between transduced with EV, $BACH2_{OE}$, $BACH2_{DE\text{-}10\%}$ and $BACH2_{DE\text{-}5\%}$. **b**, Heatmap displaying all differentially expressed genes (DEGs, $q < 0.05$, $\log_2(FC) > 1$) between EV, $BACH2_{OE}$, $BACH2_{DE\text{-}10\%}$ and $BACH2_{DE\text{-}10\%}$. Z-score obtained normalizing gene expression by row and represented by colours. Black bars in the right-hand side indicates genes bound by BACH2 based on chromatin immunoprecipitation sequencing (ChIP-seq) analysis from Roychoudhuri *et al*., 2016. **c**, Alignment plots displaying (from top to bottom) BACH2 ChIP-seq data and assay for transposase-accessible chromatin sequencing (ATAC-seq) performed in a previous study, and bulk RNA-seq data from EV, $BACH2_{OE}$, $BACH2_{DE\text{-}10\%}$ and $BACH2_{DE\text{-}5\%}$ for *Cxcr6*, *Ccr2* and *Havcr2*. **d**, Comparison between chronically stimulated OT-I T cells transduced with EV and $BACH2_{OE}$, $BACH2_{DE\text{-}10\%}$ and $BACH2_{DE\text{-}5\%}$ through GSEA analysis using Tpex (left) or Ttex (right) DEGs as reference genes. NES, normalised enrichment score.

4.2.5 Partial attenuation of AP-1 binding enables $BACH2_{DE}$ to selectively regulate genes with high levels of AP-1-dependency

Following the observation that dosed levels of BACH2 enable retention of certain stem-like characteristics without compromising the acquisition of effector functions, I sought to investigate the molecular mechanisms underpinning this phenotype.

The prior RNA-seq analysis of EV-, $BACH2_{OE}$- and $BACH2_{DE}$-transduced cells revealed two clusters of genes that are of particular interest: Cluster E and Cluster F (**Fig. 2-7b**). Cluster E contained genes whose expression relative to EV was specifically suppressed under conditions of high BACH2 but not dosed BACH2 expression (downregulated only in $BACH2_{OE}$-transduced cells), whereas genes in Cluster F were downregulated under both high and dose-optimised BACH2 expression (downregulated in both $BACH2_{OE}$- and $BACH2_{DE}$-transduced cells) (**Fig. 2-8a**). Therefore, I hypothesised that the identification differences between the regulatory elements in genes belonging to Cluster E and Cluster F may enable me to discern sequence-level determinants of gene regulation under conditions of high and low BACH2 expression.

To test this, I performed motif analysis in the promoter regions of genes in Cluster E and Cluster F (**Fig. 2-8b**). This analysis revealed that promoters of Cluster F genes were more highly enriched for bZIP motifs containing the AP-1 consensus TRE palindromic sequence (TGASTCA), including motifs associated with BATF, Jun-AP1, BATF, and JunB (**Fig. 2-8c**). Consistent with this, the frequency of TRE-containing bZIP motifs was consistently higher in Cluster F promoters compared to Cluster E, as well as to their genome-wide frequency across all promoters) (**Fig. 2-8d**).

These findings suggest that genes in Cluster F are more dependent on AP-1–mediated regulation. Since BACH2 is known to regulate transcription primarily by binding to and sterically hindering TRE-containing motifs, it is likely this increased dependency in AP-1 regulation makes genes in Cluster F more susceptible to BACH2-mediated suppression at lower doses. An additional determinant may be the density of TRE-containing motifs within a given locus, with promoters containing a higher "concentration" of these motifs functioning as high-affinity targets for BACH2 even at low expression levels.

In addition to differences in the set of target genes, the prior transcriptomic analysis also revealed changes in the overall dose of expression of BACH2 target genes under different levels of BACH2 expression. This could represent an additional layer of mechanistic regulation

leading to distinct overall functional and phenotypic outcomes. To investigate how this may occur, I performed genome-wide measurement of chromatin accessibility and occupancy of the AP-1 transcription factor JunB in chronically stimulated $CD8^+$ T cells transduced with vectors enforcing conventional high-dose overexpression and dose-optimised expression of BACH2.

This analysis revealed that while chromatin accessibility at BACH2 binding sites was minimally altered by $BACH2_{OE}$ and $BACH2_{DE}$, binding of the AP-1 factor JunB was substantially affected (**Fig. 2-8e-f**). Notably, $BACH2_{OE}$ resulted in substantial loss of JunB binding at BACH2 target sites, whereas $BACH2_{DE}$ resulted in only partial attenuation of JunB binding at these sites. This was apparent at known and putative enhancers of key genes associated with T cell effector differentiation and terminal differentiation including *Ttc39c*, *Havcr2* and *Entpd1*, as well as other known BACH2 target genes. Consistent with the dampening of AP-1 binding, transcript levels reflected a graded expression mRNA expression of target genes, with $BACH2_{DE}$ typically yielding intermediate expression between EV and $BACH2_{OE}$ (**Fig. 2-8g**).

In summary, these data suggest that AP-1 dependency at the gene regulatory level and the degree of occupancy of AP-1 factors such as JunB are an important determinant of the downstream functional consequences derived from dose-optimised BACH2 expression. Together, these findings provide mechanistic insight into how BACH2 regulates gene expression under low-dose conditions.

4.3 Discussion

Throughout this section, I have investigated the functional consequences of modulating the level of expression of BACH2 in $CD8^+$ T cells under conditions of acute and chronic stimulation. This hypothesis originated from an initial observation in which different intratumoral T cell subsets displayed varying levels of expression of BACH2, suggesting a potential functional role in the regulation of its dose throughout the anti-tumour response.

Both transcriptomic data from human samples and the *Bach2*$^{tdRFP/+}$ mouse model were used to understand the dynamics of BACH2 expression in intratumoral $CD8^+$ T cells. However, clear caveats exist with the methodology employed. For instance, none of the two methods took into account levels of protein BACH2 and instead relied on mRNA expression and a fluorescent reporter. In the case of the transcriptomic data, despite being a method that can enable detailed biological insights in many contexts, scRNA-seq can lack the resolution needed to accurately subdivide different subsets of a given cell type. This makes the technique more appropriate for

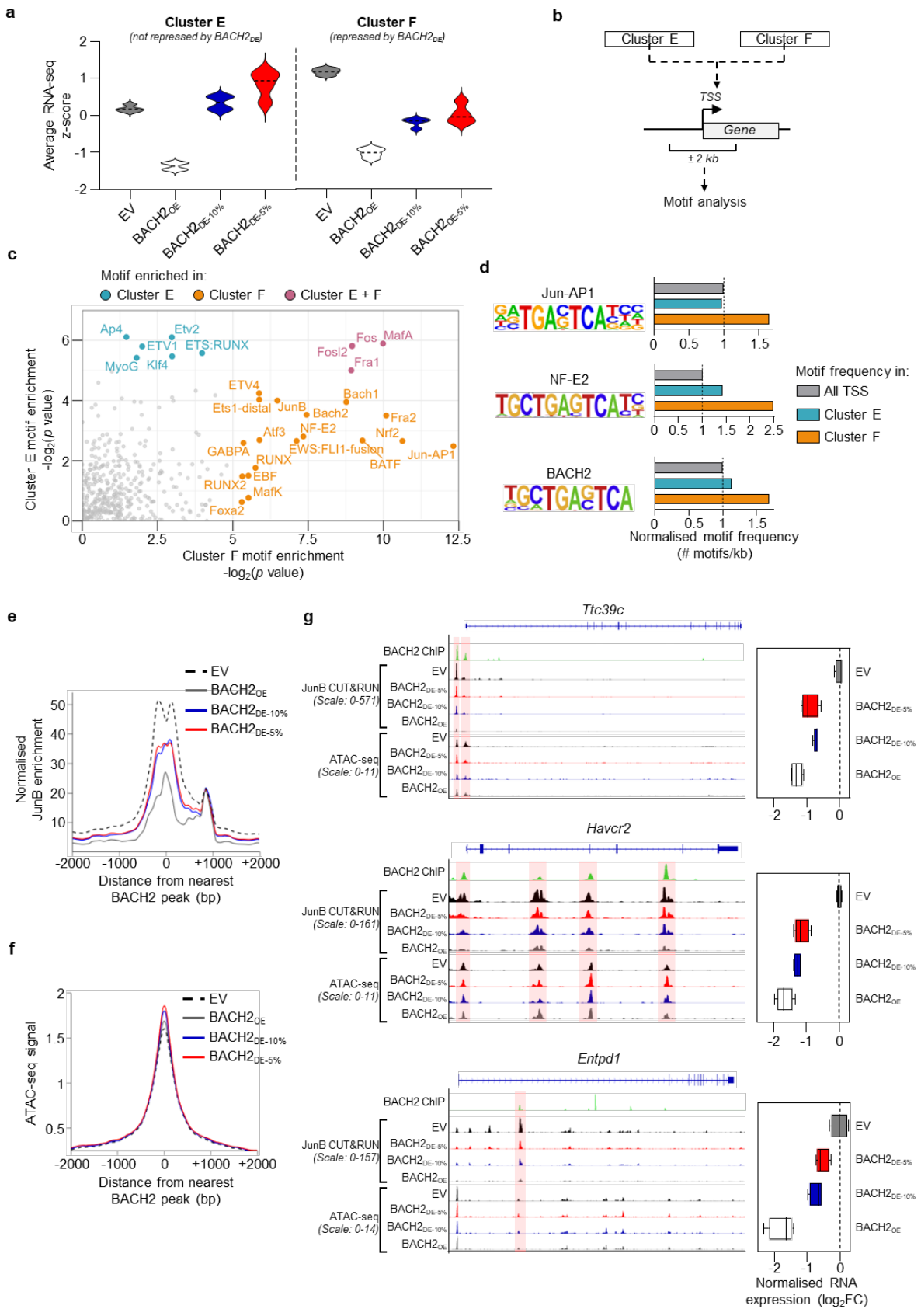
a
Cluster E
(not repressed by BACH2DE)
Cluster F
(repressed by BACH2DE)
Average RNA-seq z-score
EV
BACH2OE
BACH2DE-10%
BACH2DE-5%
b
Cluster E
Cluster F
TSS
Gene
±2 kb
Motif analysis
c
Motif enriched in:
Cluster E
Cluster F
Cluster E + F
Cluster E motif enrichment -log2(p value)
Cluster F motif enrichment -log2(p value)
Ap4
Etv2
ETV1
ETS:RUNX
MyoG
Klf4
Fos
MafA
Fosl2
Fra1
ETV4
Bach1
Ets1-distal
JunB
Bach2
Fra2
Atf3
NF-E2
Nrf2
GABPA
RUNX
EWS:FLI1-fusion
BATF
Jun-AP1
EBF
RUNX2
MafK
Foxa2
d
Jun-AP1
NF-E2
BACH2
Motif frequency in:
All TSS
Cluster E
Cluster F
Normalised motif frequency (# motifs/kb)
e
EV
BACH2OE
BACH2DE-10%
BACH2DE-5%
Normalised JunB enrichment
Distance from nearest BACH2 peak (bp)
f
ATAC-seq signal
Distance from nearest BACH2 peak (bp)
g
Ttc39c
Havcr2
Entpd1
BACH2 ChIP
JunB CUT&RUN (Scale: 0-571)
JunB CUT&RUN (Scale: 0-161)
JunB CUT&RUN (Scale: 0-157)
ATAC-seq (Scale: 0-11)
ATAC-seq (Scale: 0-14)
Normalised RNA expression (log2FC)

Figure 2-8. AP-1 motif enrichment and attenuated JunB binding are associated with sensitivity to repression by $BACH2_{DE}$. a, Average normalised expression of genes belonging to Clusters E and F from the RNA-seq dataset shown in Fig. 2-7b. **b**, Schematic representation of TF motif enrichment analysis. Regions spanning ±2 kb from the transcriptional start site (TSS) of genes in Clusters E and F were analysed for motif enrichment. **c**, TF motifs significantly enriched near TSS of Cluster E and F genes ($-\log_2$ p-value > 5). **d**, Relative frequency of selected TF motifs within ±2 kb of Cluster E and F TSS, normalised against their occurrence near all annotated TSS across the mouse genome. **e-f**, JunB binding measured by CUT&RUN (e) and chromatin accessibility measured by ATAC-seq (**f**) in chronically stimulated cells transduced with the indicated vectors, plotted relative to BACH2 binding peak centers. **g**, Alignments showing JunB occupancy and chromatin accessibility at representative loci in chronically stimulated cells transduced with the indicated vectors (left). Corresponding normalised RNA-seq $\log_2$ fold changes for these genes are shown (right).

situations where different cell types need to be distinguished (i.e. T cells, macrophages, Tregs, NK cells, etc…), as opposed to different subsets (i.e. effector $CD8^+$ T cells, memory $CD8^+$ T cells, Tpex, Ttex, etc…). Furthermore, while the use of RFP as a reporter of *Bach2* expression has several benefits (as described previously), its stability and turn-over rate differ from that of BACH2 – particularly considering how post-translational modifications driven by TCR signalling can influence its rate of degradation.

Importantly, the overall direction of my doctoral research has been shaped not just by the biological questions at hand, but also by time and resource constraints. As such, I decided to focus on exploring the hypothesis that dosed BACH2 expression can be implemented in therapeutic applications, instead of characterising its role in physiological anti-tumour responses. Nonetheless, the latter certainly remains a relevant area of further research. Sorting techniques (e.g. FACS or magnetic sorting) in combination with methods for characterising the behaviour and levels of BACH2 in different subsets (e.g. proteomics, ChIP-seq, evaluation of binding partners, etc…) could be used to confirm the observations that different subsets display differences in BACH2 expression throughout the anti-tumour response, as well as to reveal the corresponding functional implications.

One set of interesting findings from this Chapter are the insights into the mechanism underpinning the differences observed with BACH2 dosing. These revealed an increase in the frequency of AP-1 motifs within the promoter regions of genes regulated by dosed levels of BACH2, which could represent a plausible mechanism through which different genes are regulated in this system. However, it is important to acknowledge that the data presented herein does not conclusively show this is the case, as it is purely correlational in nature. Further experiment would be required to understand whether this is the case, as well as to quantify how the 'concentration' of BACH2 target sites in particular promoters affects its affinity towards such loci. The use of biochemical techniques such as electrophoretic mobility shift assays to measure the affinity of BACH2 towards DNA sequences with varying number of AP-1 motifs, or genetic engineering of T cells using reporter genes with multiple copies of BACH2 binding sites in its promoter region, could be interesting strategies to test this.

It is also worth noting that, despite the wide use of *in vitro* chronic stimulation assays, there are likely important differences between this model and the exhausted phenotype of tumour-specific T cells *in vivo*. In the *in vitro* model used here, activation is induced via antibody-mediated cross-linking of CD3, which forms part of the TCR complex. While this mechanism

of activation attempts to emulate the TCR clustering that occurs when $CD8^+$ T cells encounter tumour cells expressing a complementary pMHC, differences in the affinity and duration of the binding are likely to result in functional and phenotypic discrepancies. A clear example of this is the level of cytokine suppression in following restimulation of cells derived from *in vitro* versus *in vivo* assays in BACH2-overexpressing cells. As shown in prior data, *in vivo*-derived tumour-specific cells transduced with $BACH2_{OE}$ show minimal levels of cytokine secretion upon restimulation (**Fig. 1-6b**). Nonetheless, after using the same restimulation method in chronically stimulated cells, well over half of all $BACH2_{OE}$ cells produced cytokines at detectable levels (even if at lower levels than EV or $BACH2_{DE}$ cells) (**Fig. 2-6d**). Thus, it remains important to account for this caveat when interpreting data from these types of assays.

To this end, I proceeded to evaluate how BACH2 dosing affects tumour-specific $CD8^+$ T cells in an *in vivo* setting. The observation that stemness features can be retained without compromising effector functions are a promising indication that this could be a viable method for protecting T cells from the detrimental effects of terminal differentiation. This will be the main focus of the next chapter.

5. Chapter 3: BACH2 and FOXO1 dosing enhance anti-tumour responses *in vivo*

5.1 Background

Having identified a method to successfully modulate the dose of BACH2 and demonstrated that it preserves $CD8^+$ stemness in the context of chronic stimulation without compromising effector functions, I moved to testing this setting *in vivo*. While the previously observed *in vitro* results are a promising, it is not guaranteed that the same phenotype will be maintained in an *in vivo* setting. For instance, the duration of stimulation within a tumour is days or weeks, and many other microenvironmental factors can play a role in T cells' ability to maintain effector functions. More importantly, even if $CD8^+$ T cells modified with dosed BACH2 did maintain a higher degree of stemness, the extent to which the overall anti-tumour response would change is uncertain. Hence, I will focus on elucidating whether (I) an improvement in the anti-tumour response is observed, and (II) what are the phenotypic and transcriptomic changes enforced by BACH2 dosing in an *in vivo* setting. A third question that will be addressed, relevant to the broader context of dosing memory-associated factors for improving T cell therapy responses, is whether the observed biological outcomes are relevant just to BACH2 or is an idea that can be expanded to other TFs.

5.2 Results

5.2.1 Low-dose expression of BACH2 enhances anti-tumour $CD8^+$ T cell therapy responses in vivo

To test whether dosed expression of BACH2 has an impact in $CD8^+$ T cell-mediated anti-tumour immunity, I relied on the previously optimised ACT model. B16-OVA cells were subcutaneously injected into the flanks of WT mice to induce tumour growth. In parallel, OT-I T cells were isolated and transduced with one of four different constructs: $BACH2_{OE}$, $BACH2_{DE\text{-}10\%}$, $BACH2_{DE\text{-}5\%}$ or EV. Once visible and established tumours had been formed, mice were irradiated using 3.5 Gy and treated with transduced OT-I T cells (**Fig. 1-5a**). Notably, while mice treated with $BACH2_{OE}$-transduced T cells displayed a moderately worse tumour control compared to EV consistent with previous observations, mice treated with OT-I T cells expressing the $BACH2_{DE\text{-}10\%}$, $BACH2_{DE\text{-}5\%}$ constructs showed a significant improvement in anti-tumour control (**Fig. 3-1a-b**).

Since both the phenomenon of terminal differentiation and the effects of ectopic BACH2 expression are most likely cell-intrinsic, I hypothesised that the benefits of low-dose BACH2 expression may be broadly applicable to other types of tumours. To test this hypothesis, I repeated the experiment using a different, yet still widely used, tumour model: MC38-OVA. Like B16-OVA, MC38-OVA is a murine-derived tumour cell line (colon adenocarcinoma as opposed to melanoma) expressing OVA and hence also recognised by OT-I T cells. Since MC38-OVA cells are known to be more susceptible to irradiation, a reduced dose to 2.5 Gy (as opposed to 3.5 Gy) was used based on prior optimisation performed by other members in my laboratory (data not shown).

Using the MC38-OVA cell line and implementing the reduced irradiation dose, I repeated the experiment with the EV, $BACH2_{DE\text{-}10\%}$, $BACH2_{DE\text{-}5\%}$. Consistent with the results observed using the B16-OVA model, low-dose expression of BACH2 led to a significantly increased anti-tumour response as observed by a reduction in the final size of tumours (**Fig. 3-1c-d**).

Notably, these results represent consistent and reproducible evidence that inducing low-dose expression of BACH2 in $CD8^+$ T cells can enhance the efficacy of ACT. This not only suggests that protecting cells from terminal differentiation can have a real impact in the therapeutic efficacy of ACT and has important implications for the design of the next-generation of T cell therapies.

5.2.2 Low-dose expression of BACH2 results in higher number of intratumoral T cells but does not affect the proportion of Tpex and Ttex

Following the observation that dosing the expression of BACH2 improves anti-tumour immunity in *in vivo* models of ACT, I sought to understand its effect in the phenotype of transduced intratumoral OT-I T cells. To do this, I performed the ACT experiments as previously described, except treated tumour-bearing mice were sacrificed approximately three weeks following initial treatment for dissection and analysis of tumour tissues (**Fig. 1-5a**).

Firstly, I wanted to determine whether there were any differences in the number of intratumoral OT-I T cells between different groups. To account for sample-to-sample variability caused by tumour size differences, I normalised the number of cells to the total mass of tumour dissected from each individual mouse. When gating on OT-I T cells with a Tpex phenotype ($PD\text{-}1^+$ $TIM\text{-}3^-$ $TCF1^+$), I observed that cells in the $BACH2_{OE}$ group displayed a significant increase in the number of tumour-specific T cells that was several folds higher compared to the EV group (**Fig. 3-2a**). Instead, when shifting the focus to more differentiated subsets such as Ttex ($PD\text{-}1^+$ TIM-

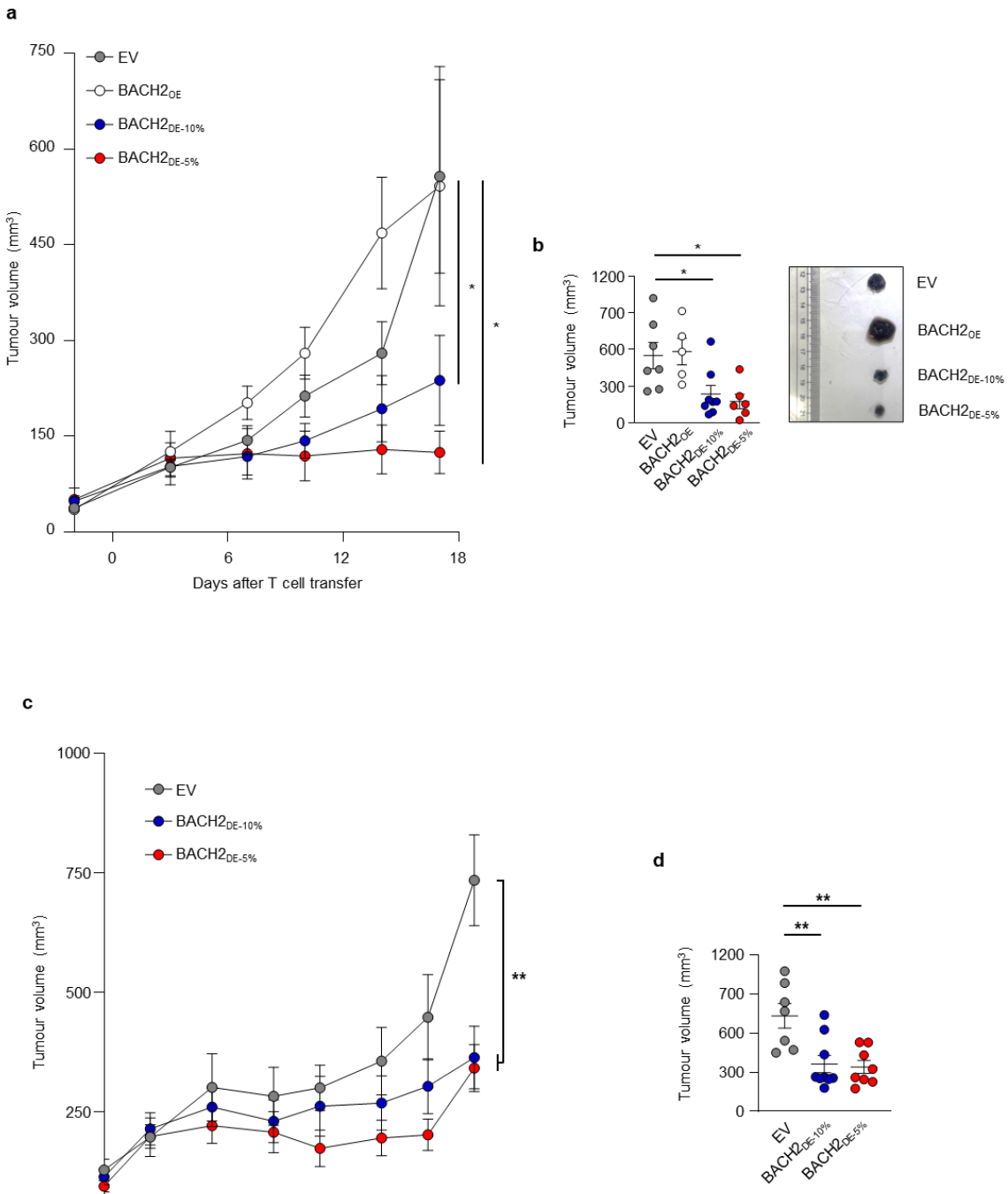
a
750
600
450
300
150
0
EV
BACH2OE
BACH2DE-10%
BACH2DE-5%
Tumour volume (mm3)
0
6
12
18
Days after T cell transfer
*
*
b
1200
700
600
300
0
Tumour volume (mm3)
*
*
EV
BACH2OE
BACH2DE-10%
BACH2DE-5%
c
1000
750
500
250
0
EV
BACH2DE-10%
BACH2DE-5%
Tumour volume (mm3)
0
7
14
21
Days after T cell transfer
**
d
1200
700
600
300
0
Tumour volume (mm3)
**
**
EV
BACH2DE-10%
BACH2DE-5%

Figure 3-1. Low-dose expression of BACH2 enhances anti-tumour CD8$^+$ T cell therapy responses *in vivo*. **a-b**, Tumour volume of mice bearing B16-OVA after sublethal irradiation (3.5 Gy) and adoptive transfer of 0.5×10^6 transduced OT-I T cells (**a**), and tumour volumes at day 15-17 post-T cell transfer (**b**). **c-d**, Tumour volume of mice bearing MC38-OVA after sublethal irradiation (2.5 Gy) and adoptive transfer of 0.5×10^6 transduced OT-I T cells (**c**), and tumour volumes at day 21 post-T cell transfer (**d**). ns, non-significant ($P > 0.05$); *, $P < 0.05$; **, $P < 0.01$; ****, $P < 0.0001$. One-way ANOVA with Dunnett's multiple comparison correction (**a-d**). Points indicate average measurement at the indicated day (**a, c**), horizontal bars indicate mean (**b, d**), error bars indicate ± SEM.

3^+ $TCF1^-$), $BACH2_{OE}$ cells were nearly entirely absent, consistent with previous observations of high levels of BACH2 preventing differentiation (**Fig. 3-2b**).

Interestingly, the number on intratumoral OT-I T cells from both $BACH2_{DE}$ groups was significant increased compared to EV, not just in Tpex, but also in the Ttex population (**Fig. 3-2a-b**). This difference between the distribution of cells across subpopulations in $BACH2_{OE}$ and $BACH2_{DE}$ suggests that ectopic expression of modulated levels of BACH2 may enhance the persistence and/or expansion potential of intratumoral T cells without compromising differentiation into effector subsets, unlike high levels of BACH2.

Following tumour excision and lymphocyte enrichment, part of the samples underwent a 4-hour anti-CD3 stimulation to assess cytokine expression. Consistent with *in vitro* observations, cells transduced with the $BACH2_{OE}$ construct displayed an overall significantly lower frequency of cells expressing effector molecules compared to EV-transduced cells. On the other hand, there were no statistically significant differences between EV and either of the $BACH2_{DE}$, reiterating the notion that dosed levels of BACH2 do not compromise acquisition of effector functions (**Fig. 3-2c-d**). Nonetheless, when evaluating relative numbers of transduced cytokine-expressing T cells per gram of tumour, both $BACH2_{DE\text{-}10\%}$ and $BACH2_{DE\text{-}5\%}$ groups displayed a significantly higher number than EV consistent with an overall higher number of intratumoral OT-I T cells with retained effector functions (**Fig. 3-2e**).

Next, I sought to study how dosing BACH2 expression affects the differentiation rate of Tpex and Ttex within the tumour. EV cells showed a balanced distribution between Tpex and Ttex, while overexpression of BACH2 at high levels curtailed T cell differentiation and led to almost all transduced cells retaining a Tpex phenotype. This is consistent with the results observed previously. However, when focusing on the $BACH2_{DE\text{-}10\%}$ and $BACH2_{DE\text{-}5\%}$ groups, the data diverged from what I expected based on prior *in vitro* assays. While previously the phenotype of $BACH2_{DE}$-transduced cells was skewed towards a Tpex state, the results from the *in vivo* models suggests that the proportion of Tpex and Ttex cells remains minimally altered compared to EV (**Fig. 3-2f**).

In conclusion, the data from the *in vivo* ACT models reveals two key insights about the effect of dosing BACH2 in anti-tumour $CD8^+$ T cells. The first is that dosing BACH2 drives an increase in the number of intratumoral T cells with preserved effector function, which may well underpin the enhanced anti-tumour responses observed in the *in vivo* ACT models. The second observation is that, despite leading to a preserved Tpex phenotype *in vitro*, intratumoral T cells

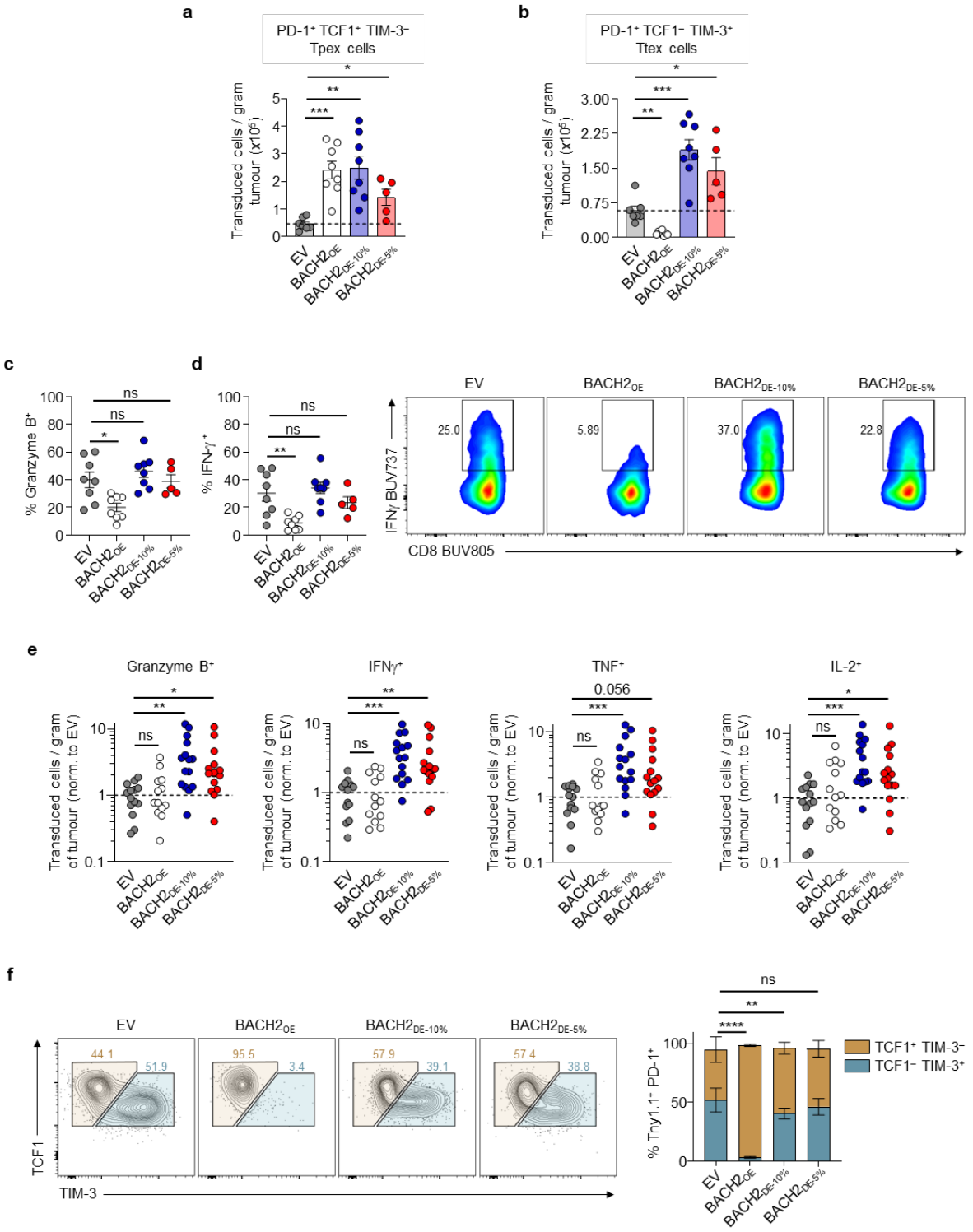
a
PD-1+ TCF1+ TIM-3−
Tpex cells
Transduced cells / gram tumour (x10⁵)
EV
BACH2OE
BACH2DE-10%
BACH2DE-5%
b
PD-1+ TCF1− TIM-3+
Ttex cells
c
% Granzyme B+
d
% IFN-γ+
EV
BACH2OE
BACH2DE-10%
BACH2DE-5%
IFNγ BUV737
CD8 BUV805
25.0
5.89
37.0
22.8
e
Granzyme B+
IFNγ+
TNF+
IL-2+
0.056
Transduced cells / gram of tumour (norm. to EV)
f
TCF1
TIM-3
44.1
51.9
95.5
3.4
57.9
39.1
57.4
38.8
% Thy1.1+ PD-1+
TCF1+ TIM-3−
TCF1− TIM-3+

Figure 3-2. Low-dose expression of BACH2 results in higher number of intratumoral T cells but does not affect the proportion of Tpex and Ttex. a-b, Number of intratumoral transduced OT-I T cells per gram of tumour in the indicated groups, gated on Tpex (**a**) and Ttex (**b**) populations. **c**, Absolute difference in the frequency of intratumoral OT-I T cells transduced with the indicated vectors and normalised to EV, (co)-expressing the indicated number effector molecules (IL-2, Granzyme B, IFN-γ and TNF) upon anti-CD3-mediated *ex vivo* restimulation. Pie charts represent the average cell frequency from each group that are expressing different number of effector molecules. Statistical significance represents differences compared to EV. **c-d,** Proportion of Granzyme B^+ (**c**) and IFN-γ^+ (**d**) intratumoral OT-I T cells transduced with the indicated vectors following *ex vivo* 4-hour restimulation and representative flow cytometry plots (**d**). **e**, Quantification of the absolute number of tumour-infiltrating transduced OT-I T cells per gram of tumour expressing the indicated effector molecule normalised to EV. Data are representative of three independent experiments. **f**, Quantification of TCF1 and TIM-3 frequency of expression in tumour-infiltrating transduced PD-1^+ OT-I T cells and representative flow cytometry plots. Statistical significance represents difference in frequency of $TCF1^+$ $TIM\text{-}3^-$ cells with that of the EV population. Data in (**e-f**) were pooled from two independent experiments. ns, non-significant ($P > 0.05$); *, $P < 0.05$; **, $P < 0.01$; ****, $P < 0.0001$. One-way ANOVA with Dunnett's multiple comparison correction (**a-f**). Bars and error indicate mean ± SEM.

expressing low levels of BACH2 differentiated towards a Ttex state at approximately the same rate as EV-transduced cells.

5.2.3 BACH2 dosing induces transcriptional changes in a subset-specific manner

After observing that modulating BACH2 expression influenced the phenotype and abundance of tumour-specific T cells *in vivo*, I asked what transcriptomic differences would drive this phenotype and whether these could help clarify how BACH2 dosing affects cells at the mechanistic level. Furthermore, I hypothesised that the transcriptomic changes driven by BACH2 dosing may differ at different stages of differentiation. Thus, I decided to use the surface marker Slamf6, which has been previously reported to be a reliable surrogate marker indicating TCF1 expression, to sort subsets in a higher (Slamf6^{-}, associated with an effector and Ttex phenotypes) and lower (Slamf6^{+}) state of differentiation[75].

OT-I T cells transduced with EV, BACH2$_{OE}$, BACH2$_{DE\text{-}10\%}$ or BACH2$_{DE\text{-}5\%}$ vectors were administered to mice bearing established B16-OVA tumours following irradiation, as previously described. After 18 days, mice were sacrificed, and tumour tissues were dissected and processed into single-cell suspensions. Subsequently, FACS was used to enrich for transduced Slamf6^{-} and Slamf6^{+} OT-I T cells, resulting in 8 different experimental groups (EV, BACH2$_{OE}$, BACH2$_{DE\text{-}10\%}$ or BACH2$_{DE\text{-}5\%}$, with Slamf6^{-} and Slamf6^{+} populations for each vector). Nonetheless, as previously observed, high levels of BACH2 restricts T cell differentiation, and thus too few cells were recovered for BACH2$_{OE}$ Slamf6^{-}, forcing me to exclude this group form the experiment and limit subsequent analyses to 7 experimental groups (**Fig. 3-3a**). Once sorted, bulk RNA-seq was used to gather transcriptomic data of the different groups.

Next, I aimed to identify the key transcriptional differences between groups that might explain the observed phenotypic variations. Hierarchical cluster analysis of DEGs revealed differential expression of genes among Slamf6^{+} and Slamf6^{-} compartments (**Fig. 3-3b-c**). Both EV and BACH2$_{DE}$ Slamf6^{+} cells showed higher expression of genes associated with a Tpex cell phenotype when compared to Slamf6^{-} cells, such as *Id3* and *Cxcr5* (Cluster A). *Slamf6* was also included in the same cluster, consistent the use of Slamf6 expression during the enrichment of the different populations. However, BACH2$_{DE}$ cells showed transcriptional programmes that diverged from those observed in EV. Notably, I observed a subset of genes appearing to become downregulated upon Slamf6^{-} differentiation in EV-transduced cells, which were instead retained in BACH2$_{DE}$-transduced cells (Cluster B), including memory-associated genes such

as *Klf3* and *Tcf7*. In addition, a smaller gene subset (Cluster C) showed similar levels of expression between EV Slamf6$^-$ cells and both BACH2$_{DE}$ Slamf6$^+$ and Slamf6$^-$ cells, while a fourth set (Cluster D) included a group of genes either upregulated in Slamf6$^-$ cells across both EV and BACH2$_{DE}$, or displaying a similar expression mean across all cell subsets.

Notably, many of the identified DEGs between EV Slamf6$^+$ and Slamf6$^-$ also showed changes in the BACH2$_{DE}$-transduced Slamf6$^+$ and Slamf6$^-$ cells, but at considerably lower scale. This is clear when comparing normalised counts in genes such as *Tcf7* and *Klf3*. EV cells undergoing Slamf6$^+$ to Slamf6$^-$ differentiation are known to lose expression of memory-associated genes like *Tcf7* and *Klf3*, which is consistent with the observed reduction in normalised counts (**Fig. 3-3d**). The same comparison in cells from both BACH2$_{DE}$ groups also show a noticeable decrease in normalised counts, but the magnitude of this change is far lower (and hence does not reach the significance threshold).

In all, these data suggests that low-dose expression of BACH2 affects the transcriptional profile of CD8$^+$ T cells in a subset-specific manner, leading to unique transcriptional profiles in Slamf6$^+$ to Slamf6$^-$ populations compared to EV-transduced cells. Furthermore, transcriptional programmes generally associated with less differentiated Slamf6$^+$, such as the expression of memory-associated genes, are maintained upon Slamf6$^-$ differentiation in cells ectopically expressing low levels of BACH2. This maintained expression of Slamf6$^+$-associated programmes in more differentiated T cells may be key for the mechanism underlying the improved performance of anti-tumour responses observed previously.

5.2.4 BACH2 dosing preserves Slamf6$^+$ transcriptional features upon Slamf6$^-$ differentiation

The observations that dosed expression of BACH2 preserves the expression of memory-associated genes in Slamf6$^-$ cells to levels comparable to those found in Slamf6$^+$ cells led me to investigate the overall transcriptional similarity between the two populations in cells transduced with EV and BACH2$_{DE}$ vectors. To do this, I used unbiased hierarchical clustering in a Pearson similarity matrix to compare the distribution of samples from different conditions (**Fig. 3-4a**). Slamf6$^+$ and Slamf6$^-$ samples for all vectors were appropriately distributed at opposite halves of the matrix. Notably, EV Slamf6$^+$ and Slamf6$^-$ groups displayed the lowest degree of similarity and were clustered at opposite ends of the matrix. On the other hand, Slamf6$^+$ and Slamf6$^-$ samples transduced with BACH2$_{DE}$ clustered more closely and displayed an overall lower Pearson distance among them. Notably, as previously observed, there was high

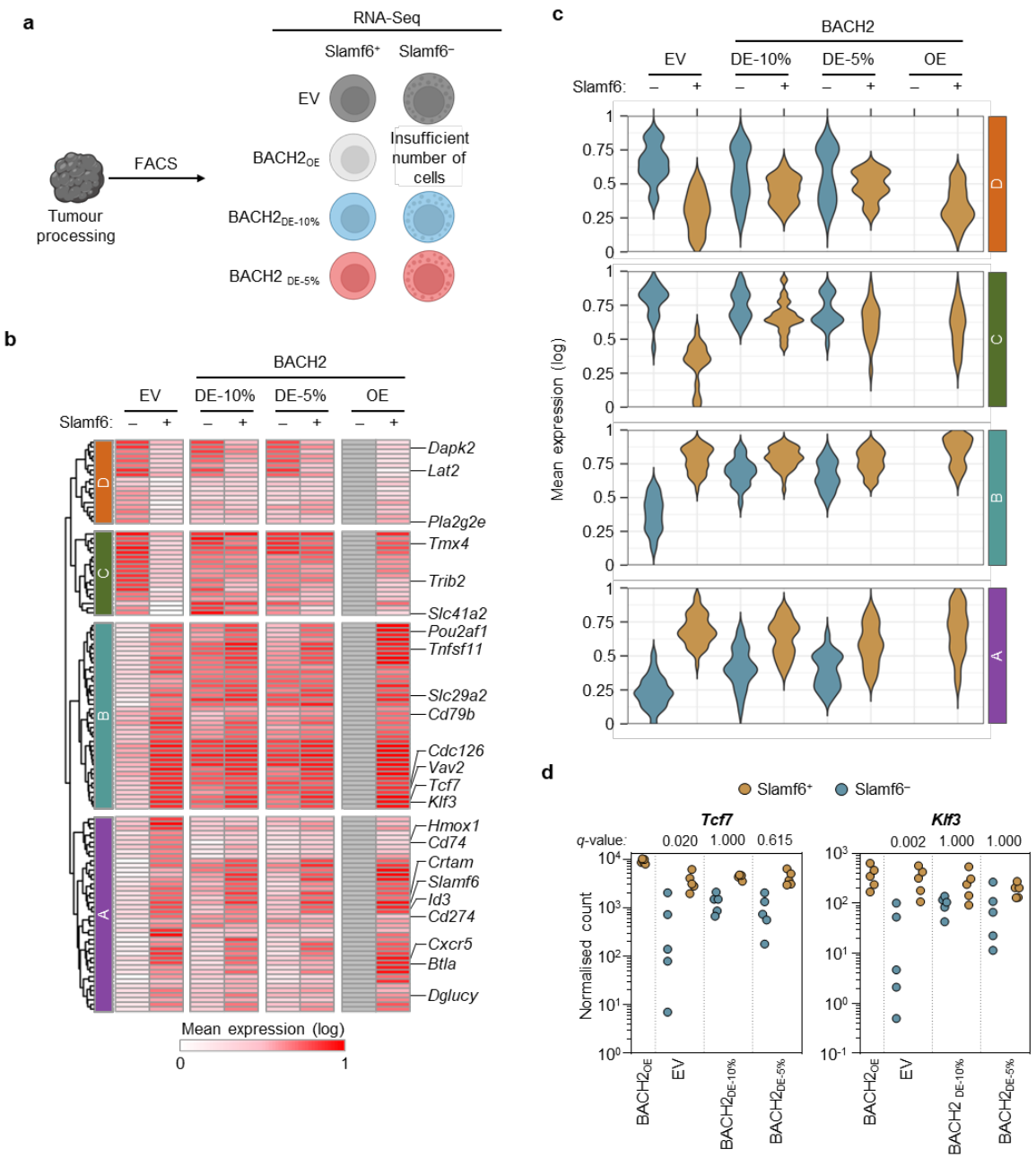
a
RNA-Seq
Slamf6+
Slamf6−
EV
BACH2OE
BACH2DE-10%
BACH2 DE-5%
Insufficient number of cells
FACS
Tumour processing
b
BACH2
EV
DE-10%
DE-5%
OE
Slamf6:
Dapk2
Lat2
Pla2g2e
Tmx4
Trib2
Slc41a2
Pou2af1
Tnfsf11
Slc29a2
Cd79b
Cdc126
Vav2
Tcf7
Klf3
Hmox1
Cd74
Crtam
Slamf6
Id3
Cd274
Cxcr5
Btla
Dglucy
Mean expression (log)
0
1
c
BACH2
EV
DE-10%
DE-5%
OE
Slamf6:
Mean expression (log)
d
Slamf6+
Slamf6−
Tcf7
Klf3
q-value:
0.020
1.000
0.615
0.002
1.000
1.000
Normalised count
BACH2OE
EV
BACH2DE-10%
BACH2DE-5%

Figure 3-3. BACH2 dosing induces subset-specific transcriptomic differences in Slamf6^{+} and Slamf6^{-} populations. a, Diagram depicting experimental workflow. Tumour-infiltrating OT-I T cells transduced with the indicated vectors were isolated from B16-OVA tumour-bearing mice 18 days post-T cell transfer and sorted via FACS into Slamf6^{+} and Slamf6^{-} subsets for analysis via RNA-seq. Insufficient number of Slamf6^{-} cells were obtained in mice treated with BACH2$_{OE}$-transduced cells. **b**, Heatmap displaying the average log(normalised count), where replicate values within each gene were normalised from 0 to 1, in the indicated groups. Genes displayed correspond to all DEGs ($q < 0.05$, $\log2(FC) > 1$) between Slamf6^{+} and Slamf6^{-} in EV and BACH2$_{DE}$. **c**, Violin plots displaying the distribution of values of the indicated populations in each of the clusters from (**c**). **d**, Normalised expression counts of *Tcf7* and *Klf3* from the indicated groups. *q*-values comparing normalised counts between Slamf6^{+} and Slamf6^{-} in each condition are shown.

transcriptional similarity between $BACH2_{DE\text{-}10\%}$ and $BACH2_{DE\text{-}5\%}$, and both groups appeared intermixed in the hierarchical ranking.

The overall transcriptional similarity between $Slamf6^{+}$ and $Slamf6^{-}$ populations in cells of the $BACH2_{DE}$ condition and the preservation of the expression certain memory-associated genes raises the question of whether controlled BACH2 expression allows $Slamf6^{-}$ cells to maintain a transcriptional profile that more closely resembles that of Tpex cells than to their EV-transduced counterparts. To answer this, I used GSEA to compare $Slamf6^{-}$ from EV and $BACH2_{DE}$ conditions using different Tpex gene sets. Notably, the transcriptome of $Slamf6^{-}$ cells transduced with both $BACH2_{DE\text{-}10\%}$ and $BACH2_{DE\text{-}5\%}$ showed a significant enrichment in Tpex-associated genes compared to $Slamf6^{-}$ cells. Moreover, this was true across a number of different publicly available gene sets, which have been derived from both tumour and chronic viral infectious models, and using different Tpex-associated markers during enrichment (e.g. TCF1, ID3, CXCR5) (**Fig. 3-4b-c**)[73,75,167,168].

Based on these observations, I decided to test whether differences at the protein level were observed in tumour-specific $Slamf6^{-}$ adoptive T cells reflective of a less differentiated phenotype within this population. The previously described B16-OVA model was used, with transduced OT-I T cells transferred a day after irradiation and analysed ~18 days following T cell transfer. Notably, several markers, including Ki67, CCR7 and CD62L, displayed a significantly higher MFI in both $BACH2_{DE\text{-}10\%}$ and $BACH2_{DE\text{-}5\%}$ cells in the $Slamf6^{-}$ population, despite displaying no differences in the $Slamf6^{+}$ compartment (Fig. **Fig. 3-4d**).

In conclusion, constitutive low-level BACH2 expression promote the maintenance of $Slamf6^{+}$ transcriptomic features in $Slamf6^{-}$ cells. This similarity is reflected in lower Pearson correlation scores among samples from $BACH2_{DE}$ groups. Consistent with this, this population also showed a significantly higher enrichment of Tpex-associated genes in these populations relative to their EV counterpart and showed higher expression of memory-associated markers such as CD62L and CCR7 within the TME.

5.2.5 Low-dose expression of $FOXO1^{AAA}$ enhances anti-tumour $CD8^{+}$ T cell therapy responses in vivo

Finally, to test whether the principles uncovered in this thesis are specific to BACH2 or could be generalizable to other TFs, I decided to expand the analysis to a new Tpex-associated TF: FOXO1.

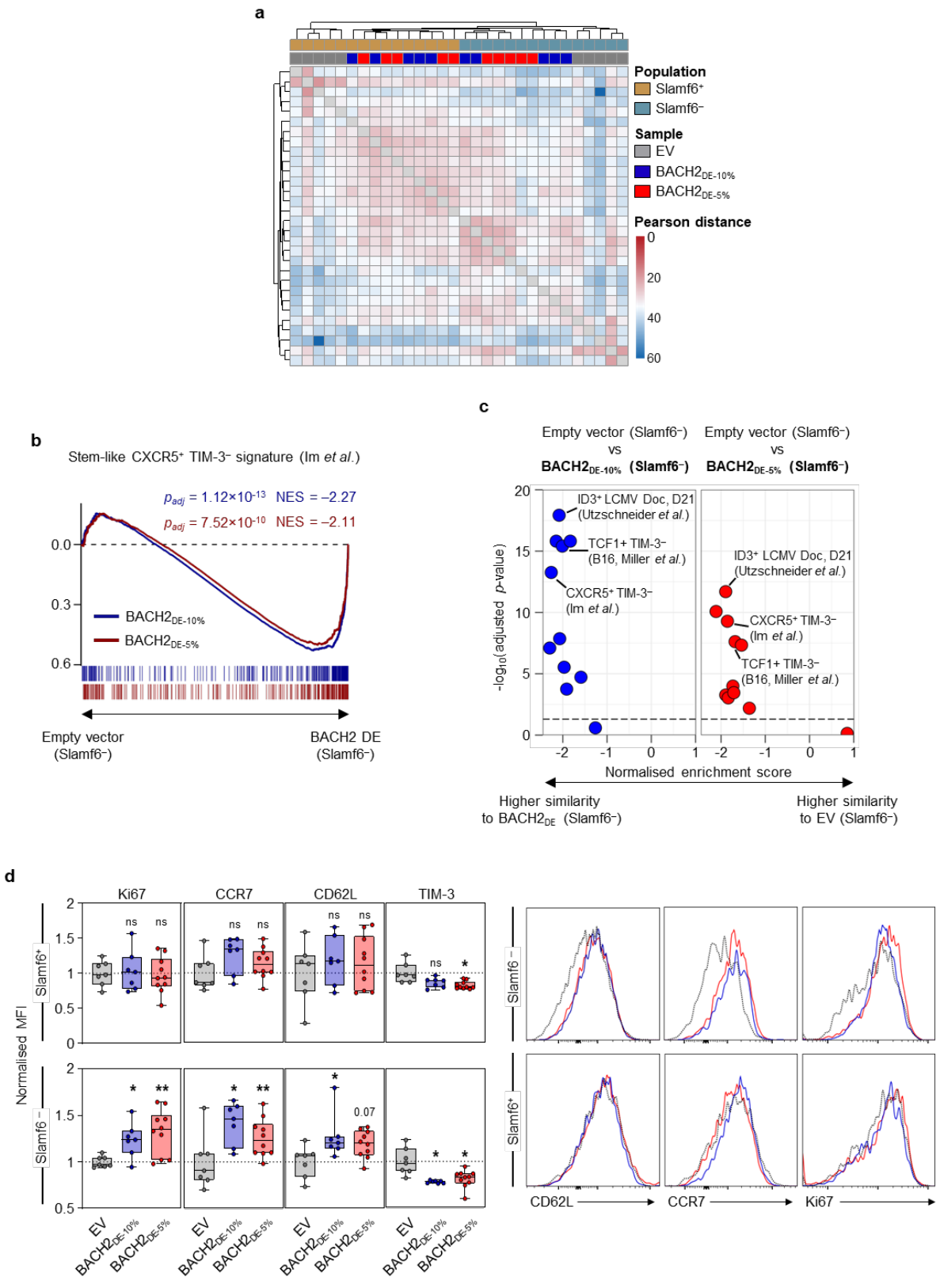
a
Population
Slamf6+
Slamf6−
Sample
EV
BACH2DE-10%
BACH2DE-5%
Pearson distance
0
20
40
60
b
Stem-like CXCR5+ TIM-3− signature (Im et al.)
padj = 1.12×10-13 NES = –2.27
padj = 7.52×10-10 NES = –2.11
BACH2DE-10%
BACH2DE-5%
Empty vector (Slamf6−)
BACH2 DE (Slamf6−)
c
Empty vector (Slamf6−) vs BACH2DE-10% (Slamf6−)
Empty vector (Slamf6−) vs BACH2DE-5% (Slamf6−)
-log10(adjusted p-value)
ID3+ LCMV Doc, D21 (Utzschneider et al.)
TCF1+ TIM-3− (B16, Miller et al.)
CXCR5+ TIM-3− (Im et al.)
Normalised enrichment score
Higher similarity to BACH2DE (Slamf6−)
Higher similarity to EV (Slamf6−)
d
Ki67
CCR7
CD62L
TIM-3
Normalised MFI
Slamf6+
Slamf6−
ns
0.07
EV
BACH2DE-10%
BACH2DE-5%
CD62L
CCR7
Ki67

Figure 3-4. BACH2 dosing preserves Slamf6^{+} transcriptional features upon Slamf6$^{–}$ differentiation. a, Pearson similarity matrix illustrating Slamf6^{+} and Slamf6$^{–}$ populations from OT-I T cells transduced with the indicated vectors. **b-c**, Comparison between Slamf6$^{–}$ EV and Slamf6$^{–}$ BACH2$_{DE\text{-}10\%}$ or BACH2$_{DE\text{-}5\%}$ transduced OT-I T cells sorted from B16-OVA tumours using GSEA with signatures derived from terminally exhausted or progenitor exhausted CD8^{+} T cells (**b**) and normalised enrichment scores of multiple publicly available Tpex signatures (**c**). **d**, Comparison of the MFI (normalised to EV) in the indicated markers between Slamf6^{+} (top) and Slamf6$^{–}$ (bottom) in tumour-infiltrating transduced OT-I T cells, and representative flow cytometry histograms. ns, non-significant ($P > 0.05$); *, $P < 0.05$; **, $P < 0.01$; ****, $P < 0.0001$. One-way ANOVA with Dunnett's multiple comparison correction (**d**). Bars and error indicate mean ± SEM.

Recently, Doan *et al*. and Chan *et al*. have independently shown that full overexpression of FOXO1 improves the anti-tumour responses in different CAR T cell models[128,129]. FOXO1 is related to BACH2, not just in that they are both involved in T cell memory differentiation, but also in the fact that FOXO1 directly binds the *BACH2* locus and induces its expression. Indeed, part of the functions of FOXO1 are thought to be directly attributable to BACH2[89]. Importantly, however, the function of FOXO1 is highly susceptible to its post-translational state: phosphorylation of three different residues (T24, S256 and S319 in humans; T24, S253 and S316 in mice), induced downstream of TCR signalling, halts FOXO1 translocation into the nucleus and prevents its function from being exerted[145]. Therefore, substituting the three sites with alanine residues (not susceptible to phosphorylation) to generate the triple-alanine mutant $FOXO1^{AAA}$ results in a constitutively active variant of FOXO1 that is permanently active.

Prior work studying the function of FOXO1 in $CD8^+$ T cells relied on $FOXO1^{AAA}$ overexpression and showed results similar to those observed with full BACH2 overexpression: while a Tpex-like phenotype is promoted, this occurs at the expense of acquisition of effector functions[89]. This was also demonstrated by Doan *et al*. and Chan *et al*., where they showed that full overexpression of $FOXO1^{AAA}$ disrupted anti-tumour immunity, despite the fact that full overexpression of the WT variant improved it. However, not much focus is placed on this seemingly paradoxical result, and while they mention the possibility of 'dose' as being an important factor, this is left as an open question.

My hypothesis was that they are observing a phenomenon analogous to that seen in $BACH2_{OE}$ and $BACH2_{DE}$, where the use of a $FOXO1^{AAA}$ overexpressing construct ($FOXO1^{AAA}{}_{OE}$) locks T cells in a Tpex state, while relying on a construct overexpressing the WT variant ($FOXO1_{OE}$) provides the right balance between stemness and effector function. To test this hypothesis, I decided to modulate the expression of $FOXO1^{AAA}$. If $FOXO1^{AAA}{}_{OE}$ is too high a dose and causes Tpex locking of $CD8^+$ T cells, perhaps constructs leading to dosed expression of $FOXO1^{AAA}$ ($FOXO1^{AAA}{}_{DE}$) may result in a beneficial phenotype.

Using the same $BACH2_{OE}$ and $BACH2_{DE}$ constructs, I replaced the CDS of BACH2 by that of $FOXO1^{AAA}$, resulting in three new constructs: $FOXO1^{AAA}{}_{OE}$, $FOXO1^{AAA}{}_{DE\text{-}10\%}$ and $FOXO1^{AAA}{}_{DE\text{-}5\%}$. I then transduced $CD8^+$ T cells and stimulated them using the previously described chronic stimulation assay (**Fig. 3-5a**). Interestingly, I observed very similar results to those seen previously using BACH2. $FOXO1^{AAA}{}_{OE}$ and $FOXO1^{AAA}{}_{DE}$ groups all showed a

similar degree of stemness when exposed to chronic stimulation as observed by the expression of CD62L as well as TCF1 and TIM-3, which was significantly higher than cells transduced with the EV group in all cases (**Fig. 3-5b-c**). Nonetheless, when testing their effector function, $FOXO1^{AAA}{}_{DE}$ cells displayed a comparable cytokine expression to EV, while this was substantially reduced in cells from the $FOXO1^{AAA}{}_{OE}$ group (**Fig. 3-5d**).

Since these results mirrored those obtained when using BACH2 in chronic stimulation assays, I hypothesised that dosing of $FOXO1^{AAA}$ could also enhance anti-tumour immunity. To test this, I treated B16-OVA-bearing mice with OT-I T cells transduced with EV, $FOXO1^{AAA}{}_{OE}$, $FOXO1^{AAA}{}_{DE\text{-}10\%}$ and $FOXO1^{AAA}{}_{DE\text{-}5\%}$. Indeed, as observed using the BACH2 vectors, mice treated with T cells belonging to the $FOXO1^{AAA}{}_{DE}$ experienced a significantly improved control of tumour growth and enhanced survival compared to EV, while this was not the case for $FOXO1^{AAA}{}_{OE}$ (**Fig. 3-5e-g**).

Overall, these results suggest that the concept of TF dosing to improve T cell-mediated anti-tumour responses may span beyond BACH2 and could be applicable to other memory-associated factors. This also reflects the broader importance of protecting tumour-specific T cells from the effects of terminal differentiation while simultaneously enable an appropriate degree of effector differentiation.

5.3 Discussion

Throughout this final chapter, I have continued the line of enquiry that originated in the previous section, testing the ability of antigen-specific T cells expressing low levels of quiescent factors in controlling tumour growth. Previous observations revealed that dosed expression of these types of factors can promote stemness without compromising effector functions, a phenotype I hypothesised could improve the efficacy of T cell therapies. Indeed, the results presented here demonstrate that, at least in the OT-I T cell therapy model, that is the case. Moreover, improvements in anti-tumour responses have shown to be reproducible in two distinct tumour models: B16 and MC38. These two models are characteristically distinct – B16 is generally considered an immunologically cold tumour, with high degree of Treg infiltration and elevated levels of immunosuppressive factors, while MC38 is more susceptible to immunotherapies such as cytokine treatment or immune checkpoint blockade. This suggests that dosing of memory factors is a generalisable approach and could be effective in tumours with different characteristics.

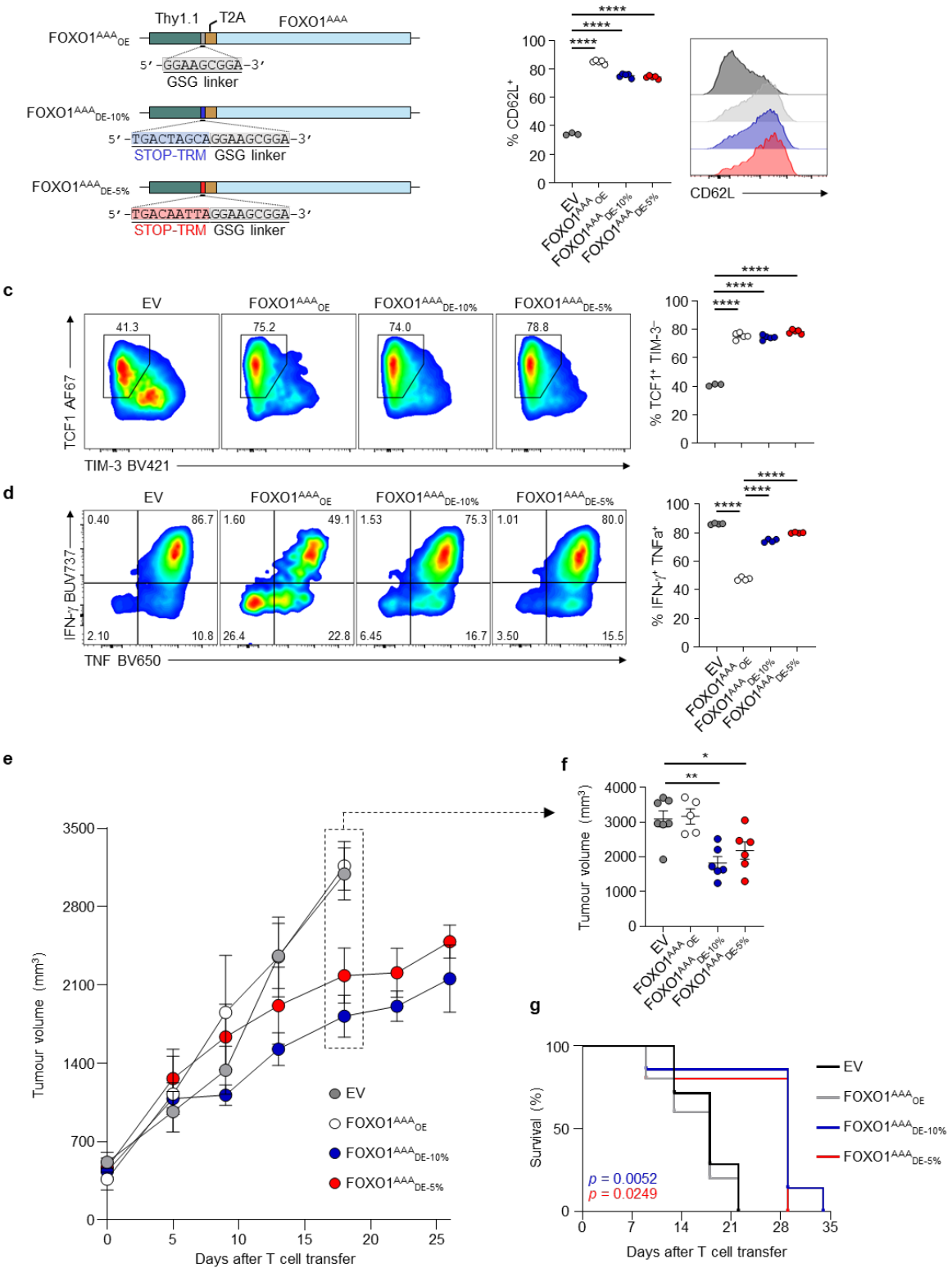
Thy1.1
T2A
FOXO1AAA
FOXO1AAA OE
5′-GGAAGCGGA-3′
GSG linker
FOXO1AAA DE-10%
5′-TGACTAGCAGGAAGCGGA-3′
STOP-TRM GSG linker
FOXO1AAA DE-5%
5′-TGACAATTAGGAAGCGGA-3′
STOP-TRM GSG linker
% CD62L+
CD62L
EV
FOXO1AAA OE
FOXO1AAA DE-10%
FOXO1AAA DE-5%
c
TCF1 AF67
TIM-3 BV421
41.3
75.2
74.0
78.8
% TCF1+ TIM-3−
d
IFN-γ BUV737
TNF BV650
0.40
86.7
2.10
10.8
1.60
49.1
26.4
22.8
1.53
75.3
6.45
16.7
1.01
80.0
3.50
15.5
% IFN-γ+ TNFa+
e
Tumour volume (mm3)
Days after T cell transfer
f
g
Survival (%)
p = 0.0052
p = 0.0249

Figure 3-5. Low-dose FOXO1^{AAA} maintains a stem-like phenotype while preserving effector function *in vitro* and improves anti-tumour T cell therapy efficacy *in vivo*. a, Schematic of FOXO1$^{AAA}{}_{OE}$ and FOXO1$^{AAA}{}_{DE}$ vectors. **b-d**, Frequency of CD62L^{+} chronically stimulated cells (**b**), TCF1^{+} TIM-3^{-} chronically stimulated cells (**c**), or IFN-γ^{+} TNF^{+} acutely stimulated cells after 4 hours of anti-CD3 restimulation in the presence of brefeldin A and monensin (**d**) from OT-I T cells transduced with the indicated vectors on day 4, with representative flow cytometry plots shown. e-f, Tumour growth in B16-OVA–bearing mice following sublethal irradiation (3.5 Gy) and adoptive transfer of 0.5 × 10^{6} OT-I T cells transduced with the indicated vectors (**e**) and tumour volume at day 18 post-transfer (**f**). For mice that were euthanised, the last recorded tumour volume was carried forward into the group average. Tumour sizes are displayed until the time point when more than 20% of mice were still alive. **g**, Kaplan–Meier survival analysis of B16-OVA tumour-bearing mice from panel (**e**). Significant differences are shown between EV and either FOXO1$^{AAA}{}_{DE\text{-}10\%}$ (blue) or FOXO1$^{AAA}{}_{DE\text{-}5\%}$ (red). Data are representative of two independent experiments. ns, not significant ($P > 0.05$); *, $P < 0.05$; **, $P < 0.01$; ****, $P < 0.0001$. Statistical tests: one-way ANOVA with Dunnett's multiple comparison test (b-d, f), Kaplan–Meier log-rank Mantel–Cox test (**e**). Horizontal bars represent mean ± SEM.

Beyond two distinct tumour models, in this section I have tested a second memory factor: FOXO1. Like BACH2, FOXO1 is a well-characterised TF involved in memory differentiation, and full overexpression of the constitutively-active mutein $FOXO1^{AAA}$ had already been shown to compromise the expression of effector cytokines (similar to BACH2 overexpression). This, therefore, raises the possibility that the dosing strategy works beyond BACH2 and FOXO1 to other TFs. Two questions emerge from this notion, however: do BACH2 and FOXO1 rely on a convergent mechanism, or do they achieve the observed phenotypes through different pathways? And, if they worked through different mechanisms, would combining multiple TFs lead to a synergistic effect? Prior studies have shown that BACH2 is a direct target of FOXO1, and that part of its function depends on BACH2[89]. Nonetheless, FOXO1 is also a pioneer TF, and it targets many other genes beyond BACH2[169]. It would be of interest to evaluate specific phenotypic and transcriptomic differences between dosing FOXO1 and BACH2.

One interesting but unexpected finding from this chapter relates to the phenotype of transduced tumour-specific T cells *in vivo*. While in the previous chapter, cells transduced with $BACH2_{DE}$ vectors were able to retain a more stem-like phenotype *in vitro* upon chronic stimulation as characterised by lower expression of TIM-3 (a finding also observed with $FOXO1^{AAA}{}_{DE}$ in this chapter), phenotyping of cells derived from the *in vivo* setting did not show stark differences in the overall expression of TIM-3 or TCF1 across EV, $BACH2_{DE\text{-}10\%}$ and $BACH2_{DE\text{-}5\%}$. One potential explanation could be that of the difference in the strength and duration of the stimulation – cells subjected to tumours *in vivo* get stimulated for long periods of time (up to ~3 weeks) and are exposed to microenvironmental factors that may favour differentiation. This may cause cells lacking high levels of BACH2 to advance further in the effector differentiation trajectory than they may do *in vitro*. Nonetheless, this hypothesis cannot be corroborated with the existing data, and further investigation in the differences between anti-CD3-driven activation and stimulation in an intratumoral context would be warranted.

Nonetheless, an observation consistent among both $BACH2_{DE\text{-}10\%}$ and $BACH2_{DE\text{-}5\%}$ is the fact that the transcriptional profile of $Slamf6^{-}$ cells exposed to dosed levels of BACH2 retains features characteristic of less differentiated $Slamf6^{+}$ populations. I decided to use Slamf6 as a marker for degree of differentiation as it is widely acknowledged to strongly correlate with TCF1, one of the *de facto* markers identifying Tpex[75]. While I could have included other markers in the selection criteria (such as TIM-3), this could have made studying the distinction between different subsets more challenging, both technically for the increased number of populations and for the reduced number of cells; as well as conceptually due to the notion that

cell differentiation is a ‘spectrum’ rather than a selection of clearly distinct populations and further subdivision may blur differences among subpopulations.

Overall, the work in this chapter has helped elucidate the potential of dosing memory factors as a novel strategy for enhancing the performance of tumour-specific T cells in an ACT setting. While data on the phenotype and transcriptomic profile of the cells upon memory TF dosing is useful to expand our understanding of what characteristics may enable T cells to clear tumours more effectively, a number of important elements remain to be elucidated, such as the specific mechanism through which this happens. The relevance of this work in the context of the existing work and literature on T cell therapy and memory factors, as well as potential areas of improvement and future work, will be discussed in the subsequent section.

6. Thesis Discussion

6.1 Summary of key findings

In this thesis, I present a novel and previously unexplored method for using memory-associated factors to enhance the persistence of tumour-targeting T cells in the context of ACT. As with many research-based projects that explore uncharted territory, my work began with a hypothesis informed by prior observations, which upon further experimentation, was refined to a new hypothesis that, eventually, proved to be correct. Here, I summarise the key findings throughout the project and describe how my understanding of the influence of memory-associated factors in T cell therapy evolved throughout the progression of my work.

The project started upon multiple reported observations that Tpex, also commonly referred to as stem-like $CD8^+$ T cells, were correlated with improved persistence and anti-tumour responses[75,79]. Previous work carried out by my laboratory, as well as other groups, had shown that BACH2, a transcriptional repressor associated with T cell memory differentiation and highly expressed in naïve and memory T cells, could enforce a Tpex phenotype[92,131]. Yet, to my knowledge, there had been no prior attempt at testing overexpression of BACH2 (or other memory-associated TFs) to improve anti-tumour responses in ACT.

As such, **Chapter 1** explores the hypothesis that BACH2 overexpression can promote a Tpex state and, consequentially, improve anti-tumour responses. After setting up and optimising a tumour ACT model by testing different doses of lymphodepleting irradiation prior to T cell administration, I treated tumour-bearing mice with antigen-specific T cells genetically edited via a conventional retroviral vector to overexpress BACH2. Data from these experiments showed that, indeed, high levels of BACH2 were sufficient to enforce a Tpex state in tumour-targeting T cells while preventing terminal differentiation, as observed by high expression of the Tpex markers TCF1 and Slamf6. Nonetheless, contrary to initial expectations, the increased levels of BACH2 significantly disrupted the ability of these T cells to engage in effector functions like production of pro-inflammatory cytokines or expression of Granzyme B. Consequently, despite promoting a Tpex state and preventing terminal differentiation, heightened expression of BACH2 compromised *in vivo* anti-tumour responses.

Undeterred, I decided to keep exploring BACH2 biology in tumour-specific T cells. In particular, I was intrigued by an apparent paradox resulting from my results in Chapter 1: the presence of Tpex in tumours is associated with improved anti-tumour ACT responses, and

BACH2 is associated (even required) for Tpex differentiation; yet overexpression of BACH2 worsened anti-tumour responses.

Therefore, in **Chapter 2**, I delved into how BACH2 regulation occurs under physiological anti-tumour responses, with the aim of better understanding how its expression pattern and dose influences T cell differentiation and acquisition of effector functions. An initial look at existing scRNA-seq data suggested an interesting idea: that BACH2 expression is 'dosed' across different T cell subsets, with potential indications for their function. Subsequent experiments using a murine transgenic model edited with a fluorescent reporter to track the expression of BACH2 in different cell states revealed a similar story: while bystander non-activated (PD-1^{-}) cells expressed high levels of BACH2, cells in Tpex and effector states showed intermediate levels of expression. These observations led to a question that became the central theme of my doctoral work: what if, rather than using supraphysiological levels of BACH2 resulting from conventional retroviral transduction, I instead delivered a lower, more physiologically relevant dose?

To do this, I employed the STOP-TRM system – a simple method for modulating the expression of transgenes of interest by employing a premature STOP codon followed by a TRM sequence and the payload of interest. Through this method, I was able to show that conventional BACH2 overexpression leads to supraphysiological levels of BACH2 expression (referred to as $BACH2_{OE}$), while dosed expression through the STOP-TRM system (referred to as $BACH2_{DE}$) led to levels of BACH2 that are closer to physiological levels of expression.

To test whether differences in quantitative levels of BACH2 lead to alterations in function, I subjected T cells expressing BACH2 at high or low doses to chronic stimulation assays. As expected, cells belonging to the $BACH2_{OE}$ group showed maintained stemness upon repeated antigen exposure relative to EV, but this was accompanied by a loss in effector functions such as production of IFN-γ. However, notably, while $BACH2_{DE}$-transduced cells showed comparable levels of stemness to $BACH2_{OE}$, they displayed no loss of effector function. These changes were also reflected at the transcriptional level, where $BACH2_{DE}$-transduced cells displayed a transcriptomic signature with significant enrichment of Tpex-associated genes relative to EV.

Motif enrichment analysis of the sequences of genes differentially regulated $BACH2_{DE}$ and $BACH2_{OE}$ cells revealed a that dosed expression of BACH2 preferentially represses highly AP-1-dependent genes with an increased concentration of AP-1 motifs near their TSS.

Furthermore, while high levels of BACH2 caused a stark reduction in the binding of the AP-1 factor JunB near known BACH2-binding sites, dosed levels of BACH2 caused only partial displacement of AP-1 binding, likely resulting in changes in the levels of mRNA expression of the respective genes with potential downstream functional implications.

Following these observations, I moved to testing this system *in vivo* throughout **Chapter 3**. Using the ACT model established in Chapter 1, I tested the ability of cells with dosed-optimised BACH2 expression to control tumour growth and found that cells transduced with both $BACH2_{DE\text{-}10\%}$ and $BACH2_{DE\text{-}5\%}$ vectors displayed superior anti-tumour immunity compared to EV or $BACH2_{OE}$-transduced cells. This was also accompanied by an increase in the number of cells per gram of tumour of both Tpex and Ttex populations, though the balance of these was not altered relative to EV. Functionally, as observed *in vitro*, only $BACH2_{OE}$ but not $BACH2_{DE}$ compromised the production of effector molecules. At a transcriptional level, more differentiated $BACH2_{DE}$ $Slamf6^{-}$ retained higher expression of Tpex-associated genes compared to their EV counterpart. This was consistent with protein-level observations of Tpex markers, such as CCR7 and CD62L, being more highly expressed in $BACH2_{DE}$ $Slamf6^{-}$ relative to EV $Slamf6^{-}$ cells, indicating retention of at least some stem-like features in more differentiated states.

Finally, I concluded my doctoral research by testing the concept beyond BACH2 with a well-characterised TF: FOXO1. Like BACH2, FOXO1 is involved in memory and Tpex differentiation, and high levels of FOXO1 activity also promote stemness while restricting the acquisition of effector functions. I therefore employed the same system used previously to generate FOXO1 dosed-optimised vectors. Again, I observed maintenance of stem-like features without compromising effector functions, leading to enhanced anti-tumour responses *in vivo*.

6.2 Limitations and future perspectives

Before delving into a detailed discussion of the conclusions of this work, its repercussions and potential future directions of research, I'd like to first cover the strengths and limitations of the methodology used.

The strength of the results and conclusions of any research depend highly on the strengths of the models used. For this reason, I have tried, as much as it was technically feasible, to use validated and well-described models, where both strengths and limitations are known and well-understood. One such example is the use of cell lines expressing model antigens for ACT experiments. As explained in Chapter 1, a good model requires a compromise between fidelity

and practicality. The *in vivo* use of cell lines such as B16-OVA and MC38-OVA enable modelling of T cell responses during ACT in a context where I know T cells are actively recognising a tumour-specific antigen, while preserving an intact TME containing many types of immune and non-immune populations[170]. As this heterogenous mix of cell types, and the soluble factors they secrete into the TME, are likely to impact T cell signalling and differentiation, I believe these to be good models to assess T cell's functional anti-tumour performance and a good compromise between technical feasibility and fidelity to a real-world disease setting. Notwithstanding, cell line-based models have clear limitations too, such as the lack the heterogeneity and varying levels of antigen expression characteristic of real tumours, but since the focus of this study has been primarily on the T cell compartment I believe these drawbacks to be of tolerable.

Another approach of major relevance to the present thesis is the use of the STOP-TRM system to modulate the expression of payloads of interest. Since ensuring this tool works as originally described is pivotal for the interpretation of the conclusions, I've sought to independently validate it in various ways[146]. This includes multiple measurements of the expression of BACH2 and using two individual techniques (flow cytometry, proteomics). Furthermore, an additional layer of confidence in the results obtained comes from the use of two individual doses throughout the entirety of the study ($BACH2_{DE\text{-}10\%}$ and $BACH2_{DE\text{-}5\%}$). In all results, both doses resulted in very similar functional and transcriptional outcomes, consistent with the expected similarity in transgene dose from both vectors.

One limitation of the STOP-TRM system, however, is the restriction in the range of doses that can be produced. This is because the highest level of expression that can be achieved using this system results in a ~10-fold decrease in expression (based on MFI signal) compared to lack of a STOP codon[146]. This means that I have been unable to test any dose of BACH2 between those obtained by the $BACH2_{OE}$ and $BACH2_{DE\text{-}10\%}$ vectors. Thus, whether a level of expression within this range would be better suited to maintaining appropriate T cell function in the context of ACT remains to be assessed.

An alternative method to achieve dosed expression of transgenes of interest while providing a more flexible range of expression is the use of mutant IRES sequences. An IRES is a sequence that enables ribosome binding and translation initiation anywhere in an mRNA transcript and is routinely used for expressing multiple payloads in a polycistronic manner. While IRES enables a relatively high expression of multiple payloads of interest from a single transgenic

cassette, mutant versions of this sequence can be used to modulate the resulting dose of expression[161]. And unlike the STOP-TRM system, a wide range of mutations enables fine-tuning the dose from close to 100% of the WT IRES version down to near complete lack of expression. Therefore, this system could be used to further examine the effect of different doses of BACH2 or other TFs more precisely and across a wider set of ranges.

Two factors from the IRES system, however, led me to select STOP-TRMs to evaluate dosed expression of BACH2. The first one is the fact that IRES sequences are over 500 bp in length, increasing the overall size of the vectors with potential consequences with the production and concentration of viral particles used for T cell transduction. And the second factor is that, while the STOP-TRM system had been originally validated in primary T cells, this was not the case for the IRES mutants which had only been tested in immortalised cell lines[146,161].

One important additional consideration is that the *in vivo* models I have employed throughout this thesis make use of T cells with a transgenic TCR, specific for the model antigen OVA. Such a setup avoids having to modify T cells further with the addition of an antigen receptor, which would increase the size requirements of the vectors and complicate production of retroviral vectors. Nonetheless, the specific affinity of a TCR towards its target, as well as the abundance of the antigen of interest, can influence the degree of signal received by the T cell. This, in turn, can have consequences on its function and differentiation trajectory[81,114]. Therefore, whether the results obtained here apply more broadly to TCRs of different affinity, different levels of antigen exposure, or even other non-TCR antigen receptors, is an aspect that warrants further investigation.

This is particularly relevant in the context of CAR T cell therapies. This type of therapies, as discussed during the introduction, involve modifying T cells with a synthetic antigen receptor composed by the fusion of an extracellular binding domain, usually derived from an antibody's scFv, with an intracellular signalling structure containing signalling domains derived from natural stimulatory and co-stimulatory receptors. CARs have revolutionised the treatment of cancer and the use of immune cells as part of the therapeutic arsenal in cancer and autoimmune indications, but differences in the degree of antigen-driven signalling between CARs and TCRs have been shown to carry functional implications. For instance, CARs generally produce 'stronger' signal when recognising an antigen than TCRs, which has shown to have a substantial impact in the rate of T cell differentiation and persistence in a clinical setting[171]. Therefore, while the overall mechanisms guiding T cell differentiation or acquisition of effector

functions is conserved among both TCR- and CAR-expressing T cells, it would be of interest to explore whether the results observed in our studies apply also to CAR T cell models and, if so, determine whether dose requirements between models changes as a consequence of signalling strength differences.

The increase of T cell therapies in the clinical setting has also highlighted the importance of maintaining cells in a low state of differentiation during *ex vivo* manufacturing and expansion[112,172]. Indeed, while long culturing times can yield a higher number of gene-modified T cells through T cell proliferation, it is also correlated with a higher degree of differentiation and overall worse anti-tumour responses[173]. Furthermore, CARs have also been observed to induce a low but constant level of CAR-driven signalling even in the absence of an antigen. This phenomenon, known as tonic signalling, can exacerbate the loss of stemness and lead to reduced persistence upon administration into patients[174]. This raises the possibility that the expression of dose-optimised BACH2 could be beneficial, not just during the active anti-tumour response, but also during prior manufacturing stages by preventing further differentiation without compromising proliferation. This is an idea that I have not formally tested in this thesis, but that would be of relevance for clinical translation.

Finally, perhaps the most obvious limitation to clinical translatability pertaining to the models I have used is the lack of testing in human T cells. This stems primarily from a time constraint, as well as from the focus of my laboratory being primarily on mouse genetics and synthetic immunology using murine *in vivo* systems (though the group is gradually expanding to perform more human experimental work). Nonetheless, I believe it is highly likely the concept is reproducible and translatable to human T cells. Functionally, BACH2 and FOXO1 have been shown to play similar roles in both human and mice, which is also reflected by a high degree of sequence conservation (>90% sequence identity for both BACH2 and FOXO1)[133,175,176].

While I have been unable to test the concepts of TF dosing to extend the persistence and enhance the function of T cells in a CAR system or using human T cells, additional work does suggest these findings are translatable in these contexts. For instance, during the final stages of my doctoral research and the preparation of manuscripts for publication of the work, I became aware of two additional laboratories investigating the use of BACH2 for mitigating the effects of terminal differentiation in the context of human CAR T cells. Their findings (not yet published and available as preprints) are complementary to my work, showing similar principles to those presented here apply to human CAR T cells, as well as that BACH2 is

capable of mitigating the effects of CAR-driven tonic signalling[177-179]. As of the time of writing, three manuscripts (one prepared by our laboratory containing the data presented in this thesis, and two additional pieces of work from the aforementioned laboratories with data on human CAR T cell models) are being jointly considered for publication.

In addition to the work on BACH2, recent published work on FOXO1 is consistent with my conclusions, as previously discussed in the Results section. These publications show that overexpression of FOXO1, but not the constitutively active mutein $FOXO1^{AAA}$, improves anti-tumour in a manner similar to that observed in my experiments[128,129]. Notably, these results were obtained also using human CAR T cell models.

My hypothesis is that the principles behind the FOXO1-driven enhancement of CAR T anti-tumour function are similar to those proposed here, though this cannot be confirmed with the data made available in those publications alone. Furthermore, the function of FOXO1 is known to be at least partially dependent on BACH2[89]. This raises several interesting questions: are the observations from the FOXO1 publications directly dependent on BACH2? And would the same principle presented here apply to other Tpex-associated TFs not directly dependent on BACH2, such as ID3? Using a model permitting gene KO and transgene overexpression simultaneously (i.e. WT FOXO1 overexpression + BACH2 KO), as well as expanding the STOP-TRM system to other TFs, would constitute useful ways to answer these questions.

Beyond the expansion of this work to other TFs, another aspect that I have not explored in my thesis is whether these principles can also be expanded to other cell types. Like in $CD8^+$ T cells, immune subsets including $CD4^+$ T cells, NK cells and Tregs display phenotypes analogous to terminal differentiation when exposed to excessive stimulation (i.e. loss of proliferative potential and function)[180-183]. And, like in $CD8^+$ T cells, BACH2 also plays a role as a negative regulator of differentiation[91,133,141,158,184-186]. Therefore, this raises the possibility that dose-optimisation of BACH2, or other TFs, can be employed therapeutically in a broader range of cell therapy contexts that go beyond $CD8^+$ T cells.

6.3 Proposed conceptual model

The data gathered throughout this work, together with the current understanding of T cell biology and differentiation, have allowed me to formulate a model to explain how BACH2 dosing alters the functions of T cells in the context of chronic stimulation, which I will summarise here.

The exposure of $CD8^+$ T cells to sustained periods of stimulation, like in the context of anti-tumour responses, induces their differentiation away from naïve or memory T cells and into states possessing effector functions. While it is practical to speak of these states as discrete subpopulations, in reality these should be thought of as a continuum of differentiation states. Along this spectrum, cells initially acquire potent effector functions but, as they progress further, approach terminally differentiated states characterised by reduced proliferative capacity, impaired cytotoxicity, and diminished effector molecule secretion. Importantly, this loss of function should not be considered pathological; rather, it likely represents an evolutionary safeguard against excessive or damaging immune responses.

This differentiation trajectory is tightly regulated by networks of transcription factors that both promote and restrain effector programmes. Among these regulators, BACH2 functions primarily as a brake on differentiation.

Here, I propose a model in which BACH2 functions as a cellular "thermostat" of differentiation, with its abundance dictating how far a $CD8^+$ T cell can advance along the differentiation continuum. In this framework, BACH2 establishes a lower "floor" of differentiation that T cells cannot cross. Physiologically, this is consistent with the notion that BACH2 expression is gradually suppressed as T cells are exposed to antigen stimulation, enabling cells to progress further into effector states. Supporting this model, complementary work from my laboratory (currently *in press*) demonstrates an analogous effect occurring in the thymus, where BACH2 levels fine-tune signalling thresholds and thereby influence the stringency of negative selection in developing T cells.

This framework would also explain the results obtained in this thesis. The high levels of BACH2 found in $BACH2_{OE}$-transduced T cells 'lock' them in an undifferentiated state, preventing them from accessing phenotypes associated with acquisition of cytotoxic functions. In this case, the limit of differentiation is set prior to the loss of Slamf6 expression, yielding a high proportion of $Slamf6^+$ cells. In contrast, lowering this threshold through dose-optimised BACH2 expression enables cells to advance to an effector state, while restraining them from becoming terminally differentiated and thus maintaining more functional phenotype. With the limit of differentiation being set beyond a $Slamf6^+$ state, cells have now the capacity to advance into $Slamf6^-$ with high cytotoxic potential. Nonetheless, differentiation is constrained before full loss of stemness characteristics, yielding cells in a state that, while effector-like, retains some features of Tpex and effector populations.

Mechanistically, this appears to be achieved through two complementary processes: (i) a dose-dependent bias in gene targeting, whereby lower BACH2 levels preferentially suppress genes more reliant on AP-1 activity; and (ii) partial displacement of AP-1 binding, reducing but not abolishing AP-1 occupancy. Together, these mechanisms provide a molecular explanation for how graded BACH2 expression calibrates the balance between effector differentiation and long-term persistence.

7. Conclusion

In conclusion, my doctoral thesis demonstrates that precise control of the expression levels of quiescent factors like BACH2 and FOXO1 can enhance the anti-tumour function of $CD8^+$ T cells in the context of ACT. While the overexpression of these factors using conventional methods that result in supraphysiological levels of expression lead to compromised acquisition of effector functions, fine-tuning their expression to yield more physiologically relevant levels enables retention of certain stem-like features while maintaining, or even improving, their cytotoxic potential.

Importantly, I believe the implication of these findings go beyond the use of quiescent factors. As interest grows in armouring T cells with transcription factors, signalling modules, or synthetic circuits, our results emphasise that the therapeutic impact depends not simply on expression, but on identifying the optimal level of expression. The contrasting functional outcomes I observed with high versus dosed expression of BACH2 and FOXO1 suggest that many otherwise promising modifications may have been overlooked, not due to lack of activity, but because they were tested at non-ideal expression levels.

But ultimately, these principles must apply beyond the field of T cell therapy itself. My work is rooted in the understanding that life is far too complex to rely on simple on/off switches or binary outcomes, and that dose must therefore be a critical mechanistic layer used to regulate many aspects of biology, not the least of which is something so critical as gene expression and cell differentiation. Looking ahead, I believe embedding systematic ‘dose-response’ readouts into synthetic biology studies and therapeutic development of cell and gene therapies could potentially let us uncover a new set of principles and produce a new generation of drugs that are currently beyond reach.

8. References

1. Dobosz, P., and Dzieciatkowski, T. (2019). The Intriguing History of Cancer Immunotherapy. Front Immunol *10*, 2965. 10.3389/fimmu.2019.02965.
2. Oiseth, S.J., and Aziz, M.S. (2017). Cancer immunotherapy: a brief review of the history, possibilities, and challenges ahead. Journal of Cancer Metastasis and Treatment *3*, 250-261.
3. McCarthy, E.F. (2006). The toxins of William B. Coley and the treatment of bone and soft-tissue sarcomas. Iowa Orthop J *26*, 154-158.
4. Coley, W.B. (1991). The treatment of malignant tumors by repeated inoculations of erysipelas. With a report of ten original cases. 1893. Clin Orthop Relat Res, 3-11.
5. Coley, W.B. (1910). The Treatment of Inoperable Sarcoma by Bacterial Toxins (the Mixed Toxins of the Streptococcus erysipelas and the Bacillus prodigiosus). Proc R Soc Med *3*, 1-48. 10.1177/003591571000301601.
6. Fefer, A., McCoy, J.L., and Glynn, J.P. (1967). Induction and regression of primary moloney sarcoma virus-induced tumors in mice. Cancer Res *27*, 1626-1631.
7. Stutman, O. (1975). Delayed tumour appearance and absence of regression in nude mice infected with murine sarcoma virus. Nature *253*, 142-144. 10.1038/253142a0.
8. Stanton, M.F., Law, L.W., and Ting, R.C. (1968). Some biologic, immunogenic, and morphologic effects in mice after infection with a murine sarcoma virus. II. Morphologic studies. J Natl Cancer Inst *40*, 1113-1129.
9. Miller, J.F., Mitchell, G.F., and Weiss, N.S. (1967). Cellular basis of the immunological defects in thymectomized mice. Nature *214*, 992-997. 10.1038/214992a0.
10. Zinkernagel, R.M., and Doherty, P.C. (1974). Immunological surveillance against altered self components by sensitised T lymphocytes in lymphocytic choriomeningitis. Nature *251*, 547-548. 10.1038/251547a0.
11. Zinkernagel, R.M., and Doherty, P.C. (1974). Restriction of in vitro T cell-mediated cytotoxicity in lymphocytic choriomeningitis within a syngeneic or semiallogeneic system. Nature *248*, 701-702. 10.1038/248701a0.
12. Steinman, R.M., and Cohn, Z.A. (1973). Identification of a novel cell type in peripheral lymphoid organs of mice. I. Morphology, quantitation, tissue distribution. J Exp Med *137*, 1142-1162. 10.1084/jem.137.5.1142.
13. Kiessling, R., Klein, E., and Wigzell, H. (1975). "Natural" killer cells in the mouse. I. Cytotoxic cells with specificity for mouse Moloney leukemia cells. Specificity and

distribution according to genotype. Eur J Immunol *5*, 112-117. 10.1002/eji.1830050208.

14. Kiessling, R., Klein, E., Pross, H., and Wigzell, H. (1975). "Natural" killer cells in the mouse. II. Cytotoxic cells with specificity for mouse Moloney leukemia cells. Characteristics of the killer cell. Eur J Immunol *5*, 117-121. 10.1002/eji.1830050209.
15. Herberman, R.B., Nunn, M.E., and Lavrin, D.H. (1975). Natural cytotoxic reactivity of mouse lymphoid cells against syngeneic acid allogeneic tumors. I. Distribution of reactivity and specificity. Int J Cancer *16*, 216-229. 10.1002/ijc.2910160204.
16. Herberman, R.B., Nunn, M.E., Holden, H.T., and Lavrin, D.H. (1975). Natural cytotoxic reactivity of mouse lymphoid cells against syngeneic and allogeneic tumors. II. Characterization of effector cells. Int J Cancer *16*, 230-239. 10.1002/ijc.2910160205.
17. Allison, J.P., McIntyre, B.W., and Bloch, D. (1982). Tumor-specific antigen of murine T-lymphoma defined with monoclonal antibody. J Immunol *129*, 2293-2300.
18. van der Bruggen, P., Traversari, C., Chomez, P., Lurquin, C., De Plaen, E., Van den Eynde, B., Knuth, A., and Boon, T. (1991). A gene encoding an antigen recognized by cytolytic T lymphocytes on a human melanoma. Science *254*, 1643-1647. 10.1126/science.1840703.
19. Shankaran, V., Ikeda, H., Bruce, A.T., White, J.M., Swanson, P.E., Old, L.J., and Schreiber, R.D. (2001). IFNgamma and lymphocytes prevent primary tumour development and shape tumour immunogenicity. Nature *410*, 1107-1111. 10.1038/35074122.
20. Ishida, Y., Agata, Y., Shibahara, K., and Honjo, T. (1992). Induced expression of PD-1, a novel member of the immunoglobulin gene superfamily, upon programmed cell death. EMBO J *11*, 3887-3895. 10.1002/j.1460-2075.1992.tb05481.x.
21. Leach, D.R., Krummel, M.F., and Allison, J.P. (1996). Enhancement of antitumor immunity by CTLA-4 blockade. Science *271*, 1734-1736. 10.1126/science.271.5256.1734.
22. Chen, D.S., and Mellman, I. (2013). Oncology meets immunology: the cancer-immunity cycle. Immunity *39*, 1-10. 10.1016/j.immuni.2013.07.012.
23. Mellman, I., Chen, D.S., Powles, T., and Turley, S.J. (2023). The cancer-immunity cycle: Indication, genotype, and immunotype. Immunity *56*, 2188-2205. 10.1016/j.immuni.2023.09.011.

24. Ferguson, T.A., Choi, J., and Green, D.R. (2011). Armed response: how dying cells influence T-cell functions. Immunol Rev *241*, 77-88. 10.1111/j.1600-065X.2011.01006.x.

25. Speiser, D.E., Chijioke, O., Schaeuble, K., and Munz, C. (2023). CD4(+) T cells in cancer. Nat Cancer *4*, 317-329. 10.1038/s43018-023-00521-2.

26. Marzo, A.L., Lake, R.A., Lo, D., Sherman, L., McWilliam, A., Nelson, D., Robinson, B.W., and Scott, B. (1999). Tumor antigens are constitutively presented in the draining lymph nodes. J Immunol *162*, 5838-5845.

27. Prokhnevska, N., Cardenas, M.A., Valanparambil, R.M., Sobierajska, E., Barwick, B.G., Jansen, C., Reyes Moon, A., Gregorova, P., delBalzo, L., Greenwald, R., et al. (2023). CD8(+) T cell activation in cancer comprises an initial activation phase in lymph nodes followed by effector differentiation within the tumor. Immunity *56*, 107-124 e105. 10.1016/j.immuni.2022.12.002.

28. Sautes-Fridman, C., Petitprez, F., Calderaro, J., and Fridman, W.H. (2019). Tertiary lymphoid structures in the era of cancer immunotherapy. Nat Rev Cancer *19*, 307-325. 10.1038/s41568-019-0144-6.

29. Teillaud, J.L., Houel, A., Panouillot, M., Riffard, C., and Dieu-Nosjean, M.C. (2024). Tertiary lymphoid structures in anticancer immunity. Nat Rev Cancer *24*, 629-646. 10.1038/s41568-024-00728-0.

30. Nolz, J.C., Starbeck-Miller, G.R., and Harty, J.T. (2011). Naive, effector and memory CD8 T-cell trafficking: parallels and distinctions. Immunotherapy *3*, 1223-1233. 10.2217/imt.11.100.

31. Slaney, C.Y., Kershaw, M.H., and Darcy, P.K. (2014). Trafficking of T cells into tumors. Cancer Res *74*, 7168-7174. 10.1158/0008-5472.CAN-14-2458.

32. Haabeth, O.A.W., Fauskanger, M., Manzke, M., Lundin, K.U., Corthay, A., Bogen, B., and Tveita, A.A. (2018). CD4(+) T-cell-Mediated Rejection of MHC Class II-Positive Tumor Cells Is Dependent on Antigen Secretion and Indirect Presentation on Host APCs. Cancer Res *78*, 4573-4585. 10.1158/0008-5472.CAN-17-2426.

33. Seliger, B., Kloor, M., and Ferrone, S. (2017). HLA class II antigen-processing pathway in tumors: Molecular defects and clinical relevance. Oncoimmunology *6*, e1171447. 10.1080/2162402X.2016.1171447.

34. Barry, M., and Bleackley, R.C. (2002). Cytotoxic T lymphocytes: all roads lead to death. Nat Rev Immunol *2*, 401-409. 10.1038/nri819.

35. Haen, S.P., Loffler, M.W., Rammensee, H.G., and Brossart, P. (2020). Towards new horizons: characterization, classification and implications of the tumour antigenic repertoire. Nat Rev Clin Oncol *17*, 595-610. 10.1038/s41571-020-0387-x.

36. Falkenburg, W.J., Melenhorst, J.J., van de Meent, M., Kester, M.G., Hombrink, P., Heemskerk, M.H., Hagedoorn, R.S., Gostick, E., Price, D.A., Falkenburg, J.H., et al. (2011). Allogeneic HLA-A*02-restricted WT1-specific T cells from mismatched donors are highly reactive but show off-target promiscuity. J Immunol *187*, 2824-2833. 10.4049/jimmunol.1100852.

37. Schmitt, T.M., Aggen, D.H., Stromnes, I.M., Dossett, M.L., Richman, S.A., Kranz, D.M., and Greenberg, P.D. (2013). Enhanced-affinity murine T-cell receptors for tumor/self-antigens can be safe in gene therapy despite surpassing the threshold for thymic selection. Blood *122*, 348-356. 10.1182/blood-2013-01-478164.

38. Shah, K., Al-Haidari, A., Sun, J., and Kazi, J.U. (2021). T cell receptor (TCR) signaling in health and disease. Signal Transduct Target Ther *6*, 412. 10.1038/s41392-021-00823-w.

39. Richards, D.M., Ruggiero, E., Hofer, A.C., Sefrin, J.P., Schmidt, M., von Kalle, C., and Feuerer, M. (2015). The Contained Self-Reactive Peripheral T Cell Repertoire: Size, Diversity, and Cellular Composition. J Immunol *195*, 2067-2079. 10.4049/jimmunol.1500880.

40. Li, D., and Wu, M. (2021). Pattern recognition receptors in health and diseases. Signal Transduct Target Ther *6*, 291. 10.1038/s41392-021-00687-0.

41. Chen, L., and Flies, D.B. (2013). Molecular mechanisms of T cell co-stimulation and co-inhibition. Nat Rev Immunol *13*, 227-242. 10.1038/nri3405.

42. Jenkins, M.K., and Schwartz, R.H. (1987). Antigen presentation by chemically modified splenocytes induces antigen-specific T cell unresponsiveness in vitro and in vivo. J Exp Med *165*, 302-319. 10.1084/jem.165.2.302.

43. Schwartz, R.H. (2003). T cell anergy. Annu Rev Immunol *21*, 305-334. 10.1146/annurev.immunol.21.120601.141110.

44. Mescher, M.F., Curtsinger, J.M., Agarwal, P., Casey, K.A., Gerner, M., Hammerbeck, C.D., Popescu, F., and Xiao, Z. (2006). Signals required for programming effector and memory development by CD8+ T cells. Immunol Rev *211*, 81-92. 10.1111/j.0105-2896.2006.00382.x.

45. Curtsinger, J.M., and Mescher, M.F. (2010). Inflammatory cytokines as a third signal for T cell activation. Curr Opin Immunol *22*, 333-340. 10.1016/j.coi.2010.02.013.

46. Kenneth Murphy, C.W. (2017). Janeway's Immunobiology, 9th Edition (Garland Science).
47. Chmielewski, M., and Abken, H. (2015). TRUCKs: the fourth generation of CARs. Expert Opin Biol Ther *15*, 1145-1154. 10.1517/14712598.2015.1046430.
48. Steffin, D., Ghatwai, N., Montalbano, A., Rathi, P., Courtney, A.N., Arnett, A.B., Fleurence, J., Sweidan, R., Wang, T., Zhang, H., et al. (2025). Interleukin-15-armoured GPC3 CAR T cells for patients with solid cancers. Nature *637*, 940-946. 10.1038/s41586-024-08261-8.
49. Govaerts, A. (1960). Cellular antibodies in kidney homotransplantation. J Immunol *85*, 516-522.
50. Cantor, H., and Boyse, E.A. (1975). Functional subclasses of T-lymphocytes bearing different Ly antigens. I. The generation of functionally distinct T-cell subclasses is a differentiative process independent of antigen. J Exp Med *141*, 1376-1389. 10.1084/jem.141.6.1376.
51. Kisielow, P., Hirst, J.A., Shiku, H., Beverley, P.C., Hoffman, M.K., Boyse, E.A., and Oettgen, H.F. (1975). Ly antigens as markers for functionally distinct subpopulations of thymus-derived lymphocytes of the mouse. Nature *253*, 219-220. 10.1038/253219a0.
52. Fyfe, G., Fisher, R.I., Rosenberg, S.A., Sznol, M., Parkinson, D.R., and Louie, A.C. (1995). Results of treatment of 255 patients with metastatic renal cell carcinoma who received high-dose recombinant interleukin-2 therapy. J Clin Oncol *13*, 688-696. 10.1200/JCO.1995.13.3.688.
53. Cameron, F., Whiteside, G., and Perry, C. (2011). Ipilimumab: first global approval. Drugs *71*, 1093-1104. 10.2165/11594010-000000000-00000.
54. Voskoboinik, I., Whisstock, J.C., and Trapani, J.A. (2015). Perforin and granzymes: function, dysfunction and human pathology. Nat Rev Immunol *15*, 388-400. 10.1038/nri3839.
55. Villa-Morales, M., and Fernandez-Piqueras, J. (2012). Targeting the Fas/FasL signaling pathway in cancer therapy. Expert Opin Ther Targets *16*, 85-101. 10.1517/14728222.2011.628937.
56. Gebhardt, T., Park, S.L., and Parish, I.A. (2023). Stem-like exhausted and memory CD8(+) T cells in cancer. Nat Rev Cancer. 10.1038/s41568-023-00615-0.
57. Giles, J.R., Globig, A.M., Kaech, S.M., and Wherry, E.J. (2023). CD8(+) T cells in the cancer-immunity cycle. Immunity *56*, 2231-2253. 10.1016/j.immuni.2023.09.005.

58. Chang, J.T., Wherry, E.J., and Goldrath, A.W. (2014). Molecular regulation of effector and memory T cell differentiation. Nat Immunol *15*, 1104-1115. 10.1038/ni.3031.

59. Joshi, N.S., Cui, W., Chandele, A., Lee, H.K., Urso, D.R., Hagman, J., Gapin, L., and Kaech, S.M. (2007). Inflammation directs memory precursor and short-lived effector CD8(+) T cell fates via the graded expression of T-bet transcription factor. Immunity *27*, 281-295. 10.1016/j.immuni.2007.07.010.

60. Mueller, S.N., and Mackay, L.K. (2016). Tissue-resident memory T cells: local specialists in immune defence. Nat Rev Immunol *16*, 79-89. 10.1038/nri.2015.3.

61. Zajac, A.J., Blattman, J.N., Murali-Krishna, K., Sourdive, D.J., Suresh, M., Altman, J.D., and Ahmed, R. (1998). Viral immune evasion due to persistence of activated T cells without effector function. J Exp Med *188*, 2205-2213. 10.1084/jem.188.12.2205.

62. Gallimore, A., Glithero, A., Godkin, A., Tissot, A.C., Pluckthun, A., Elliott, T., Hengartner, H., and Zinkernagel, R. (1998). Induction and exhaustion of lymphocytic choriomeningitis virus-specific cytotoxic T lymphocytes visualized using soluble tetrameric major histocompatibility complex class I-peptide complexes. J Exp Med *187*, 1383-1393. 10.1084/jem.187.9.1383.

63. Zheng, L., Qin, S., Si, W., Wang, A., Xing, B., Gao, R., Ren, X., Wang, L., Wu, X., Zhang, J., et al. (2021). Pan-cancer single-cell landscape of tumor-infiltrating T cells. Science *374*, abe6474. 10.1126/science.abe6474.

64. McLane, L.M., Abdel-Hakeem, M.S., and Wherry, E.J. (2019). CD8 T Cell Exhaustion During Chronic Viral Infection and Cancer. Annu Rev Immunol *37*, 457-495. 10.1146/annurev-immunol-041015-055318.

65. Rudloff, M.W., Zumbo, P., Favret, N.R., Roetman, J.J., Detres Roman, C.R., Erwin, M.M., Murray, K.A., Jonnakuti, S.T., Dundar, F., Betel, D., and Philip, M. (2023). Hallmarks of CD8(+) T cell dysfunction are established within hours of tumor antigen encounter before cell division. Nat Immunol *24*, 1527-1539. 10.1038/s41590-023-01578-y.

66. Khan, O., Giles, J.R., McDonald, S., Manne, S., Ngiow, S.F., Patel, K.P., Werner, M.T., Huang, A.C., Alexander, K.A., Wu, J.E., et al. (2019). TOX transcriptionally and epigenetically programs CD8(+) T cell exhaustion. Nature *571*, 211-218. 10.1038/s41586-019-1325-x.

67. Wherry, E.J., and Kurachi, M. (2015). Molecular and cellular insights into T cell exhaustion. Nat Rev Immunol *15*, 486-499. 10.1038/nri3862.

68. Blank, C.U., Haining, W.N., Held, W., Hogan, P.G., Kallies, A., Lugli, E., Lynn, R.C., Philip, M., Rao, A., Restifo, N.P., et al. (2019). Defining 'T cell exhaustion'. Nat Rev Immunol *19*, 665-674. 10.1038/s41577-019-0221-9.

69. Scott, A.C., Dundar, F., Zumbo, P., Chandran, S.S., Klebanoff, C.A., Shakiba, M., Trivedi, P., Menocal, L., Appleby, H., Camara, S., et al. (2019). TOX is a critical regulator of tumour-specific T cell differentiation. Nature *571*, 270-274. 10.1038/s41586-019-1324-y.

70. Wherry, E.J. (2011). T cell exhaustion. Nat Immunol *12*, 492-499. 10.1038/ni.2035.

71. Blackburn, S.D., Shin, H., Freeman, G.J., and Wherry, E.J. (2008). Selective expansion of a subset of exhausted CD8 T cells by alphaPD-L1 blockade. Proc Natl Acad Sci U S A *105*, 15016-15021. 10.1073/pnas.0801497105.

72. He, R., Hou, S., Liu, C., Zhang, A., Bai, Q., Han, M., Yang, Y., Wei, G., Shen, T., Yang, X., et al. (2016). Follicular CXCR5- expressing CD8(+) T cells curtail chronic viral infection. Nature *537*, 412-428. 10.1038/nature19317.

73. Im, S.J., Hashimoto, M., Gerner, M.Y., Lee, J., Kissick, H.T., Burger, M.C., Shan, Q., Hale, J.S., Lee, J., Nasti, T.H., et al. (2016). Defining CD8+ T cells that provide the proliferative burst after PD-1 therapy. Nature *537*, 417-421. 10.1038/nature19330.

74. Utzschneider, D.T., Charmoy, M., Chennupati, V., Pousse, L., Ferreira, D.P., Calderon-Copete, S., Danilo, M., Alfei, F., Hofmann, M., Wieland, D., et al. (2016). T Cell Factor 1-Expressing Memory-like CD8(+) T Cells Sustain the Immune Response to Chronic Viral Infections. Immunity *45*, 415-427. 10.1016/j.immuni.2016.07.021.

75. Miller, B.C., Sen, D.R., Al Abosy, R., Bi, K., Virkud, Y.V., LaFleur, M.W., Yates, K.B., Lako, A., Felt, K., Naik, G.S., et al. (2019). Subsets of exhausted CD8(+) T cells differentially mediate tumor control and respond to checkpoint blockade. Nat Immunol *20*, 326-336. 10.1038/s41590-019-0312-6.

76. Siddiqui, I., Schaeuble, K., Chennupati, V., Fuertes Marraco, S.A., Calderon-Copete, S., Pais Ferreira, D., Carmona, S.J., Scarpellino, L., Gfeller, D., Pradervand, S., et al. (2019). Intratumoral Tcf1(+)PD-1(+)CD8(+) T Cells with Stem-like Properties Promote Tumor Control in Response to Vaccination and Checkpoint Blockade Immunotherapy. Immunity *50*, 195-211 e110. 10.1016/j.immuni.2018.12.021.

77. Jansen, C.S., Prokhnevska, N., Master, V.A., Sanda, M.G., Carlisle, J.W., Bilen, M.A., Cardenas, M., Wilkinson, S., Lake, R., Sowalsky, A.G., et al. (2019). An intra-tumoral niche maintains and differentiates stem-like CD8 T cells. Nature *576*, 465-470. 10.1038/s41586-019-1836-5.

78. Zehn, D., Thimme, R., Lugli, E., de Almeida, G.P., and Oxenius, A. (2022). 'Stem-like' precursors are the fount to sustain persistent CD8(+) T cell responses. Nat Immunol *23*, 836-847. 10.1038/s41590-022-01219-w.

79. Krishna, S., Lowery, F.J., Copeland, A.R., Bahadiroglu, E., Mukherjee, R., Jia, L., Anibal, J.T., Sachs, A., Adebola, S.O., Gurusamy, D., et al. (2020). Stem-like CD8 T cells mediate response of adoptive cell immunotherapy against human cancer. Science *370*, 1328-1334. 10.1126/science.abb9847.

80. Vignali, P.D.A., DePeaux, K., Watson, M.J., Ye, C., Ford, B.R., Lontos, K., McGaa, N.K., Scharping, N.E., Menk, A.V., Robson, S.C., et al. (2023). Hypoxia drives CD39-dependent suppressor function in exhausted T cells to limit antitumor immunity. Nat Immunol *24*, 267-279. 10.1038/s41590-022-01379-9.

81. Daniel, B., Yost, K.E., Hsiung, S., Sandor, K., Xia, Y., Qi, Y., Hiam-Galvez, K.J., Black, M., C, J.R., Shi, Q., et al. (2022). Divergent clonal differentiation trajectories of T cell exhaustion. Nat Immunol *23*, 1614-1627. 10.1038/s41590-022-01337-5.

82. Kasmani, M.Y., Zander, R., Chung, H.K., Chen, Y., Khatun, A., Damo, M., Topchyan, P., Johnson, K.E., Levashova, D., Burns, R., et al. (2023). Clonal lineage tracing reveals mechanisms skewing CD8+ T cell fate decisions in chronic infection. J Exp Med *220*. 10.1084/jem.20220679.

83. Pauken, K.E., Sammons, M.A., Odorizzi, P.M., Manne, S., Godec, J., Khan, O., Drake, A.M., Chen, Z., Sen, D.R., Kurachi, M., et al. (2016). Epigenetic stability of exhausted T cells limits durability of reinvigoration by PD-1 blockade. Science *354*, 1160-1165. 10.1126/science.aaf2807.

84. Gill, A.L., Wang, P.H., Lee, J., Hudson, W.H., Ando, S., Araki, K., Hu, Y., Wieland, A., Im, S., Gavora, A., et al. (2023). PD-1 blockade increases the self-renewal of stem-like CD8 T cells to compensate for their accelerated differentiation into effectors. Sci Immunol *8*, eadg0539. 10.1126/sciimmunol.adg0539.

85. Odorizzi, P.M., Pauken, K.E., Paley, M.A., Sharpe, A., and Wherry, E.J. (2015). Genetic absence of PD-1 promotes accumulation of terminally differentiated exhausted CD8+ T cells. J Exp Med *212*, 1125-1137. 10.1084/jem.20142237.

86. Wei, J., Luo, C., Wang, Y., Guo, Y., Dai, H., Tong, C., Ti, D., Wu, Z., and Han, W. (2019). PD-1 silencing impairs the anti-tumor function of chimeric antigen receptor modified T cells by inhibiting proliferation activity. J Immunother Cancer *7*, 209. 10.1186/s40425-019-0685-y.

87. Henning, A.N., Klebanoff, C.A., and Restifo, N.P. (2018). Silencing stemness in T cell differentiation. Science *359*, 163-164. 10.1126/science.aar5541.

88. Wang, X., He, Q., Shen, H., Xia, A., Tian, W., Yu, W., and Sun, B. (2019). TOX promotes the exhaustion of antitumor CD8(+) T cells by preventing PD1 degradation in hepatocellular carcinoma. J Hepatol *71*, 731-741. 10.1016/j.jhep.2019.05.015.

89. Delpoux, A., Marcel, N., Hess Michelini, R., Katayama, C.D., Allison, K.A., Glass, C.K., Quinones-Parra, S.M., Murre, C., Loh, L., Kedzierska, K., et al. (2021). FOXO1 constrains activation and regulates senescence in CD8 T cells. Cell Rep *34*, 108674. 10.1016/j.celrep.2020.108674.

90. Chen, Z., Ji, Z., Ngiow, S.F., Manne, S., Cai, Z., Huang, A.C., Johnson, J., Staupe, R.P., Bengsch, B., Xu, C., et al. (2019). TCF-1-Centered Transcriptional Network Drives an Effector versus Exhausted CD8 T Cell-Fate Decision. Immunity *51*, 840-855 e845. 10.1016/j.immuni.2019.09.013.

91. Roychoudhuri, R., Hirahara, K., Mousavi, K., Clever, D., Klebanoff, C.A., Bonelli, M., Sciume, G., Zare, H., Vahedi, G., Dema, B., et al. (2013). BACH2 represses effector programs to stabilize T(reg)-mediated immune homeostasis. Nature *498*, 506-510. 10.1038/nature12199.

92. Yao, C., Lou, G., Sun, H.W., Zhu, Z., Sun, Y., Chen, Z., Chauss, D., Moseman, E.A., Cheng, J., D'Antonio, M.A., et al. (2021). BACH2 enforces the transcriptional and epigenetic programs of stem-like CD8(+) T cells. Nat Immunol *22*, 370-380. 10.1038/s41590-021-00868-7.

93. Rosenberg, S.A., and Restifo, N.P. (2015). Adoptive cell transfer as personalized immunotherapy for human cancer. Science *348*, 62-68. 10.1126/science.aaa4967.

94. Rosenberg, S.A., Packard, B.S., Aebersold, P.M., Solomon, D., Topalian, S.L., Toy, S.T., Simon, P., Lotze, M.T., Yang, J.C., Seipp, C.A., and et al. (1988). Use of tumor-infiltrating lymphocytes and interleukin-2 in the immunotherapy of patients with metastatic melanoma. A preliminary report. N Engl J Med *319*, 1676-1680. 10.1056/NEJM198812223192527.

95. Dudley, M.E., Wunderlich, J.R., Robbins, P.F., Yang, J.C., Hwu, P., Schwartzentruber, D.J., Topalian, S.L., Sherry, R., Restifo, N.P., Hubicki, A.M., et al. (2002). Cancer regression and autoimmunity in patients after clonal repopulation with antitumor lymphocytes. Science *298*, 850-854. 10.1126/science.1076514.

96. Gattinoni, L., Finkelstein, S.E., Klebanoff, C.A., Antony, P.A., Palmer, D.C., Spiess, P.J., Hwang, L.N., Yu, Z., Wrzesinski, C., Heimann, D.M., et al. (2005). Removal of

homeostatic cytokine sinks by lymphodepletion enhances the efficacy of adoptively transferred tumor-specific CD8+ T cells. J Exp Med *202*, 907-912. 10.1084/jem.20050732.

97. Dudley, M.E., Yang, J.C., Sherry, R., Hughes, M.S., Royal, R., Kammula, U., Robbins, P.F., Huang, J., Citrin, D.E., Leitman, S.F., et al. (2008). Adoptive cell therapy for patients with metastatic melanoma: evaluation of intensive myeloablative chemoradiation preparative regimens. J Clin Oncol *26*, 5233-5239. 10.1200/JCO.2008.16.5449.
98. FDA, U. (2014). FDA Approves First Cellular Therapy to Treat Patients with Unresectable or Metastatic Melanoma.
99. Morgan, R.A., Dudley, M.E., Wunderlich, J.R., Hughes, M.S., Yang, J.C., Sherry, R.M., Royal, R.E., Topalian, S.L., Kammula, U.S., Restifo, N.P., et al. (2006). Cancer regression in patients after transfer of genetically engineered lymphocytes. Science *314*, 126-129. 10.1126/science.1129003.
100. Baulu, E., Gardet, C., Chuvin, N., and Depil, S. (2023). TCR-engineered T cell therapy in solid tumors: State of the art and perspectives. Sci Adv *9*, eadf3700. 10.1126/sciadv.adf3700.
101. Winstead, E. (2024). FDA Approves Engineered Cell Therapy for Advanced Synovial Sarcoma.
102. June, C.H., O'Connor, R.S., Kawalekar, O.U., Ghassemi, S., and Milone, M.C. (2018). CAR T cell immunotherapy for human cancer. Science *359*, 1361-1365. 10.1126/science.aar6711.
103. Mitra, A., Barua, A., Huang, L., Ganguly, S., Feng, Q., and He, B. (2023). From bench to bedside: the history and progress of CAR T cell therapy. Front Immunol *14*, 1188049. 10.3389/fimmu.2023.1188049.
104. FDA, U. (2024). FDA approves obecabtagene autoleucel for adults with relapsed or refractory B-cell precursor acute lymphoblastic leukemia.
105. Pietrobon, V., Todd, L.A., Goswami, A., Stefanson, O., Yang, Z., and Marincola, F. (2021). Improving CAR T-Cell Persistence. Int J Mol Sci *22*. 10.3390/ijms221910828.
106. Ren, H., Cao, K., and Wang, M. (2021). A Correlation Between Differentiation Phenotypes of Infused T Cells and Anti-Cancer Immunotherapy. Front Immunol *12*, 745109. 10.3389/fimmu.2021.745109.
107. Cieri, N., Camisa, B., Cocchiarella, F., Forcato, M., Oliveira, G., Provasi, E., Bondanza, A., Bordignon, C., Peccatori, J., Ciceri, F., et al. (2013). IL-7 and IL-15 instruct the

generation of human memory stem T cells from naive precursors. Blood *121*, 573-584. 10.1182/blood-2012-05-431718.

108. Crompton, J.G., Sukumar, M., Roychoudhuri, R., Clever, D., Gros, A., Eil, R.L., Tran, E., Hanada, K., Yu, Z., Palmer, D.C., et al. (2015). Akt inhibition enhances expansion of potent tumor-specific lymphocytes with memory cell characteristics. Cancer Res *75*, 296-305. 10.1158/0008-5472.CAN-14-2277.

109. Klebanoff, C.A., Crompton, J.G., Leonardi, A.J., Yamamoto, T.N., Chandran, S.S., Eil, R.L., Sukumar, M., Vodnala, S.K., Hu, J., Ji, Y., et al. (2017). Inhibition of AKT signaling uncouples T cell differentiation from expansion for receptor-engineered adoptive immunotherapy. JCI Insight *2*. 10.1172/jci.insight.95103.

110. Kong, W., Dimitri, A., Wang, W., Jung, I.Y., Ott, C.J., Fasolino, M., Wang, Y., Kulikovskaya, I., Gupta, M., Yoder, T., et al. (2021). BET bromodomain protein inhibition reverses chimeric antigen receptor extinction and reinvigorates exhausted T cells in chronic lymphocytic leukemia. J Clin Invest *131*. 10.1172/JCI145459.

111. Ghassemi, S., Nunez-Cruz, S., O'Connor, R.S., Fraietta, J.A., Patel, P.R., Scholler, J., Barrett, D.M., Lundh, S.M., Davis, M.M., Bedoya, F., et al. (2018). Reducing Ex Vivo Culture Improves the Antileukemic Activity of Chimeric Antigen Receptor (CAR) T Cells. Cancer Immunol Res *6*, 1100-1109. 10.1158/2326-6066.CIR-17-0405.

112. Gattinoni, L., Klebanoff, C.A., Palmer, D.C., Wrzesinski, C., Kerstann, K., Yu, Z., Finkelstein, S.E., Theoret, M.R., Rosenberg, S.A., and Restifo, N.P. (2005). Acquisition of full effector function in vitro paradoxically impairs the in vivo antitumor efficacy of adoptively transferred CD8+ T cells. J Clin Invest *115*, 1616-1626. 10.1172/JCI24480.

113. Weber, E.W., Parker, K.R., Sotillo, E., Lynn, R.C., Anbunathan, H., Lattin, J., Good, Z., Belk, J.A., Daniel, B., Klysz, D., et al. (2021). Transient rest restores functionality in exhausted CAR-T cells through epigenetic remodeling. Science *372*. 10.1126/science.aba1786.

114. Shakiba, M., Zumbo, P., Espinosa-Carrasco, G., Menocal, L., Dundar, F., Carson, S.E., Bruno, E.M., Sanchez-Rivera, F.J., Lowe, S.W., Camara, S., et al. (2022). TCR signal strength defines distinct mechanisms of T cell dysfunction and cancer evasion. J Exp Med *219*. 10.1084/jem.20201966.

115. Ghorashian, S., Kramer, A.M., Onuoha, S., Wright, G., Bartram, J., Richardson, R., Albon, S.J., Casanovas-Company, J., Castro, F., Popova, B., et al. (2019). Enhanced CAR T cell expansion and prolonged persistence in pediatric patients with ALL treated with a low-affinity CD19 CAR. Nat Med *25*, 1408-1414. 10.1038/s41591-019-0549-5.

116. Feucht, J., Sun, J., Eyquem, J., Ho, Y.J., Zhao, Z., Leibold, J., Dobrin, A., Cabriolu, A., Hamieh, M., and Sadelain, M. (2019). Calibration of CAR activation potential directs alternative T cell fates and therapeutic potency. Nat Med *25*, 82-88. 10.1038/s41591-018-0290-5.

117. Lynn, R.C., Weber, E.W., Sotillo, E., Gennert, D., Xu, P., Good, Z., Anbunathan, H., Lattin, J., Jones, R., Tieu, V., et al. (2019). c-Jun overexpression in CAR T cells induces exhaustion resistance. Nature *576*, 293-300. 10.1038/s41586-019-1805-z.

118. Seo, H., Gonzalez-Avalos, E., Zhang, W., Ramchandani, P., Yang, C., Lio, C.J., Rao, A., and Hogan, P.G. (2021). BATF and IRF4 cooperate to counter exhaustion in tumor-infiltrating CAR T cells. Nat Immunol *22*, 983-995. 10.1038/s41590-021-00964-8.

119. Beltra, J.C., Abdel-Hakeem, M.S., Manne, S., Zhang, Z., Huang, H., Kurachi, M., Su, L., Picton, L., Ngiow, S.F., Muroyama, Y., et al. (2023). Stat5 opposes the transcription factor Tox and rewires exhausted CD8(+) T cells toward durable effector-like states during chronic antigen exposure. Immunity *56*, 2699-2718 e2611. 10.1016/j.immuni.2023.11.005.

120. Garcia, J., Daniels, J., Lee, Y., Zhu, I., Cheng, K., Liu, Q., Goodman, D., Burnett, C., Law, C., Thienpont, C., et al. (2024). Naturally occurring T cell mutations enhance engineered T cell therapies. Nature. 10.1038/s41586-024-07018-7.

121. Chen, J., Lopez-Moyado, I.F., Seo, H., Lio, C.J., Hempleman, L.J., Sekiya, T., Yoshimura, A., Scott-Browne, J.P., and Rao, A. (2019). NR4A transcription factors limit CAR T cell function in solid tumours. Nature *567*, 530-534. 10.1038/s41586-019-0985-x.

122. Mai, D., Johnson, O., Reff, J., Fan, T.J., Scholler, J., Sheppard, N.C., and June, C.H. (2023). Combined disruption of T cell inflammatory regulators Regnase-1 and Roquin-1 enhances antitumor activity of engineered human T cells. Proc Natl Acad Sci U S A *120*, e2218632120. 10.1073/pnas.2218632120.

123. Wei, J., Long, L., Zheng, W., Dhungana, Y., Lim, S.A., Guy, C., Wang, Y., Wang, Y.D., Qian, C., Xu, B., et al. (2019). Targeting REGNASE-1 programs long-lived effector T cells for cancer therapy. Nature *576*, 471-476. 10.1038/s41586-019-1821-z.

124. Sutra Del Galy, A., Menegatti, S., Fuentealba, J., Lucibello, F., Perrin, L., Helft, J., Darbois, A., Saitakis, M., Tosello, J., Rookhuizen, D., et al. (2021). In vivo genome-wide CRISPR screens identify SOCS1 as intrinsic checkpoint of CD4(+) T(H)1 cell response. Sci Immunol *6*, eabe8219. 10.1126/sciimmunol.abe8219.

125. FDA, U. (2023). FDA Investigating Serious Risk of T-cell Malignancy Following BCMA-Directed or CD19-Directed Autologous Chimeric Antigen Receptor (CAR) T cell Immunotherapies.

126. Yu, H., and Jove, R. (2004). The STATs of cancer--new molecular targets come of age. Nat Rev Cancer *4*, 97-105. 10.1038/nrc1275.

127. Mallette, F.A., Calabrese, V., Ilangumaran, S., and Ferbeyre, G. (2010). SOCS1, a novel interaction partner of p53 controlling oncogene-induced senescence. Aging (Albany NY) *2*, 445-452. 10.18632/aging.100163.

128. Doan, A.E., Mueller, K.P., Chen, A.Y., Rouin, G.T., Chen, Y., Daniel, B., Lattin, J., Markovska, M., Mozarsky, B., Arias-Umana, J., et al. (2024). FOXO1 is a master regulator of memory programming in CAR T cells. Nature. 10.1038/s41586-024-07300-8.

129. Chan, J.D., Scheffler, C.M., Munoz, I., Sek, K., Lee, J.N., Huang, Y.K., Yap, K.M., Saw, N.Y.L., Li, J., Chen, A.X.Y., et al. (2024). FOXO1 enhances CAR T cell stemness, metabolic fitness and efficacy. Nature. 10.1038/s41586-024-07242-1.

130. Shan, Q., Hu, S., Chen, X., Danahy, D.B., Badovinac, V.P., Zang, C., and Xue, H.H. (2021). Ectopic Tcf1 expression instills a stem-like program in exhausted CD8(+) T cells to enhance viral and tumor immunity. Cell Mol Immunol *18*, 1262-1277. 10.1038/s41423-020-0436-5.

131. Roychoudhuri, R., Clever, D., Li, P., Wakabayashi, Y., Quinn, K.M., Klebanoff, C.A., Ji, Y., Sukumar, M., Eil, R.L., Yu, Z., et al. (2016). BACH2 regulates CD8 + T cell differentiation by controlling access of AP-1 factors to enhancers. Nature Immunology. 10.1038/ni.3441.

132. Reinke, A.W., Baek, J., Ashenberg, O., and Keating, A.E. (2013). Networks of bZIP protein-protein interactions diversified over a billion years of evolution. Science *340*, 730-734. 10.1126/science.1233465.

133. Igarashi, K., Kurosaki, T., and Roychoudhuri, R. (2017). BACH transcription factors in innate and adaptive immunity. Nat Rev Immunol *17*, 437-450. 10.1038/nri.2017.26.

134. Amoutzias, G.D., Veron, A.S., Weiner, J., 3rd, Robinson-Rechavi, M., Bornberg-Bauer, E., Oliver, S.G., and Robertson, D.L. (2007). One billion years of bZIP transcription factor evolution: conservation and change in dimerization and DNA-binding site specificity. Mol Biol Evol *24*, 827-835. 10.1093/molbev/msl211.

135. Escriva, H., Manzon, L., Youson, J., and Laudet, V. (2002). Analysis of lamprey and hagfish genes reveals a complex history of gene duplications during early vertebrate evolution. Mol Biol Evol *19*, 1440-1450. 10.1093/oxfordjournals.molbev.a004207.

136. Sun, J., Hoshino, H., Takaku, K., Nakajima, O., Muto, A., Suzuki, H., Tashiro, S., Takahashi, S., Shibahara, S., Alam, J., et al. (2002). Hemoprotein Bach1 regulates enhancer availability of heme oxygenase-1 gene. EMBO J *21*, 5216-5224. 10.1093/emboj/cdf516.

137. Vardaka, P., Lozano, T., Bot, C., Ellery, J., Whiteside, S.K., Imianowski, C.J., Farrow, S., Walker, S., Okkenhaug, H., Yang, J., et al. (2020). A cell-based bioluminescence assay reveals dose-dependent and contextual repression of AP-1-driven gene expression by BACH2. Sci Rep *10*, 18902. 10.1038/s41598-020-75732-z.

138. Kuwahara, M., Ise, W., Ochi, M., Suzuki, J., Kometani, K., Maruyama, S., Izumoto, M., Matsumoto, A., Takemori, N., Takemori, A., et al. (2016). Bach2-Batf interactions control Th2-type immune response by regulating the IL-4 amplification loop. Nat Commun *7*, 12596. 10.1038/ncomms12596.

139. Tanaka, H., Muto, A., Shima, H., Katoh, Y., Sax, N., Tajima, S., Brydun, A., Ikura, T., Yoshizawa, N., Masai, H., et al. (2016). Epigenetic Regulation of the Blimp-1 Gene (Prdm1) in B Cells Involves Bach2 and Histone Deacetylase 3. J Biol Chem *291*, 6316-6330. 10.1074/jbc.M116.713842.

140. Muto, A., Tashiro, S., Nakajima, O., Hoshino, H., Takahashi, S., Sakoda, E., Ikebe, D., Yamamoto, M., and Igarashi, K. (2004). The transcriptional programme of antibody class switching involves the repressor Bach2. Nature *429*, 566-571. 10.1038/nature02596.

141. Tsukumo, S., Unno, M., Muto, A., Takeuchi, A., Kometani, K., Kurosaki, T., Igarashi, K., and Saito, T. (2013). Bach2 maintains T cells in a naive state by suppressing effector memory-related genes. Proc Natl Acad Sci U S A *110*, 10735-10740. 10.1073/pnas.1306691110.

142. Kuwahara, M., Suzuki, J., Tofukuji, S., Yamada, T., Kanoh, M., Matsumoto, A., Maruyama, S., Kometani, K., Kurosaki, T., Ohara, O., et al. (2014). The Menin-Bach2 axis is critical for regulating CD4 T-cell senescence and cytokine homeostasis. Nat Commun *5*, 3555. 10.1038/ncomms4555.

143. Itoh-Nakadai, A., Hikota, R., Muto, A., Kometani, K., Watanabe-Matsui, M., Sato, Y., Kobayashi, M., Nakamura, A., Miura, Y., Yano, Y., et al. (2014). The transcription

repressors Bach2 and Bach1 promote B cell development by repressing the myeloid program. Nat Immunol *15*, 1171-1180. 10.1038/ni.3024.

144. Herndler-Brandstetter, D., Ishigame, H., Shinnakasu, R., Plajer, V., Stecher, C., Zhao, J., Lietzenmayer, M., Kroehling, L., Takumi, A., Kometani, K., et al. (2018). KLRG1(+) Effector CD8(+) T Cells Lose KLRG1, Differentiate into All Memory T Cell Lineages, and Convey Enhanced Protective Immunity. Immunity *48*, 716-729 e718. 10.1016/j.immuni.2018.03.015.

145. Tang, E.D., Nunez, G., Barr, F.G., and Guan, K.L. (1999). Negative regulation of the forkhead transcription factor FKHR by Akt. J Biol Chem *274*, 16741-16746. 10.1074/jbc.274.24.16741.

146. Sillibourne, J.E., Agliardi, G., Righi, M., Smetanova, K., Rowley, G., Speller, S., Dolor, A., Lamb, K., Allen, C., Karattil, R., et al. (2022). A compact and simple method of achieving differential transgene expression by exploiting translational readthrough. Biotechniques *72*, 143-154. 10.2144/btn-2021-0079.

147. Nowicka, M., Krieg, C., Crowell, H.L., Weber, L.M., Hartmann, F.J., Guglietta, S., Becher, B., Levesque, M.P., and Robinson, M.D. (2017). CyTOF workflow: differential discovery in high-throughput high-dimensional cytometry datasets. F1000Res *6*, 748. 10.12688/f1000research.11622.3.

148. Tyanova, S., Temu, T., Sinitcyn, P., Carlson, A., Hein, M.Y., Geiger, T., Mann, M., and Cox, J. (2016). The Perseus computational platform for comprehensive analysis of (prote)omics data. Nat Methods *13*, 731-740. 10.1038/nmeth.3901.

149. Love, M.I., Huber, W., and Anders, S. (2014). Moderated estimation of fold change and dispersion for RNA-seq data with DESeq2. Genome Biol *15*, 550. 10.1186/s13059-014-0550-8.

150. Overwijk, W.W., and Restifo, N.P. (2001). B16 as a mouse model for human melanoma. Curr Protoc Immunol *Chapter 20*, Unit 20 21. 10.1002/0471142735.im2001s39.

151. Wang, C., Barnoud, C., Cenerenti, M., Sun, M., Caffa, I., Kizil, B., Bill, R., Liu, Y., Pick, R., Garnier, L., et al. (2023). Dendritic cells direct circadian anti-tumour immune responses. Nature *614*, 136-143. 10.1038/s41586-022-05605-0.

152. Whiteside, S.K., Grant, F.M., Alvisi, G., Clarke, J., Tang, L., Imianowski, C.J., Zhang, B., Evans, A.C., Wesolowski, A.J., Conti, A.G., et al. (2023). Acquisition of suppressive function by conventional T cells limits antitumor immunity upon T(reg) depletion. Sci Immunol *8*, eabo5558. 10.1126/sciimmunol.abo5558.

153. Yang, J., Yamashita-Kanemaru, Y., Morris, B.I., Contursi, A., Trajkovski, D., Xu, J., Patrascan, I., Benson, J., Evans, A.C., Conti, A.G., et al. (2025). Aspirin prevents metastasis by limiting platelet TXA(2) suppression of T cell immunity. Nature *640*, 1052-1061. 10.1038/s41586-025-08626-7.

154. Wittenborn, T.R., Fahlquist Hagert, C., Ferapontov, A., Fonager, S., Jensen, L., Winther, G., and Degn, S.E. (2021). Comparison of gamma and x-ray irradiation for myeloablation and establishment of normal and autoimmune syngeneic bone marrow chimeras. PLoS One *16*, e0247501. 10.1371/journal.pone.0247501.

155. Ascierto, M.L., McMiller, T.L., Berger, A.E., Danilova, L., Anders, R.A., Netto, G.J., Xu, H., Pritchard, T.S., Fan, J., Cheadle, C., et al. (2016). The Intratumoral Balance between Metabolic and Immunologic Gene Expression Is Associated with Anti-PD-1 Response in Patients with Renal Cell Carcinoma. Cancer Immunol Res *4*, 726-733. 10.1158/2326-6066.CIR-16-0072.

156. Hamann, D., Kostense, S., Wolthers, K.C., Otto, S.A., Baars, P.A., Miedema, F., and van Lier, R.A. (1999). Evidence that human CD8+CD45RA+CD27- cells are induced by antigen and evolve through extensive rounds of division. Int Immunol *11*, 1027-1033. 10.1093/intimm/11.7.1027.

157. Lee, S.W., Choi, H.Y., Lee, G.W., Kim, T., Cho, H.J., Oh, I.J., Song, S.Y., Yang, D.H., and Cho, J.H. (2021). CD8(+) TILs in NSCLC differentiate into TEMRA via a bifurcated trajectory: deciphering immunogenicity of tumor antigens. J Immunother Cancer *9*. 10.1136/jitc-2021-002709.

158. Imianowski, C.J., Whiteside, S.K., Lozano, T., Evans, A.C., Benson, J.D., Courreges, C.J.F., Sadiyah, F., Lau, C.M., Zandhuis, N.D., Grant, F.M., et al. (2022). BACH2 restricts NK cell maturation and function, limiting immunity to cancer metastasis. J Exp Med *219*. 10.1084/jem.20211476.

159. Kansy, B.A., Concha-Benavente, F., Srivastava, R.M., Jie, H.B., Shayan, G., Lei, Y., Moskovitz, J., Moy, J., Li, J., Brandau, S., et al. (2017). PD-1 Status in CD8(+) T Cells Associates with Survival and Anti-PD-1 Therapeutic Outcomes in Head and Neck Cancer. Cancer Res *77*, 6353-6364. 10.1158/0008-5472.CAN-16-3167.

160. Beltra, J.C., Manne, S., Abdel-Hakeem, M.S., Kurachi, M., Giles, J.R., Chen, Z., Casella, V., Ngiow, S.F., Khan, O., Huang, Y.J., et al. (2020). Developmental Relationships of Four Exhausted CD8(+) T Cell Subsets Reveals Underlying Transcriptional and Epigenetic Landscape Control Mechanisms. Immunity *52*, 825-841 e828. 10.1016/j.immuni.2020.04.014.

161. Koh, E.Y., Ho, S.C., Mariati, Song, Z., Bi, X., Bardor, M., and Yang, Y. (2013). An internal ribosome entry site (IRES) mutant library for tuning expression level of multiple genes in mammalian cells. PLoS One *8*, e82100. 10.1371/journal.pone.0082100.

162. Zhang, F., Carothers, J.M., and Keasling, J.D. (2012). Design of a dynamic sensor-regulator system for production of chemicals and fuels derived from fatty acids. Nat Biotechnol *30*, 354-359. 10.1038/nbt.2149.

163. Ohnuki, M., Tanabe, K., Sutou, K., Teramoto, I., Sawamura, Y., Narita, M., Nakamura, M., Tokunaga, Y., Nakamura, M., Watanabe, A., et al. (2014). Dynamic regulation of human endogenous retroviruses mediates factor-induced reprogramming and differentiation potential. Proc Natl Acad Sci U S A *111*, 12426-12431. 10.1073/pnas.1413299111.

164. Schueren, F., Lingner, T., George, R., Hofhuis, J., Dickel, C., Gartner, J., and Thoms, S. (2014). Peroxisomal lactate dehydrogenase is generated by translational readthrough in mammals. Elife *3*, e03640. 10.7554/eLife.03640.

165. Wu, J.E., Manne, S., Ngiow, S.F., Baxter, A.E., Huang, H., Freilich, E., Clark, M.L., Lee, J.H., Chen, Z., Khan, O., et al. (2023). In vitro modeling of CD8(+) T cell exhaustion enables CRISPR screening to reveal a role for BHLHE40. Sci Immunol *8*, eade3369. 10.1126/sciimmunol.ade3369.

166. Belk, J.A., Yao, W., Ly, N., Freitas, K.A., Chen, Y.T., Shi, Q., Valencia, A.M., Shifrut, E., Kale, N., Yost, K.E., et al. (2022). Genome-wide CRISPR screens of T cell exhaustion identify chromatin remodeling factors that limit T cell persistence. Cancer Cell *40*, 768-786 e767. 10.1016/j.ccell.2022.06.001.

167. Utzschneider, D.T., Gabriel, S.S., Chisanga, D., Gloury, R., Gubser, P.M., Vasanthakumar, A., Shi, W., and Kallies, A. (2020). Early precursor T cells establish and propagate T cell exhaustion in chronic infection. Nat Immunol *21*, 1256-1266. 10.1038/s41590-020-0760-z.

168. Wherry, E.J., Ha, S.J., Kaech, S.M., Haining, W.N., Sarkar, S., Kalia, V., Subramaniam, S., Blattman, J.N., Barber, D.L., and Ahmed, R. (2007). Molecular signature of CD8+ T cell exhaustion during chronic viral infection. Immunity *27*, 670-684. 10.1016/j.immuni.2007.09.006.

169. Hatta, M., and Cirillo, L.A. (2007). Chromatin opening and stable perturbation of core histone:DNA contacts by FoxO1. J Biol Chem *282*, 35583-35593. 10.1074/jbc.M704735200.

170. Albelda, S.M. (2024). CAR T cell therapy for patients with solid tumours: key lessons to learn and unlearn. Nat Rev Clin Oncol *21*, 47-66. 10.1038/s41571-023-00832-4.

171. Wachsmann, T.L.A., Wouters, A.K., Remst, D.F.G., Hagedoorn, R.S., Meeuwsen, M.H., van Diest, E., Leusen, J., Kuball, J., Falkenburg, J.H.F., and Heemskerk, M.H.M. (2022). Comparing CAR and TCR engineered T cell performance as a function of tumor cell exposure. Oncoimmunology *11*, 2033528. 10.1080/2162402X.2022.2033528.

172. Klaver, Y., van Steenbergen, S.C., Sleijfer, S., Debets, R., and Lamers, C.H. (2016). T Cell Maturation Stage Prior to and During GMP Processing Informs on CAR T Cell Expansion in Patients. Front Immunol *7*, 648. 10.3389/fimmu.2016.00648.

173. Zhang, X., Lv, X., and Song, Y. (2018). Short-term culture with IL-2 is beneficial for potent memory chimeric antigen receptor T cell production. Biochem Biophys Res Commun *495*, 1833-1838. 10.1016/j.bbrc.2017.12.041.

174. Long, A.H., Haso, W.M., Shern, J.F., Wanhainen, K.M., Murgai, M., Ingaramo, M., Smith, J.P., Walker, A.J., Kohler, M.E., Venkateshwara, V.R., et al. (2015). 4-1BB costimulation ameliorates T cell exhaustion induced by tonic signaling of chimeric antigen receptors. Nat Med *21*, 581-590. 10.1038/nm.3838.

175. Fabre, S., Carrette, F., Chen, J., Lang, V., Semichon, M., Denoyelle, C., Lazar, V., Cagnard, N., Dubart-Kupperschmitt, A., Mangeney, M., et al. (2008). FOXO1 regulates L-Selectin and a network of human T cell homing molecules downstream of phosphatidylinositol 3-kinase. J Immunol *181*, 2980-2989. 10.4049/jimmunol.181.5.2980.

176. Kim, M.V., Ouyang, W., Liao, W., Zhang, M.Q., and Li, M.O. (2013). The transcription factor Foxo1 controls central-memory CD8+ T cell responses to infection. Immunity *39*, 286-297. 10.1016/j.immuni.2013.07.013.

177. Chang, T.C., Heard, A., Lattin, J., Barrett, A., Landmann, J.H., Warrington, J., Tenzin, Y., Afrin, S., Gupta, D.K., Chang, J.F., et al. (2025). BACH2 regulates T cell lineage states to overcome dysfunction driven by tonic CAR signaling. Research Square.

178. Hu, T., Zhu, Z., Luo, Y., Wizzard, S., Hoar, J., Shinde, S.S., Yihunie, K., Yao, C., and Wu, T. (2025). BACH2 dosage establishes the hierarchy of stemness and finetunes antitumor immunity in CAR T cells. bioRxiv.

179. Chang, T.C., Heard, A., Warrington, J., Landmann, J., Afrin, S., Chang, J., Selli, M.E., Hsu, Y.S., and Singh, N. (2023). Regulation of the Transcriptional Repressor BACH2 Overcomes Tonic Signaling-Driven CAR T Cell Dysfunction. 65th ASH Annual Meeting.

180. Merino, A.M., Kim, H., Miller, J.S., and Cichocki, F. (2020). Unraveling exhaustion in adaptive and conventional NK cells. J Leukoc Biol *108*, 1361-1368. 10.1002/JLB.4MR0620-091R.

181. Dean, I., Lee, C.Y.C., Tuong, Z.K., Li, Z., Tibbitt, C.A., Willis, C., Gaspal, F., Kennedy, B.C., Matei-Rascu, V., Fiancette, R., et al. (2024). Rapid functional impairment of natural killer cells following tumor entry limits anti-tumor immunity. Nat Commun *15*, 683. 10.1038/s41467-024-44789-z.

182. Lamarche, C., Ward-Hartstonge, K., Mi, T., Lin, D.T.S., Huang, Q., Brown, A., Edwards, K., Novakovsky, G.E., Qi, C.N., Kobor, M.S., et al. (2023). Tonic-signaling chimeric antigen receptors drive human regulatory T cell exhaustion. Proc Natl Acad Sci U S A *120*, e2219086120. 10.1073/pnas.2219086120.

183. Miggelbrink, A.M., Jackson, J.D., Lorrey, S.J., Srinivasan, E.S., Waibl-Polania, J., Wilkinson, D.S., and Fecci, P.E. (2021). CD4 T-Cell Exhaustion: Does It Exist and What Are Its Roles in Cancer? Clin Cancer Res *27*, 5742-5752. 10.1158/1078-0432.CCR-21-0206.

184. Grant, F.M., Yang, J., Nasrallah, R., Clarke, J., Sadiyah, F., Whiteside, S.K., Imianowski, C.J., Kuo, P., Vardaka, P., Todorov, T., et al. (2020). BACH2 drives quiescence and maintenance of resting Treg cells to promote homeostasis and cancer immunosuppression. J Exp Med *217*. 10.1084/jem.20190711.

185. Sidwell, T., Liao, Y., Garnham, A.L., Vasanthakumar, A., Gloury, R., Blume, J., Teh, P.P., Chisanga, D., Thelemann, C., de Labastida Rivera, F., et al. (2020). Attenuation of TCR-induced transcription by Bach2 controls regulatory T cell differentiation and homeostasis. Nat Commun *11*, 252. 10.1038/s41467-019-14112-2.

186. Li, S., Bern, M.D., Miao, B., Fan, C., Xing, X., Inoue, T., Piersma, S.J., Wang, T., Colonna, M., Kurosaki, T., and Yokoyama, W.M. (2022). The transcription factor Bach2 negatively regulates murine natural killer cell maturation and function. Elife *11*. 10.7554/eLife.77294.